University of Southampton

Mathematical Modelling of Creep in Weldments using the Cosserat Theory of Plates and Shells

by

Michael Geoffery Newman

Thesis submitted for degree of Doctor of Philosophy

Faculty of Mathematical Studies

This thesis was submitted for examination in September 1993

UNIVERSITY OF SOUTHAMPTON

ABSTRACT

FACULTY OF MATHEMATICAL STUDIES
DEPARTMENT OF MATHEMATICS

Doctor of Philosophy

MATHEMATICAL MODELLING OF CREEP IN WELDMENTS USING THE COSSERAT THEORY OF PLATES AND SHELLS

by Michael Geoffery Newman

Long term problems arising from creep deformation occur frequently in industry. In the power generation industry, for instance, knowledge of the high temperature performance of plates and pipes containing weldments is of particular importance, since the majority of plant failures are associated with weldments. One mode of failure identified by metallurgists is called type IV cracking, and this mode occurs close to the weld in material which has been softened by the welding process

This thesis extends the models of a weldment developed by Nicol(1985) and Hawkes(1989), which are based on the Cosserat theory of plates and shells.

The ultimate aim of this investigation is to predict the time to failure of weldments under applied loads. In order to achieve this goal we introduce the basic concepts of Continuum Damage Mechanics into both the Cosserat model introduced by Nicol and the alternative approach suggested by Hawkes. The lifetimes of a welded plate comprising the parent material, low and high temperature heat affected zones and weld metal, are calculated for both methods, for values of the parameters associated with type IV cracking. It is found that the corresponding solutions from each model display similar characteristics for the initial strain rates but the calculated rupture times can differ significantly.

A different Cosserat model of a plate, in which the assumed stress distribution is zero on the top and bottom surfaces, is next presented. Finally, we investigate the behaviour of a V-shaped weld, obtaining results which imply that the presence of the angled interfaces reduces the lifetime of the weldment.

TABLE OF CONTENTS

ACKNOWLEDGEMENTS

I would like to thank my supervisor Dr. R.E. Craine, for his invaluable advice and assistance over the past few years. I would also like to thank Dr. J.A. Williams for many informative and enjoyable discussions on the subject.

This work would never have been completed without the financial support of the Science and Engineering Research Council and Powergen through the awarding of a CASE studentship.

DEDICATION

Much love and thanks to my parents for all of their help and support, and especially to Louise for all her patience.

Chapter 1

INTRODUCTION

In the last twenty years the design life of components in power plant has been an area of increasing interest. The high temperature creep regime is one area of particular interest since knowledge of the performance and lifetime of plant components is of considerable importance, for both safety and economic reasons.

The majority of problems in weldments occur due to material inhomogeneities in, or around, the weld. These inhomogeneities are caused during the welding process and arise mainly due to different local rates of cooling within the metal being welded which lead, in practice, to the production of metallurgically different zones contained in the weldment. These different zones have been confirmed by observation, Coleman (1978). Within each zone the material properties are almost uniform and from one zone to the next the changes in properties occur over very small length scales, typically $100\mu m$, Hence it is reasonable to model a weldment containing zones using a material with piecewise constant material properties.

Metallurgists suggest that a ferritic weld, containing $\frac{1}{2}$Chromium $\frac{1}{2}$Molybdenum $\frac{1}{4}$Vanadium weld material, consists of four basic regions. The first region is the untransformed parent material. Adjacent to this is a narrow partially transformed or overtempered region, known as the type IV region (after a German classification of the weld crack mode which occurs in this region) or, alternatively, as the low temperature heat affected zone. The type IV region is much more ductile than the parent material. Next to this region is the narrow fully transformed high temperature heat affected zone (HAZ), which is much

stronger than the parent material. Finally in the centre of the weldment is the weld material itself. The weld material is usually weaker than the parent material but not as weak as the material in the type IV region. The weldment is generally the weak feature of any component and often causes welded plates not to reach their design life.

There are three main modes of cracking associated with the structure of the weldment as described in the previous paragraph. The first of these is called stress relief or HAZ cracking, which is attributed to the high creep strength and low ductility of the heat affected zone. The second, referred to as transverse weld metal cracking, occurs within an incorrectly heat-treated weld metal. Both of these forms of cracking are promoted by the existence of residual stresses created by the welding process. The third type of cracking is called type IV cracking, which gives its name to the previously mentioned partially transformed region between the HAZ and the parent material. Type IV cracking is mainly influenced by the applied loading and since it occurs frequently in practice it is important to understand the process more fully.

Changes to the welding process, through varying the local rates of cooling and the maximum temperature in the fusion zone of the weld, make it is possible to maintain some control over the width and material properties of the narrow HAZ and type IV region. Hence, knowing how changes to the parameters affect the lifetime of a weld should lead to improvements in the welding process.

The introduction,by Kachanov (1958, 1986), of the concept of "effective stress" into the steady state creep equation of Norton (1929), allowed much progress to be made on the modelling of the tertiary stage of creep, and thus creep rupture. The approach introduced by Kachanov, and later modified by Rabotnov (1969), incorporates the coupling effect between the material deterioration and the mechanical behaviour of the specimen. These pioneering efforts led to the development of a new field of applied mathematics called Continuum Damage Mechanics (CDM), in which a single damage variable represents the accumulated damage in a material arising from the microscopic level of dislocations

(Ashby and Embury (1985)), slip bands, void growth and coalescence (Giessen and Tvergaard(1991), Dyson (1983)) , the initiation of microcracks and crack propagation (Cocks and Ashby (1981)) to the macroscopic level of the influence of material damage on physical quantities such as density change (Jonas and Baudelet (1977)) and the mechanical change of the material as measured by effective stress. The basic assumption involving effective stress is that a volume of damaged material under an applied stress displays the same strain response as a volume of the undamaged material subject to an effective stress. To measure the damage of the material, and thus the effective stress, Kachanov introduces into the steady state creep equation a damage variable D which takes the value 0 in the undamaged state and 1 at failure. A more detailed discussion of CDM can be found in Chaboche (1989).

The concept of effective stress has been extensively used in obtaining constitutive equations for creep and creep rupture (see, for example Hayhurst (1972), Leckie and Hayhurst (1977), Leckie (1986)). An alternative model for creep and creep rupture has been proposed more recently by Evans, Parker and Wilshire (1982) and Wilshire (1991), called the theta-concept. This method allows data obtained from short term high precision experiments to be extrapolated to predict rupture times. Maruyama, Tanaka and Oikawa (1990) have used a modification of this theta concept model to predict the long term creep rupture of CrMoV ferritic steels.

Other recent work has used the Kachanov-Rabotnov equations to model creep and creep rupture of some simple structures. For instance, Othman and Hayhurst (1990) modelled the creep of a two bar structure subject to a steady load. Hall and Hayhurst (1991a) have used a similar method to model the crack growth and failure behaviour in an internally cracked plate and have also examined a plate containing an external crack. The same authors have produced a model which predicts the accumulated damage and rupture time of a pipe containing a V-shaped weld (Hall and Hayhurst (1991b)). Storesund, Tu and Wu (1992) have used Norton's simple power law to investigate the

stress redistribution due to the presence of a weld in an initially flat plate, and they then made predictions as to the failure behaviour using a simplistic rupture criterion.

All the papers mentioned in the previous paragraph contain results found using finite element methods. Unfortunately, the presence of the thin distinct zones in a weldment and the fact that stress singularities occur at the corners of these regions makes choosing a suitable mesh and obtaining reliable solutions with the finite element model both very difficult and extremely time consuming. It would be very useful,therefore, to construct a simple and reliable mathematical model which will accurately predict the time and position of rupture.

Nicol (1985) introduced a model, different from that used by previous authors, based on the Cosserat theory of plates and shells. The general Cosserat theory of shells was developed during the 1960's by such authors as Green and Naghdi (1965), Green, Naghdi and Wainwright (1965), Green, Naghdi and Osborn (1968), Green Laws and Naghdi (1968) and Green, Naghdi and Wenner (1971). A full thermodynamic derivation of the Cosserat theory can be found in Naghdi (1972), and this latter article encompasses much of the work of the previous authors.

Nicol (1985) investigated a welded plate containing parent material and weld metal only, under simple uniaxial tension, by generalising the multi-axial form of Norton's Law and introducing generalised stresses and strains appropriate to Cosserat theory. Nicol examined the effect on the steady state strain-rate caused through varying the width of the weld metal and the relative creep strengths of the constituent materials. The results of Nicol's work were analysed more extensively by Nicol and Williams (1985), who obtained parametric equations defining the variation of strain-rate with the material properties at certain positions within the plate. The aim of their work was to predict the lifetime of the weld using a simple failure criterion defined by Monkman and Grant (1956), in which the strain at failure is required. Unfortunately, data on this value is scarce and hence no predictions on rupture could be made.

Hawkes (1989) applied Nicol's simple model to a more realistic weldment containing the extra two zones (namely the type IV region and the HAZ) and then obtained plots of the initial strain-rates for various material parameters associated with the weld. The results showed that it is necessary to include these thin zones in any satisfactory model of a weld. Hawkes also introduced an alternative approach, deriving the constitutive equations directly from the multiaxial form of the steady state creep law. Comparisons made between solutions obtained using Hawkes' suggested model and the original one of Nicol, for a plate containing parent material and weld metal only, showed qualitative agreement. Hawkes also used the generalised method of Nicol to examine a model more appropriate to a thicker plate by associating more directors with each point on the Cosserat surface (see Chapter 2 for more details about the Cosserat theory and 'directors'). For a simple weld, in the 'elastic case', it was found that the results were similar to those obtained by Nicol.

Hawkes then investigated the creep of a pipe containing a simple butt weld, subject to constant end loading and internal and/or external pressure, and the creep in an initially curved plate. The results obtained for the pipe showed that the thinning of the pipe about its mean radius occurred over a different lengthscale than the bending of the pipe. Although these extensions of Hawkes increased the range of applications of Nicol's theory, it was still not possible to determine the rupture time and position of rupture

In this thesis we attempt to address this outstanding problem using the basic approach of Continuum Damage Mechanics which, as mentioned earlier, was introduced by Kachanov (1958) and extended by Rabotnov (1969). In chapter 3 we shall use the multi-axial form of the Kachanov-Rabotnov equations, in conjunction with the alternative Cosserat model suggested by Hawkes, to model the creep and creep rupture of a weldment comprising parent material, type IV region, HAZ and weld metal. Although analytical results can be found for strain-rates at $t = 0$, the rupture time and position of rupture must be calculated numerically. A suitable numerical scheme is presented and numerous

results, obtained for different parameters associated with the weld, are determined and discussed.

An alternative damage evolution model has been suggested by Hayhurst (1983). This model includes a direct dependence of the damage rate on the maximum principal stress in addition to the equivalent stress, the effects on the time to rupture of using this model is also investigated in chapter 3.

In the development of their models of a plate under simple uniaxial tension, Nicol and Hawkes both used linear expressions in z (where z denotes the co-ordinate normal to the Cosserat surface) for the components of the three dimensional stress in the plate. Hawkes, in his model of a thicker plate, introduced more directors associated with each point on the Cosserat surface and, to obtain a consistent model, now used higher order terms in z for the three dimensional stress tensor. In chapter 4, by introducing a cubic in z for the three dimensional stress distribution and introducing suitable constraints, we obtain a model for the strain-rates of an initially flat plate containing a weld under uniaxial tension in which the three dimensional stress has zero shear on the plate's top and bottom surfaces.

Most real welds do not display the simple geometry described earlier in which the interfaces of each region are normal to the central surface of the plate. The usual geometry is that of a V-shaped weld, where the interfaces are at an angle θ_o to the central surface of the plate. This type of weld is modelled in chapter 5. In obtaining a model for the pipe, Hawkes generalised the derivation of Nicol to include the use of non-Cartesian co-ordinates. In chapter 5 we shall further extend Nicol's approach by introducing directors which reflect the geometry of the plate. This extension includes not only the concept of effective stress and Continuum Damage Mechanics, but directors which initially are not perpendicular to the Cosserat surface. The model leads to a complex system of partial differential equations which are solved by a suitable numerical scheme. When $\theta_o = 0$, the system reduces to Nicol's model for the strain-rate together with a damage evolution

equation. It is found that the presence of the angled interface reduces the rupture time of the weldment

Finally in chapter 6, we state some concluding remarks on the use of a Cosserat model to represent the creep and creep rupture of a plate containing a weldment. Some other problems that could be attacked in the future using the Cosserat model are also presented.

Chapter 2

BACKGROUND INFORMATION

This chapter will look at the background information required to solve the problem set out in the introduction to this thesis. We shall briefly examine the geometry of Euclidean space and present some results from differential geometry. In section §2.3 the multi-axial creep laws used throughout the thesis are introduced and, finally, sections §2.4 to §2.6 are concerned with the introduction of the general Cosserat theory and the derivation of the field equations associated with this theory.

2.1 Geometry of Euclidean Space.

This section will summarize the basic formulæ of tensor calculus and some appropriate results from the differential geometry of a surface. For a much more complete exposition the reader should consult books on the subject of tensor calculus and/or differential geometry, such as, Abram (1965).

Throughout the thesis all Latin indices (subscripts and superscripts) take the values 1,2,3 whereas Greek indices (subscripts and superscripts) have the range 1,2 only. The usual summation convention over a repeated index will apply, unless specifically stated otherwise.

Let x^i refer to a fixed right-handed orthogonal Cartesian co-ordinate system in Euclidean 3-space. Let v^i denote an arbitrary curvilinear system related to the x^i by the transformation

$$x^i = x^i\left(v^1, v^2, v^3\right), \tag{2.1}$$

$$\det\left(\frac{\partial x^i}{\partial v^j}\right) \neq 0. \tag{2.2}$$

The non-zero determinantal condition (2.2) ensures that there exists a unique inverse such that

$$v^i = v^i\left(x^1, x^2, x^3\right). \tag{2.3}$$

Let $\tilde{v}^i$ be a new set of curvilinear co-ordinates and consider the invertible transformation

$$\tilde{v}^i = \tilde{v}^i\left(v^1, v^2, v^3\right), \tag{2.4}$$

and its inverse defined by

$$v^i = v^i\left(\tilde{v}^1, \tilde{v}^2, \tilde{v}^3\right). \tag{2.5}$$

We assume that the functions defining these transformations (2.4)–(2.5) are continuous and are partially differentiable as many times as required. Hence from (2.4) and (2.5) the transformation of the differentials $dv^i, d\tilde{v}^i$ can be expressed

$$dv^i = \frac{\partial v^i}{\partial \tilde{v}^j} d\tilde{v}^j, \tag{2.6}$$

and

$$d\tilde{v}^i = \frac{\partial \tilde{v}^i}{\partial v^j} dv^j. \tag{2.7}$$

Let $T^i = \{T^1, T^2, T^3\}$ and $T_i = \{T_1, T_2, T_3\}$ be two distinct sets of 3 real numbers associated with a point P of the Euclidean space with co-ordinates v^i . Let there also be associated with the same point 2 sets of real numbers $\tilde{T}^i = \left\{\tilde{T}^1, \tilde{T}^2, \tilde{T}^3\right\}$ and $\tilde{T}_i = \left\{\tilde{T}_1, \tilde{T}_2, \tilde{T}_3\right\}$ defined with respect to a co-ordinate system $\tilde{v}^i$ introduced through (2.4). Then T^i are said to be the components of a contravariant tensor of order 1, and T_i to be the components of a covariant tensor of order 1, if the numbers T^i and $\tilde{T}^i$, and T_i and $\tilde{T}_i$, satisfy respectively the relations

$$\tilde{T}^i = \frac{\partial \tilde{v}^i}{\partial v^j} T^j \quad , \quad T^i = \frac{\partial v^i}{\partial \tilde{v}^j} \tilde{T}^j, \tag{2.8}$$

$$\tilde{T}_i = \frac{\partial v^j}{\partial \tilde{v}^i} T_j \quad , \quad T_i = \frac{\partial \tilde{v}^j}{\partial v^i} \tilde{T}_j. \tag{2.9}$$

The above relations can be generalised by letting $T_{i_1 \ldots i_r}^{j_1 \ldots j_s}$ and $\tilde{T}_{i_1 \ldots i_r}^{j_1 \ldots j_s}$ be two systems of $3^{(r+s)}$ numbers associated with a point P in the co-ordinate systems $v^i, \tilde{v}^i$ respectively. We say these numbers are the components of a mixed tensor of order $(r+s)$ at P, covariant of order r and contravariant of order s , if they transform according to the laws

$$T_{i_1 \ldots i_r}^{j_1 \ldots j_s} = \frac{\partial \tilde{v}^{k_1}}{\partial v^{i_1}} \cdots \frac{\partial \tilde{v}^{k_r}}{\partial v^{i_r}} \frac{\partial v^{j_1}}{\partial \tilde{v}^{l_1}} \cdots \frac{\partial v^{j_s}}{\partial \tilde{v}^{l_s}} \tilde{T}_{k_1 \ldots k_r}^{l_1 \ldots l_s}, \tag{2.10}$$

$$\tilde{T}_{i_1 \ldots i_r}^{j_1 \ldots j_s} = \frac{\partial v^{k_1}}{\partial \tilde{v}^{i_1}} \cdots \frac{\partial v^{k_r}}{\partial \tilde{v}^{i_r}} \frac{\partial \tilde{v}^{j_1}}{\partial v^{l_1}} \cdots \frac{\partial \tilde{v}^{j_s}}{\partial v^{l_s}} T_{k_1 \ldots k_r}^{l_1 \ldots l_s}. \tag{2.11}$$

It should be noted that only tensors of the same type can be added or subtracted.

Now, suppose

$$\mathrm{p} = \mathrm{p}\left(v^i\right) \tag{2.12}$$

is the position vector of some point in Euclidean space, then the square of the line element is

$$ds^2 = d\mathrm{p} \cdot d\mathrm{p} = g_{ij} dv^i dv^j, \tag{2.13}$$

where

$$\mathrm{g}_i = \frac{\partial \mathrm{p}}{\partial v^i} \quad , \quad g_{ij} = \mathrm{g}_i \cdot \mathrm{g}_j, \tag{2.14}$$

are the covariant base vectors and the metric tensor respectively. The reciprocal contravariant base vectors g^i and conjugate metric tensor g^{ij} are defined by

$$\mathrm{g}^i = g^{ij} \mathrm{g}_j \quad , \quad g^{ij} = g^{ji} = \mathrm{g}^i \cdot \mathrm{g}^j = \frac{\mathcal{G}^{ij}}{g}, \tag{2.15}$$

$$g = \det\left(g_{ij}\right),$$

where $\mathcal{G}^{ij}$ are the cofactors of g_{ij} in the expansion of the determinant g . The base vectors also satisfy the following relationships

$$\mathrm{g}^i \cdot \mathrm{g}_j = \delta_j^i \quad , \quad g^{ik} g_{kj} = g_{jk} g^{ki} = \delta_j^i, \tag{2.16}$$

where δ^i_j is the Kronecker delta.

It is possible to raise or lower an index of a tensor through inner multiplication by g^{ij} or g_{ij} as in the following examples

$$\begin{aligned} T_{hjk} &= g_{hi}T^i_{jk}, \\ T^i_{jk} &= g^{ih}T_{hjk}. \end{aligned} \tag{2.17}$$

The Christoffel symbols of the first and second kinds are defined by

$$\overset{*}{\Gamma}_{ijk} = g_{mk}\,\overset{*}{\Gamma}{}^m_{ij} = \frac{1}{2}\left(g_{ik,j} + g_{jk,i} - g_{ij,k}\right), \tag{2.18}$$

where $_{,i}$ denotes partial differentiation with respect to v^i and similarly with the notations $_{,j}$ and $_{,k}$.

Using (2.14), the Christoffel symbols can also be expressed as

$$\overset{*}{\Gamma}_{ijk} = \overset{*}{\Gamma}_{jik} = \mathbf{g}_k \cdot \mathbf{g}_{i,j} \quad , \quad \overset{*}{\Gamma}{}^k_{ij} = \overset{*}{\Gamma}{}^k_{ji} = \mathbf{g}^k \cdot \mathbf{g}_{i,j} = -\mathbf{g}_i \cdot \mathbf{g}^k{}_{,j}. \tag{2.19}$$

We now define covariant differentiation of a covariant tensor T_i, a contravariant tensor T^i and a mixed second order tensor T^i_j, respectively, by

$$T_{i\|k} = T_{i,k} - \overset{*}{\Gamma}{}^l_{ik}T_l, \tag{2.20}$$

$$T^i{}_{\|k} = T^i{}_{,k} + \overset{*}{\Gamma}{}^i_{lk}T^l, \tag{2.21}$$

$$T^i_{j\|k} = T^i_{j,k} + \overset{*}{\Gamma}{}^i_{lk}T^l_j - \overset{*}{\Gamma}{}^l_{jk}T^i_l. \tag{2.22}$$

For higher order tensors there is a natural generalisation of equation (2.22).

2.2 Results on the Differential Geometry of a Surface.

First we define a surface $\mathcal{S}$, by the parametric equations

$$x_i = f_i\left(v^1, v^2\right), \tag{2.23}$$

where x_i are rectangular Cartesian co-ordinates of a point P on the surface $\mathcal{S}$, v^1 and v^2 are parameters. We assume that the functions f_i are continuous and differentiable as many times as required. It immediately follows from (2.23) that the position vector $\mathbf{r}$ can be expressed as a function of the parameters v^α (usually called the curvilinear co-ordinates on the surface $\mathcal{S}$):

$$\mathbf{r} = \mathbf{r}\left(v^1, v^2\right). \tag{2.24}$$

Hence with any point P of the surface we can associate a set of base vectors $\mathbf{a}_1, \mathbf{a}_2$, defined by

$$\mathbf{a}_\alpha = \mathbf{r}_{,\alpha} \quad , \quad \mathbf{a}_1 \times \mathbf{a}_2 \neq 0, \tag{2.25}$$

where $_{,\alpha}$ denotes partial differentiation with respect to v^α. The condition $(2.25)_{(ii)}$ ensures that there exists a unique normal at each point on the surface $\mathcal{S}$. Definitions of covariant, contravariant and mixed tensors at a point P on $\mathcal{S}$ are similar to those in the previous section §2.1, and so will not be discussed here. Let $\mathbf{a}_3$ denote the outward unit normal to $\mathcal{S}$ at the point P, then it follows that

$$\mathbf{a}_3 = \frac{\mathbf{a}_1 \times \mathbf{a}_2}{|\mathbf{a}_1 \times \mathbf{a}_2|}, \tag{2.26}$$

from which we deduce

$$\mathbf{a}_3 \cdot \mathbf{a}_3 = 1 \quad , \quad \mathbf{a}_3 \cdot \mathbf{a}_\alpha = 0 \quad , \quad \mathbf{a}_3 \cdot \mathbf{a}_{3,\alpha} = 0. \tag{2.27}$$

The first and second fundamental forms are now defined. The square of a line element of the surface is given by

$$ds^2 = d\mathbf{r} \cdot d\mathbf{r} = a_{\alpha\beta} dv^\alpha dv^\beta, \tag{2.28}$$

where

$$a_{\alpha\beta} = \mathbf{a}_\alpha \cdot \mathbf{a}_\beta. \tag{2.29}$$

The quadratic form (2.28) is called the first fundamental form of the surface . The reciprocals of the base vectors $\mathbf{a}_\alpha$ and the first fundamental form $a_{\alpha\beta}$ are denoted by $\mathbf{a}^\alpha$

and $a^{\alpha\beta}$ respectively. They are defined at all non-singular points of the surface, and are given by

$$\mathbf{a}^{\alpha} = a^{\alpha\beta}\mathbf{a}_{\beta} \quad , \quad a^{\alpha\beta} = a^{\beta\alpha} = \mathbf{a}^{\alpha} \cdot \mathbf{a}^{\beta} = \frac{\mathcal{A}^{\alpha\beta}}{a}, \tag{2.30}$$

where $\mathcal{A}^{\alpha\beta}$ are the cofactors of $a_{\alpha\beta}$ in the expansion of the determinant a. All of the above quantities satisfy the relevant laws for tensor transformations. They also satisfy the relations

$$\mathbf{a}^{\alpha} \cdot \mathbf{a}_{\beta} = \delta^{\alpha}_{\beta} \quad , \quad a^{\alpha\lambda}a_{\lambda\beta} = a_{\beta\lambda}a^{\lambda\alpha} = \delta^{\alpha}_{\beta}. \tag{2.31}$$

We can use $a^{\alpha\beta}$ and $a_{\alpha\beta}$ to raise and lower indices in a similar way to that shown in (2.17).

The second fundamental form is a measure of the curvature of the surface $\mathcal{S}$ and is defined by

$$-d\mathbf{r} \cdot d\mathbf{a}_3 = b_{\alpha\beta}dv^{\alpha}dv^{\beta}, \tag{2.32}$$

and on using equations $(2.25)_{(i)}$ and $(2.27)_{(ii)}$ we obtain the relations

$$b_{\alpha\beta} = b_{\beta\alpha} = -\mathbf{a}_{\alpha} \cdot \mathbf{a}_{3,\beta} = \mathbf{a}_3 \cdot \mathbf{a}_{\alpha,\beta}. \tag{2.33}$$

The Christoffel symbols on the surface are defined in a similar fashion to the Euclidean 3-space Christoffel symbols through

$$\Gamma_{\alpha\beta\gamma} = a_{\lambda\gamma}\Gamma^{\lambda}_{\alpha\beta} = \frac{1}{2}\left(a_{\alpha\gamma,\beta} + a_{\beta\gamma,\alpha} - a_{\alpha\beta,\gamma}\right), \tag{2.34}$$

$$\Gamma_{\alpha\beta\gamma} = \Gamma_{\beta\alpha\gamma} = \mathbf{a}_{\gamma} \cdot \mathbf{a}_{\alpha,\beta}, \tag{2.35}$$

$$\Gamma^{\gamma}_{\alpha\beta} = \Gamma^{\gamma}_{\beta\alpha} = \mathbf{a}^{\gamma} \cdot \mathbf{a}_{\alpha,\beta} = -\mathbf{a}_{\alpha} \cdot \mathbf{a}^{\gamma}{}_{,\beta}. \tag{2.36}$$

The covariant derivative associated with the metric tensor $a_{\alpha\beta}$ of the surface can now be defined. Notice that the operator is represented by a single vertical bar in this case instead of the double vertical bar in the previous section, §2.1. The appropriate expressions for the derivatives are

$$T_{\alpha|\gamma} = T_{\alpha,\gamma} - \Gamma^{\lambda}_{\alpha\gamma}T_{\lambda}, \tag{2.37}$$

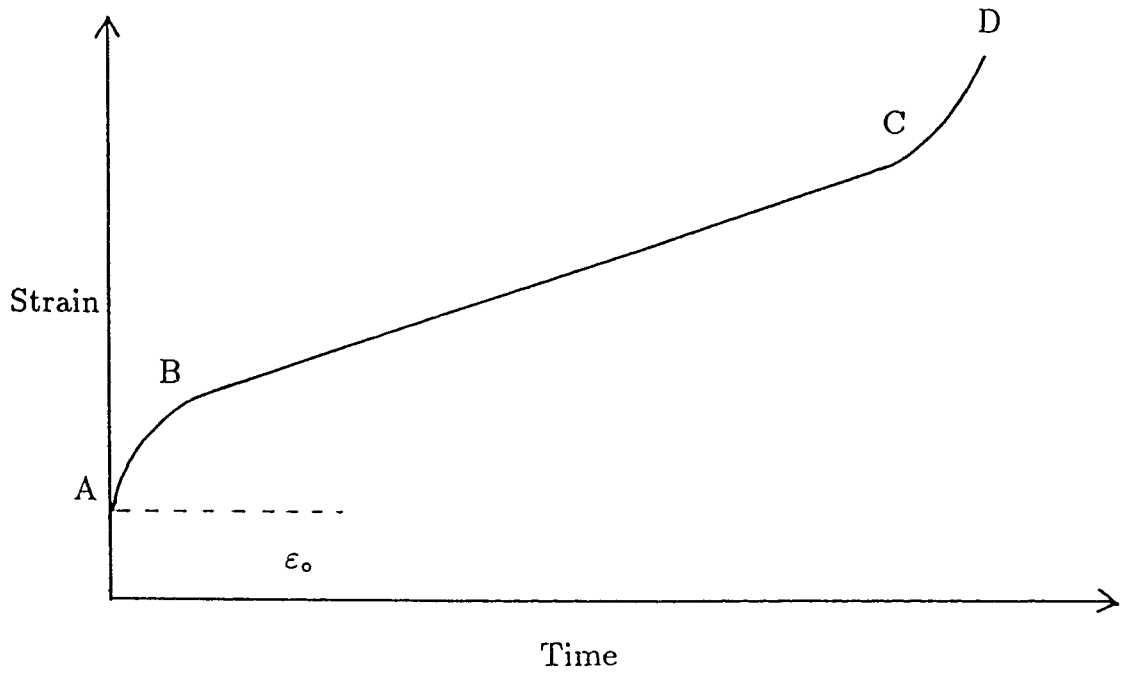

Figure 2.1: Creep diagram

$$T^{\alpha}_{\beta|\gamma} = T^{\alpha}_{\beta,\gamma} + \Gamma^{\alpha}_{\lambda\gamma} T^{\lambda}_{\beta} - \Gamma^{\lambda}_{\beta\gamma} T^{\alpha}_{\lambda}, \tag{2.38}$$

$$T^{\alpha\beta}{}_{|\gamma} = T^{\alpha\beta}{}_{,\gamma} + \Gamma^{\alpha}_{\lambda\gamma} T^{\lambda\beta} + \Gamma^{\beta}_{\lambda\gamma} T^{\alpha\lambda}. \tag{2.39}$$

2.3 Introduction to Creep and Creep Laws.

Creep is the term used to describe the phenomenon that occurs when a material, usually a metal, is subjected to a load at a high temperature (the temperature being greater than some critical value). The material undergoes a plastic time-dependent deformation. There are three main stages in the creep process and these are shown graphically in Figure (2.1).

Figure (2.1) shows how the strain in a specimen changes with time under constant load and temperature. At the instant of loading the component obtains an instantaneous elastic or elasto-plastic strain ε_o. The first portion of the curve AB, which is the primary creep regime, is where the strain-rate decreases with time. The portion BC is the secondary

creep regime, and during this time the strain-rate is approximately constant (the so called 'steady creep' regime). Finally, the third part of the curve, CD, shows the tertiary creep regime, where the strain-rate increases dramatically with time until either brittle or ductile rupture occurs.

Another factor that affects the form of the creep curve is the applied stress level. At high applied stress levels (short term creep) ductile fracture usually occurs. The main features of this type of fracture are a decrease in the cross-sectional area of the specimen and the formation of necking. Ductile fracture occurs at large strains and the creep acceleration in the tertiary stage is large.

For the case of low applied stress (long term creep) the fracture is usually brittle. This type of fracture occurs at small strains and the tertiary stage is not so important. For weldments brittle fracture is the principal failure mechanism and it is only this case which is considered in this thesis.

The most generally accepted form for the constitutive equation for uniaxial secondary creep is Norton's power law, Norton (1929), which is written

$$\frac{\partial \varepsilon}{\partial t} = A\sigma^n. \tag{2.40}$$

where A and n are material dependent constants. In practice both of these latter parameters are not only material dependent but also vary with the applied stress and the temperature. In this thesis, however, A and n will be assumed to be material dependent only.

A useful, and perhaps the simplest, way to predict failure is to use the continuum damage model first suggested by Kachanov (1958) and extended by Rabotnov (1969). In this approach one introduces an additional variable ψ and, for the uniaxial case, equation (2.40) becomes

$$\frac{\partial \varepsilon}{\partial t} = \frac{A\sigma^n}{\psi^p}. \tag{2.41}$$

where ψ satisfies an 'evolution' equation of the form

$$\frac{\partial \psi}{\partial t} = -\frac{B\sigma^m}{\psi^q}. \tag{2.42}$$

In Kachanov's original theory ψ was replaced by $(1-\omega)$, with ω representing the accumulated damage in the material. Hence $\omega = 0$ denotes the virgin state and $\omega = 1$ when the material fails. The quantity ψ is called the 'continuity'. Expressing the initial condition and rupture criterion in terms of the continuity variable, we have

$$\begin{aligned} \psi &= 1 \quad \text{at} \quad t = 0, \\ \psi &= 0 \quad \text{at} \quad t = t_r, \end{aligned} \tag{2.43}$$

where t_r is the rupture time of the specimen.

In practice, the stress state is usually multi-axial and therefore equations (2.41) and (2.42) need to be extended. On assuming that the influence of the continuum damage on the rate of deformation is scalar in character, we obtain the following coupled equations (see Hayhurst(1983))

$$\frac{\partial \gamma_{ij}}{\partial t} = \frac{3}{2}\frac{A(\sigma^*)^{n-1}}{\psi^p} s_{ij}, \tag{2.44}$$

where γ_{ij} is the three dimensional strain tensor and

$$\frac{\partial \psi}{\partial t} = -\frac{B(\sigma^*)^m}{\psi^q}. \tag{2.45}$$

In (2.44) and (2.45) σ^* is defined by

$$(\sigma^*)^2 = \frac{3}{2} s_{ij} s_{ij}, \tag{2.46}$$

where s_{ij} is the usual stress-deviation tensor given by

$$s_{ij} = \sigma_{ij} - \frac{1}{3}\delta_{ij}\sigma_{kk}, \tag{2.47}$$

δ_{ij} being, as usual, the Kronecker delta.

2.4 An Introduction to the Cosserat Theory of Plates and Shells.

Before defining a shell we shall introduce suitable co-ordinate systems. Let points in a region of Euclidean 3-space be referred to a fixed right-handed rectangular Cartesian co-ordinate system x_i, and let $\{v^1, v^2, v^3\}$ be a general material co-ordinate system such that

$$x_i = x_i\left(v^1, v^2, v^3\right), \tag{2.48}$$

Assuming that

$$\det\left(\frac{\partial x_i}{\partial v^j}\right) \neq 0, \tag{2.49}$$

then the transformation (2.48) is non-singular and has a unique inverse which is defined by

$$v^i = v^i\left(x_1, x_2, x_3\right). \tag{2.50}$$

It will be convenient for later use to set $v^3 = \xi$ and so the notation that we will use is

$$v^i = \left\{v^\alpha, \xi\right\}. \tag{2.51}$$

Consider a three-dimensional body, $\mathcal{B}$, in a region of Euclidean 3-space $\mathcal{R}$. If $\mathbf{P}$ denotes the position vector of some point in the body in the reference configuration (we can identify the reference configuration with that of the initial configuration at time $t = 0$, and hence 'reference configuration' and 'initial configuration' are interchangeable in this context), relative to a fixed origin, then

$$\mathbf{P} = \mathbf{P}\left(v^\alpha, \xi\right). \tag{2.52}$$

The position p of the point, relative to the same origin, in the deformed configuration at time t can be expressed as

$$\mathrm{p} = \mathrm{p}\left(v^\alpha, \xi, t\right). \tag{2.53}$$

It is assumed that the function p is sufficiently smooth that it is differentiable with respect to v^α, ξ and t as many times as required. Further if we impose

$$g^{\frac{1}{2}} = [\mathrm{g}_1, \mathrm{g}_2, \mathrm{g}_3] > 0, \tag{2.54}$$

then we shall have a right-handed co-ordinate system. We now commence with the description of a shell. Let $\partial\mathcal{B}$, the boundary of the body $\mathcal{B}$, be specified by:

(i) The two material surfaces

$$\xi = \alpha\left(v^\lambda\right) \text{ and } \xi = \beta\left(v^\lambda\right) \quad , \quad \alpha < 0 < \beta, \tag{2.55}$$

where the surface $\xi = 0$ lies entirely between the two surfaces α and β.

(ii) A material surface

$$f\left(v^1, v^2\right) = 0, \tag{2.56}$$

such that $\xi = constant$ are closed smooth curves on (2.56). It should be noted that we have imposed the condition (2.54), which ensures that the surfaces (2.55) and the surface $\xi = 0$ do not intersect one another.

If $\rho^*\left(v^\alpha, \xi, t\right)$ and $\rho_\circ^*\left(v^\alpha, \xi\right)$ are the mass densities of the body $\mathcal{B}$, in the deformed configuration and the reference (initial) configuration respectively, then the local equation of conservation of mass is

$$\rho^* g^{\frac{1}{2}} = \rho_\circ^* G^{\frac{1}{2}}, \tag{2.57}$$

where G is the dual of g in the reference (initial) configuration. The position of the surface $\xi = 0$ at time t can be fixed by imposing the condition

$$\int_\alpha^\beta \rho_\circ^* G^{\frac{1}{2}} \xi d\xi = 0. \tag{2.58}$$

The condition (2.58) was first introduced by Green, Laws and Naghdi (1968), and it is in effect a condition which equalizes the mass distribution above and below the surface $\xi = 0$. It should be noted that as a result of (2.57) condition (2.58) is independent of

time and hence once the relative position of the surface $\xi = 0$ is determined at some time t, it remains so determined at all subsequent times. This completes the description of a shell.

Let us now briefly introduce the Cosserat theory of plates and shells. We model the shell by introducing a two-dimensional reference surface $\mathcal{S}$, identified with the surface $\xi = 0$ above. At each material point of the surface $\mathcal{S}$ we associate an infinite number of vectors dependent on the material points v^α. In this Cosserat model the deformable vector fields are called 'directors', and these directors vary independently of the deformation of the surface. It is shown in Naghdi (1972) that the deformation of a general plate or shell, of arbitrary thickness, can be modelled exactly by a Cosserat plate or shell with an infinite number of directors. Clearly with an infinite number of directors the model is extremely complicated. To simplify the analysis we often restrict attention to a finite number of directors only and, for the simplest case, introduce a single director. The latter model would be a good approximation, we hope, for a thin plate or shell, at least.

How do we define a thin shell? If h is the thickness of the shell then

$$h = \beta\left(v^\lambda\right) - \alpha\left(v^\lambda\right), \tag{2.59}$$

and we say that a shell is thin when the thickness, h, is much smaller than the minimum radius of curvature, R, of the surface; that is

$$\frac{h}{R} \ll 1. \tag{2.60}$$

In the case of an initially flat plate (for which R is infinite) we say the plate is thin when h is much smaller than the smallest dimension of its middle plane.

Thus for a thin shell or plate we introduce a single deformable director $\mathbf{d}$ at every point on the surface $\mathcal{S}$. It should be noted that $\mathbf{d}$ is *not* necessarily normal to $\mathcal{S}$. The assigned director is expected to portray the 'thickening' about the surface $\xi = 0$ and its

component along the unit normal to this surface models in some sense the thickness of the three-dimensional shell or plate.

2.5 Kinematics of Shells.

The kinematics of the shells defined in the previous section, §2.4, is now developed from the three-dimensional theory. We assume that the position $\mathrm{p}(\upsilon^\alpha, \xi, t)$ of a point in a deformed arbitrarily thick shell is defined by the analytical function

$$\mathrm{p} = \mathrm{r}(\upsilon^\alpha, t) + \sum_{N=1}^{\infty} \xi^N \mathrm{d}_{(N)}(\upsilon^\alpha, t), \tag{2.61}$$

and its dual in the initial (reference) configuration is

$$\mathrm{P} = \mathrm{R}(\upsilon^\alpha, 0) + \sum_{N=1}^{\infty} \xi^N \mathrm{D}_{(N)}(\upsilon^\alpha, 0), \tag{2.62}$$

where r and R are the position vectors of a point in the deformed and initial configuration respectively and $\mathrm{d}_{(N)}$ and $\mathrm{D}_{(N)}$ are vector functions of υ^α and t in the deformed and initial configuration. We assume that the power series (2.61) and (2.62) are differentiable as many times as required. The velocity vector of the shell or plate is given by

$$\mathrm{v}^* = \dot{\mathrm{p}}(\upsilon^\alpha, \xi, t) = \mathrm{v} + \sum_{N=1}^{\infty} \xi^N \mathrm{w}_{(N)}, \tag{2.63}$$

where we have written

$$\mathrm{v} = \dot{\mathrm{r}} \quad , \quad \mathrm{w}_{(N)} = \dot{\mathrm{d}}_{(N)}, \tag{2.64}$$

and the superposed dot denotes differentiation with respect to time holding the other material variables constant. Recalling $(2.14)_{(i)}$ and (2.61) the base vectors g_i can be expressed

$$\mathrm{g}_\alpha = \mathrm{a}_\alpha + \sum_{N=1}^{\infty} \xi^N \frac{\partial \mathrm{d}_{(N)}}{\partial \upsilon^\alpha}, \tag{2.65}$$

$$\mathrm{g}_3 = \sum_{N=1}^{\infty} N \xi^{N-1} \mathrm{d}_{(N)}. \tag{2.66}$$

We now introduce some additional kinematical quantities. Let the three-dimensional vector fields $\mathbf{d}_{(N)}$ and their partial derivatives with respect to v^α be referred to the base vectors $\mathbf{a}_\alpha$, then

$$\mathbf{d}_{(N)} = d_{(N)i}\mathbf{a}^i = d_{(N)}{}^i\mathbf{a}_i \ , \ d_{(N)}{}^\gamma = a^{\gamma\beta}d_{(N)\beta} \ , \ d_{(N)}{}^3 = d_{(N)3}, \tag{2.67}$$

$$\frac{\partial \mathbf{d}_{(N)}}{\partial v^\alpha} = \lambda_{(N)i\alpha}\mathbf{a}^i, \tag{2.68}$$

where the components $\lambda_{(N)i\alpha}$ are given by

$$\lambda_{(N)\gamma\alpha} = \mathbf{a}_\gamma \cdot \mathbf{d}_{(N),\alpha} = d_{(N)\gamma|\alpha} - b_{\gamma\alpha}d_{(N)3} \ , \ \lambda_{(N)}{}^\gamma{}_\alpha = a^{\gamma\beta}\lambda_{(N)\beta\alpha} \tag{2.69}$$

$$\lambda_{(N)3\alpha} = \mathbf{a}_3 \cdot \mathbf{d}_{(N),\alpha} = d_{(N)3,\alpha} - b^\gamma_\alpha d_{(N)\gamma} \ , \ \lambda_{(N)}{}^3{}_\alpha = \lambda_{(N)3\alpha} \tag{2.70}$$

Let us next introduce kinematic variables $\varrho_{\alpha\beta}$, $\kappa_{(N)i\alpha}$ and $\gamma_{(N)i}$ through the definitions

$$\varrho_{\alpha\beta} = \frac{1}{2}\left(a_{\alpha\beta} - A_{\alpha\beta}\right), \tag{2.71}$$

$$\kappa_{(N)i\alpha} = \lambda_{(N)i\alpha} - \Lambda_{(N)i\alpha}, \tag{2.72}$$

$$\gamma_{(N)i} = d_{(N)i} - D_{(N)i}, \tag{2.73}$$

where $A_{\alpha\beta}$, $\Lambda_{(N)i\alpha}$ and $D_{(N)i}$ are the values of $a_{\alpha\beta}$, $\lambda_{(N)i\alpha}$ and $d_{(N)i}$ respectively, in the initial (reference) configuration. In preparation for certain results derived later it is convenient to record the following expressions

$$\mathbf{d}_{(N)} \cdot \mathbf{d}_{(M)} = d_{(N)}{}^\gamma d_{(M)\gamma} + d_{(N)}{}^3 d_{(M)3}, \tag{2.74}$$

$$\mathbf{d}_{(N)} \cdot \mathbf{d}_{(M),\alpha} = d_{(N)}{}^\gamma \lambda_{(M)\gamma\alpha} + d_{(N)}{}^3 \lambda_{(M)3\alpha}, \tag{2.75}$$

$$\mathbf{d}_{(N),\alpha} \cdot \mathbf{d}_{(M),\beta} = \lambda_{(N)}{}^\gamma_\alpha \lambda_{(M)\gamma\beta} + \lambda_{(N)}{}^3_\alpha \lambda_{(M)3\beta}. \tag{2.76}$$

It should be noted that analogous expressions to (2.74)–(2.76) in the initial configuration may be written down. These are not stated here but the reader is referred to Naghdi (1972) for a full presentation of the appropriate results.

For later use we now calculate the components of g_{ij} in terms of the variables in (2.67) to (2.68), using (2.65) and (2.66), and we obtain

$$\begin{aligned} g_{\alpha\beta} &= a_{\alpha\beta} + \xi\left(\mathbf{a}_\beta \cdot \frac{\partial \mathbf{d}_{(1)}}{\partial \upsilon^\alpha} + \mathbf{a}_\alpha \cdot \frac{\partial \mathbf{d}_{(1)}}{\partial \upsilon^\beta}\right) \\ &+ \sum_{P=2}^{\infty} \xi^P \left[\mathbf{a}_\beta \cdot \frac{\partial \mathbf{d}_{(P)}}{\partial \upsilon^\alpha} + \mathbf{a}_\alpha \cdot \frac{\partial \mathbf{d}_{(P)}}{\partial \upsilon^\beta} + \sum_{M=1}^{P-1}\left(\frac{\partial \mathbf{d}_{(P-M)}}{\partial \upsilon^\alpha} \cdot \frac{\partial \mathbf{d}_{(M)}}{\partial \upsilon^\beta}\right)\right], \quad (2.77) \\ g_{\alpha 3} &= d_{(1)\alpha} + \sum_{P=2}^{\infty} \xi^{P-1}\left[P d_{(P)\alpha} + \sum_{M=1}^{P-1}\left(M \frac{\partial \mathbf{d}_{(P-M)}}{\partial \upsilon^\alpha} \cdot \mathbf{d}_{(M)}\right)\right], \quad (2.78) \end{aligned}$$

and

$$g_{33} = \sum_{P=2}^{\infty} \xi^{P-2}\left[\sum_{M=1}^{P-1}\left((P-M)M\mathbf{d}_{(P-M)} \cdot \mathbf{d}_{(M)}\right)\right]. \quad (2.79)$$

The components of G_{ij}, the values of g_{ij} in the initial (reference) configuration, can be calculated similarly.

Now recalling from Green and Zerna (1968), the result

$$\gamma^*_{ij} = \frac{1}{2}\left(\mathbf{g}_i \cdot \mathbf{g}_j - \mathbf{G}_i \cdot \mathbf{G}_j\right) = \frac{1}{2}\left(g_{ij} - G_{ij}\right), \quad (2.80)$$

where γ^*_{ij} are the covariant components of the usual three-dimensional strain tensor, and substituting for g_{ij} and G_{ij} using (2.77) to (2.79) and the corresponding expressions for G_{ij}, we obtain

$$\begin{aligned} 2\gamma^*_{\alpha\beta} &= 2\varrho_{\alpha\beta} + \xi\left(\kappa_{(1)\alpha\beta} + \kappa_{(1)\beta\alpha}\right) \\ &+ \sum_{P=2}^{\infty}\left[\kappa_{(P)\alpha\beta} + \kappa_{(P)\beta\alpha} + \sum_{M=1}^{P-1}\left(\mathbf{d}_{(P-M),\alpha} \cdot \mathbf{d}_{(M),\beta} - \mathbf{D}_{(P-M),\alpha} \cdot \mathbf{D}_{(M),\beta}\right)\right], \quad (2.81) \\ 2\gamma^*_{\alpha 3} &= \gamma_{(1)\alpha} \\ &+ \sum_{P=2}^{\infty} \xi^{P-1}\left[P\gamma_{(P)\alpha} + \sum_{M=1}^{P-1} M\left(\mathbf{d}_{(P-M),\alpha} \cdot \mathbf{d}_{(M)} - \mathbf{D}_{(P-M),\alpha} \cdot \mathbf{D}_{(M)}\right)\right], \quad (2.82) \end{aligned}$$

and

$$2\gamma^*_{33} = \sum_{P=2}^{\infty} \xi^{P-2}\left[\sum_{M=1}^{P-1}(P-M)M\left(\mathbf{d}_{(P-M)} \cdot \mathbf{d}_{(M)} - \mathbf{D}_{(P-M)} \cdot \mathbf{D}_{(M)}\right)\right]. \quad (2.83)$$

For future reference we expand the series (2.81) to (2.83) in order to show the dependence of γ^*_{ij} on $\mathbf{d}_{(1)}$, $\mathbf{d}_{(1)\alpha}$ and their reference values, and obtain

$$\begin{aligned} 2\gamma^*_{\alpha\beta} &= 2\varrho_{\alpha\beta} + \xi\left(\kappa_{(1)\alpha\beta} + \kappa_{(1)\beta\alpha}\right) \\ &+ \xi^2\left[\left(\lambda_{(1)}{}^{\vartheta}{}_{\alpha}\lambda_{(1)\vartheta\beta} - \Lambda_{(1)}{}^{\vartheta}{}_{\alpha}\Lambda_{(1)\vartheta\beta}\right) + \left(\lambda_{(1)}{}^{3}{}_{\alpha}\lambda_{(1)3\beta} - \Lambda_{(1)}{}^{3}{}_{\alpha}\Lambda_{(1)3\beta}\right)\right] + \cdots, \quad (2.84) \\ 2\gamma^*_{\alpha 3} &= \gamma_{(1)\alpha} \\ &+ \xi\left[\left(d_{(1)}{}^{\vartheta}\lambda_{(1)\vartheta\alpha} - D_{(1)}{}^{\vartheta}\Lambda_{(1)\vartheta\alpha}\right) + \left(d_{(1)}{}^{3}\lambda_{(1)3\alpha} - D_{(1)}{}^{3}\Lambda_{(1)3\alpha}\right)\right] + \cdots, \quad (2.85) \end{aligned}$$

and

$$2\gamma^*_{33} = \left(d_{(1)}{}^{\vartheta}d_{(1)\vartheta} - D_{(1)}{}^{\vartheta}D_{(1)\vartheta}\right) + \left(\left(d_{(1)3}\right)^2 - \left(D_{(1)3}\right)^2\right) + \cdots; \quad (2.86)$$

where all terms in (2.84)–(2.86) which do not appear explicitly involve the quantities $\mathbf{d}_{(N)}$, $\mathbf{D}_{(N)}$, $N \geq 2$.

Before completing this section we note that the variables used to derive the kinematic results in this section, namely $d_{(N)i}$, $\lambda_{(N)i\alpha}$ and those on the right-hand side of equations (2.71) to (2.73), all satisfy the invariance condition in that they remain unaltered under superposed rigid body rotation, and hence they are suitable for use in developing a sensible mathematical theory.

2.6 Basic Field Equations for Shells and Plates.

In this section we shall briefly derive the field equations for a shell-like body, leaving most of the mathematical manipulation to the reader. Alternatively, the reader can find the full derivation with explanations in Naghdi (1972) §11 and §12.

We must first present some preliminary results. Suppose dv and $d\sigma$ are an element of the volume of the body $\mathcal{B}$ and an element of the area of the surface $\xi = 0$, respectively, given by

$$dv = (\mathbf{g}_1 \times \mathbf{g}_2 \cdot \mathbf{g}_3)\, dv^1 dv^2 dv^3 = g^{\frac{1}{2}} dv^1 dv^2 dv^3, \quad (2.87)$$

$$d\sigma = (\mathbf{a}_1 \times \mathbf{a}_2 \cdot \mathbf{a}_3)\, dv^1 dv^2 = a^{\frac{1}{2}} dv^1 dv^2. \tag{2.88}$$

Let $\mathbf{f}^* = \mathbf{f}^*(v^\alpha, \xi, t)$, a vector field per unit mass defined for points in the body $\mathcal{B}$, represent the body force at time t, and let

$$\mathbf{n} = n_i \mathbf{g}^i = n^i \mathbf{g}_i, \tag{2.89}$$

be the outward unit normal vector on the boundary $\partial\mathcal{B}$ at time t. Suppose the vector field $\mathbf{t} = \mathbf{t}(v^\alpha, \xi, t; \mathbf{n})$ is the contact force (or the stress vector) defined for every point on the boundary $\partial\mathcal{B}$ at time t.

Under suitable continuity assumptions the principles of conservation of linear momentum and the conservation of angular momentum for non-polar media imply:

(i) That there exists a tensor field $\sigma^{ij} = \sigma^{ij}(v^\alpha, \xi, t)$ such that

$$\mathbf{t} = \frac{\mathbf{T}^i n_i}{g^{\frac{1}{2}}} = \sigma^{ij} n_i \mathbf{g}_j \quad , \quad \mathbf{T}^i = g^{\frac{1}{2}} \sigma^{ij} \mathbf{g}_j = g^{\frac{1}{2}} \sigma^i_j \mathbf{g}^j. \tag{2.90}$$

(ii) That the Cauchy equations of motion hold and hence

$$\mathbf{T}^i{}_{,i} + \rho^* \mathbf{f}^* g^{\frac{1}{2}} = \rho^* \dot{\mathbf{v}}^* g^{\frac{1}{2}} \quad , \quad \mathbf{g}_i \times \mathbf{T}^i = 0. \tag{2.91}$$

It is easily shown from $(2.90)_{(ii)}$ and $(2.91)_{(ii)}$ that the stress tensor σ^{ij} is symmetric i.e.

$$\sigma^{ij} = \sigma^{ji}. \tag{2.92}$$

We observe that if $\mathbf{n}$ is the outward unit normal to $\partial\mathcal{B}$ then $\mathbf{t}(v^\alpha, \xi, t; \mathbf{n})$ reduces to a function of position for points on $\partial\mathcal{B}$, hence

$$\mathbf{t} = \bar{\mathbf{t}}(v^\alpha, \xi, t), \tag{2.93}$$

where $\bar{\mathbf{t}}$ is the surface traction prescribed on the boundary $\partial\mathcal{B}$.

The outward unit normals to the surfaces defined through (2.55) are;

$$\begin{aligned} \mathbf{n} &= f_{(\alpha)}^{-1}\left(\alpha_{,1}\mathbf{g}^1 + \alpha_{,2}\mathbf{g}^2 - \mathbf{g}^3\right) \text{ on } \xi = \alpha\left(v^\lambda\right), \\ \mathbf{n} &= f_{(\beta)}^{-1}\left(-\beta_{,1}\mathbf{g}^1 - \beta_{,2}\mathbf{g}^2 + \mathbf{g}^3\right) \text{ on } \xi = \beta\left(v^\lambda\right), \end{aligned} \tag{2.94}$$

where

$$f_{(\alpha)} = \left[(\alpha_{,1})^2 g^{11} + (\alpha_{,2})^2 g^{22} + g^{33} + 2\left(\alpha_{,1}\alpha_{,2}\, g^{12} - \alpha_{,1}\, g^{13} - \alpha_{,2}\, g^{23}\right)\right]^{\frac{1}{2}} \tag{2.95}$$

with an analogous expression to (2.96) for $f_{(\beta)}$. The area elements on the two bounding surfaces are given by

$$\begin{aligned} da &= f_{(\alpha)} g^{\frac{1}{2}} dv^1 dv^2 \text{ on } \xi = \alpha\left(v^\lambda\right), \\ da &= f_{(\beta)} g^{\frac{1}{2}} dv^1 dv^2 \text{ on } \xi = \beta\left(v^\lambda\right). \end{aligned} \tag{2.96}$$

In all of the expressions above, (2.94)–(2.96), $\mathbf{g}^i$, g^{ij}, g are evaluated on the surfaces $\xi = \alpha\left(v^\lambda\right)$ or $\xi = \beta\left(v^\lambda\right)$. It should be noted that if α and β are constants (as in the case of the flat plate) then both expressions in (2.95) reduce to

$$da = \left(g\, g^{33}\right)^{\frac{1}{2}} dv^1 dv^2. \tag{2.97}$$

We define a two-dimensional body force by

$$\begin{aligned} \rho \mathbf{f} a^{\frac{1}{2}} &= \int_\alpha^\beta \rho^* \mathbf{f}^* g^{\frac{1}{2}} d\xi + \left[\bar{\mathbf{t}} g^{\frac{1}{2}} f_{(\beta)}\right]_{\xi=\beta} + \left[\bar{\mathbf{t}} g^{\frac{1}{2}} f_{(\alpha)}\right]_{\xi=\alpha}, \\ &= \int_\alpha^\beta \rho^* \mathbf{f}^* g^{\frac{1}{2}} d\xi \\ &+ \left[-\beta_{,1}\mathbf{T}^1 - \beta_{,2}\mathbf{T}^2 + \mathbf{T}^3\right]_{\xi=\beta} - \left[-\alpha_{,1}\mathbf{T}^1 - \alpha_{,2}\mathbf{T}^2 + \mathbf{T}^3\right]_{\xi=\alpha}, \end{aligned} \tag{2.98}$$

and two-dimensional body moments by

$$\begin{aligned} \rho \mathbf{l}^{(N)} a^{\frac{1}{2}} &= \int_\alpha^\beta \rho^* \mathbf{f}^* g^{\frac{1}{2}} \xi^N d\xi + \left[\bar{\mathbf{t}} \xi^N g^{\frac{1}{2}} f_{(\beta)}\right]_{\xi=\beta} + \left[\bar{\mathbf{t}} \xi^N g^{\frac{1}{2}} f_{(\alpha)}\right]_{\xi=\alpha}, \\ &= \int_\alpha^\beta \rho^* \mathbf{f}^* g^{\frac{1}{2}} \xi^N d\xi \\ &+ \left[\xi^N\left(-\beta_{,1}\mathbf{T}^1 - \beta_{,2}\mathbf{T}^2 + \mathbf{T}^3\right)\right]_{\xi=\beta} - \left[\xi^N\left(-\alpha_{,1}\mathbf{T}^1 - \alpha_{,2}\mathbf{T}^2 + \mathbf{T}^3\right)\right]_{\xi=\alpha}, \end{aligned} \tag{2.99}$$

where we have defined the mass density per unit area of a surface ρ through

$$\rho a^{\frac{1}{2}} = \int_{\alpha}^{\beta} k d\xi \quad \text{and} \quad \rho k^{(N)} a^{\frac{1}{2}} = \int_{\alpha}^{\beta} \xi^N k d\xi, \tag{2.100}$$

where

$$k = k(v^{\alpha}, \xi) = \rho^* g^{\frac{1}{2}} = \rho_o^* G^{\frac{1}{2}}. \tag{2.101}$$

Finally let us define N^{α} and $\mathrm{M}^{(N)\alpha}$, the resultant force vector and resultant couple vector of order N $(N = 1, 2, \ldots)$ by

$$\mathrm{N}^{\alpha} a^{\frac{1}{2}} = \int_{\alpha}^{\beta} \mathrm{T}^{\alpha} d\xi \ , \ \mathrm{M}^{(N)\alpha} a^{\frac{1}{2}} = \int_{\alpha}^{\beta} \xi^N \mathrm{T}^{\alpha} d\xi. \tag{2.102}$$

We now recall the conservation of energy for non-polar media over any part of the body $\mathcal{P}$ in the form

$$\frac{d}{dt} \int_{\mathcal{P}} \left(\frac{1}{2} \mathrm{v}^* \cdot \mathrm{v}^* \right) \rho^* dv = \int_{\mathcal{P}} \mathrm{f}^* \cdot \mathrm{v}^* \rho^* dv + \int_{\partial \mathcal{P}} \mathrm{t} \cdot \mathrm{v}^* da. \tag{2.103}$$

The left-hand side of (2.103) denotes the kinetic energy of the body and $\mathrm{t} \cdot \mathrm{v}^*$ and $\mathrm{f} \cdot \mathrm{v}^*$, are the rate of work by surface forces and the rate of work by body forces respectively. Equation (2.103) describes the conservation of the mechanical energy only with all thermodynamic terms omitted. Naghdi (1972) derives field equations for the full thermo-mechanical problem, but in our work we are considering purely isothermal situations.

It can be shown that the (three-dimensional) balance of energy, equation (2.103), can be written in terms of the two-dimensional variables as

$$\frac{d}{dt} \int_{\mathcal{P}} \rho \left(\frac{1}{2} \mathrm{v} \cdot \mathrm{v} + \sum_{N=2}^{\infty} k^{(N)} \mathrm{w}_{(N)} \cdot \mathrm{v} + \frac{1}{2} \sum_{M,N=1}^{\infty} k^{(M+N)} \mathrm{w}_{(M)} \cdot \mathrm{w}_{(N)} \right) d\sigma$$

$$= \int_{\mathcal{P}} \rho \left(\mathrm{f} \cdot \mathrm{v} + \sum_{N=1}^{\infty} \mathrm{l}^{(N)} \cdot \mathrm{w}_{(N)} \right) d\sigma + \int_{\partial \mathcal{P}} \left(\mathrm{N} \cdot \mathrm{v} + \sum_{N=1}^{\infty} \mathrm{M}^{(N)} \cdot \mathrm{w}_{(N)} \right) ds, \tag{2.104}$$

where $\partial\mathcal{P}$ is the boundary of $\mathcal{P}$, part of the two-dimensional reference surface $\xi = 0$ in the present configuration.

The local balance of energy can be written as

$$\sigma^{ij}\dot{\gamma}^{*}_{ij} = 0, \tag{2.105}$$

or, in the alternative form

$$\mathbf{T}^{i} \cdot \mathbf{v}^{*}{}_{,i} = 0. \tag{2.106}$$

Let $\phi = \phi(v^{i})$ be a scalar function, then multiplying (2.106) by $g^{-\frac{1}{2}}\phi$ and integrating over $\mathcal{P}^{*}$ gives

$$\int_{\mathcal{P}^{*}} g^{-\frac{1}{2}} \mathbf{T}^{i} \cdot \mathbf{v}^{*}{}_{,i}\, \phi dv = 0, \tag{2.107}$$

which can be expressed as

$$\int_{\mathcal{P}^{*}} g^{-\frac{1}{2}} \left(\left(\mathbf{T}^{i} \cdot \mathbf{v}^{*}\phi \right)_{,i} - \mathbf{T}^{i}{}_{,i} \cdot \mathbf{v}^{*}\phi - \mathbf{T}^{i} \cdot \mathbf{v}^{*}\phi_{,i} \right) dv = 0, \tag{2.108}$$

which implies

$$\Rightarrow \int_{\partial\mathcal{P}^{*}} (\mathbf{t} \cdot \mathbf{v}^{*})\, \phi da + \int_{\mathcal{P}^{*}} g^{-\frac{1}{2}} \left(-\mathbf{T}^{i}{}_{,i} \cdot \mathbf{v}^{*}\phi - \mathbf{T}^{i} \cdot \mathbf{v}^{*}\phi_{,i} \right) dv = 0. \tag{2.109}$$

After some manipulation and using $(2.91)_{(\mathrm{i})}$ we obtain

$$\frac{d}{dt}\int_{\mathcal{P}^{*}} \frac{1}{2}\mathbf{v}^{*} \cdot \mathbf{v}^{*}\rho^{*}\phi dv = \int_{\mathcal{P}^{*}} \left(\mathbf{f}^{*} \cdot \mathbf{v}^{*}\rho^{*}\phi - g^{-\frac{1}{2}}\mathbf{T}^{i} \cdot \mathbf{v}^{*}\phi_{,i} \right) dv + \int_{\partial\mathcal{P}^{*}} \mathbf{t} \cdot \mathbf{v}^{*}\phi\, da. \tag{2.110}$$

In particular if we use the specific substitution $\phi = \xi^{n}$ $(n = 0, 1, \ldots)$ we can deduce from (2.110) the result

$$\begin{aligned} \frac{d}{dt}\int_{\mathcal{P}} \rho \left(\frac{1}{2}k^{(n)}\mathbf{v} \cdot \mathbf{v} + \sum_{N=1}^{\infty} k^{(N+n)}\mathbf{w}_{(N)} \cdot \mathbf{v} + \frac{1}{2}\sum_{M,N=1}^{\infty} k^{(M+N+n)}\mathbf{w}_{(M)} \cdot \mathbf{w}_{(N)} \right) d\sigma = \\ \int_{\mathcal{P}} \left[\left(\mathbf{l}^{(n)} \cdot \mathbf{v} + \sum_{N=1}^{\infty} \mathbf{l}^{(N+n)} \cdot \mathbf{w}_{(N)} \right) - \mathbf{m}^{(n)} \cdot \mathbf{v} - \sum_{N=1}^{\infty} \frac{n}{N+n}\mathbf{m}^{(N+n)} \cdot \mathbf{w}_{(N)} \right] d\sigma \\ + \int_{\partial\mathcal{P}} \left[\mathbf{M}^{(n)} \cdot \mathbf{v} + \sum_{N=1}^{\infty} \mathbf{M}^{(N+n)} \cdot \mathbf{w}_{(N)} \right] ds, \end{aligned} \tag{2.111}$$

where we have introduced

$$\mathrm{m}^{(N)}a^{\frac{1}{2}} = N\int_{\alpha}^{\beta}\xi^{N-1}\mathrm{T}^{3}d\xi \ , \ (N \geq 0)\,. \tag{2.112}$$

Under suitable continuity assumptions, (2.111) can be reduced to

$$\begin{aligned}&\left(\mathrm{M}^{(n)\alpha}{}_{|\alpha} + \rho\bar{\mathrm{l}}^{(n)} - \mathrm{m}^{(n)}\right)\cdot\mathrm{v} + \mathrm{M}^{(n)\alpha}\cdot\mathrm{v}_{,\alpha}\\ &+ \sum_{N=1}^{\infty}\left(\mathrm{M}^{(N+n)\alpha}{}_{|\alpha} + \rho\bar{\mathrm{l}}^{(N+n)} - \frac{n}{N+n}\mathrm{m}^{(N+n)}\right)\cdot\mathrm{w}_{(N)}\\ &+ \sum_{N=2}^{\infty}\mathrm{M}^{(N+n)\alpha}\cdot\mathrm{w}_{(N)_{,\alpha}} = 0 \ , \ n = 0,1,\ldots\,,\end{aligned} \tag{2.113}$$

where we define

$$\begin{aligned}\bar{\mathrm{f}} = \bar{\mathrm{l}}^{(0)} &= \mathrm{f} - \dot{\mathrm{v}} - \sum_{N=1}^{\infty}k^{(N)}\dot{\mathrm{w}}_{(N)},\\ \bar{\mathrm{l}} = \bar{\mathrm{l}}^{(1)} &= \mathrm{l}^{(1)} - \sum_{M=1}^{\infty}k^{(M+1)}\dot{\mathrm{w}}_{(M)},\end{aligned} \tag{2.114}$$

and

$$\bar{\mathrm{l}}^{(N)} = \mathrm{l}^{(N)} - k^{(N)}\dot{\mathrm{v}} - \sum_{M=1}^{\infty}k^{(M+N)}\dot{\mathrm{w}}_{(M)} \ , (N \geq 2).$$

It is possible now to derive the field equations for plates or shells from the energy equations (2.113) together with invariance requirements under superposed rigid body motions. We assume that the quantities

$$\mathrm{T}_{i} \ , \ \sigma^{ij} \ , \ (\mathrm{f}^{*} - \dot{\mathrm{v}}^{*})\,, \tag{2.115}$$

are invariant under superposed rigid body motions, and so by the definitions introduced in this section it follows that

$$\mathrm{M}^{(n)\alpha} \ , \ \mathrm{m}^{(n)} \ , \ \bar{\mathrm{l}}^{(n)} \ , (n \geq 0)\,, \tag{2.116}$$

are also invariant under superposed rigid body motions.

For simple translational motion we have the transformation given by

$$\mathrm{v}^{*+} = \mathrm{v}^{*} + \mathrm{b} \tag{2.117}$$

and hence

$$\mathrm{v}^{+} = \mathrm{v} + \mathrm{b} \ , \ \mathrm{w}_{(N)}{}^{+} = \mathrm{w}_{(N)}. \tag{2.118}$$

Under a general superposed rigid body motion the energy equation (2.113) becomes

$$\begin{aligned}
&\left(\mathrm{M}^{(n)\alpha}{}^{+}{}_{|\alpha} + \rho\bar{\mathrm{I}}^{(n)+} - \mathrm{m}^{(n)+}\right) \cdot \mathrm{v}^{+} + \mathrm{M}^{(n)\alpha+} \cdot \mathrm{v}^{+}{}_{,\alpha} \\
&\quad + \sum_{N=1}^{\infty} \left(\mathrm{M}^{(N+n)\alpha}{}^{+}{}_{|\alpha} + \rho\bar{\mathrm{I}}^{(N+n)+} - \frac{n}{N+n}\mathrm{m}^{(N+n)+}\right) \cdot \mathrm{w}_{(N)}{}^{+} \\
&\quad + \sum_{N=2}^{\infty} \mathrm{M}^{(N+n)\alpha+} \cdot \mathrm{w}_{(n)}{}^{+}{}_{,\alpha} = 0.
\end{aligned} \tag{2.119}$$

Recalling that the variables in (2.116) are invariant under superposed rigid body motions and substituting (2.118) into the equation (2.119) and subtracting the resultant equation from the original energy equation (2.113) we obtain the condition that

$$\mathrm{M}^{(n)\alpha}{}_{|\alpha} + \rho\bar{\mathrm{I}}^{(n)} - \mathrm{m}^{(n)} = 0 \ , \ (n = 0, 1, \ldots), \tag{2.120}$$

and so the generalised energy equation (2.113) can be reduced to

$$\mathrm{M}^{(n)\alpha} \cdot \mathrm{v}_{,\alpha} + \sum_{N=1}^{\infty} \frac{N}{N+n}\mathrm{m}^{(N+n)} \cdot \mathrm{w}_{(N)} + \sum_{N=2}^{\infty} \mathrm{M}^{(N+n)\alpha} \cdot \mathrm{w}_{(N)_{,\alpha}} = 0. \tag{2.121}$$

If we assume next that the plate or shell undergoes a uniform rotation of the form

$$\mathrm{v}^{*+} = \mathrm{v}^{*} + \boldsymbol{\omega}_{\circ} \times \mathrm{p}, \tag{2.122}$$

then it follows that

$$\mathrm{v}^{+} = \mathrm{v} + \boldsymbol{\omega}_{\circ} \times \mathrm{r} \ , \ \mathrm{w}_{(N)}{}^{+} = \mathrm{w}_{(N)} + \boldsymbol{\omega}_{\circ} \times \mathrm{d}_{(N)}. \tag{2.123}$$

Substituting (2.123) into (2.121), recalling the list of invariant variables (2.116), subtracting equation (2.121) and then noting that $\omega_\circ$ is arbitrary, leads to the equation

$$\mathbf{M}^{(n)\alpha} \times \mathbf{a}_\alpha + \sum_{N=1}^{\infty} \left(\frac{N}{N+n} \mathbf{m}^{(N+n)} \times \mathbf{d}_{(N)} + \mathbf{M}^{(N+n)\alpha} \times \mathbf{d}_{(N),\alpha} \right) = 0. \qquad (2.124)$$

It should be observed that the equations of motion (2.120) can be obtained by direct integration of $(2.91)_{(i)}$, after multiplication by ξ^N and with use of definitions (2.98) to (2.99), (2.102) and (2.112), and hence the field equations result directly from the symmetry of the stress tensor σ^{ij}.

The quantities $\mathbf{M}^{(N)\alpha}$ and $\mathbf{m}^{(N)\alpha}$ transform as contravariant surface vectors and may be written in component form, referred to the base vectors $\mathbf{a}_i$, as

$$\mathbf{M}^{(N)\alpha} = M^{(N)\alpha i}\mathbf{a}_i \ , \ \mathbf{m}^{(N)} = m^{(N)i}\mathbf{a}_i. \qquad (2.125)$$

Similarly the variables in (2.114) can be expressed through

$$\bar{\mathbf{f}} = \bar{\mathbf{l}}_\circ = \bar{f}^i \mathbf{a}_i \ , \ \bar{\mathbf{l}}^{(n)} = \bar{l}^{(n)i}\mathbf{a}_i \ , \ (n \geq 1), \qquad (2.126)$$

and so using (2.125) and (2.126) we can express (2.120) in the component forms

$$N^{\alpha\beta}{}_{|\alpha} - b^\beta_\alpha N^{\alpha 3} + \rho \bar{f}^\beta = 0, \qquad (2.127)$$

$$N^{\alpha 3}{}_{|\alpha} + b_{\alpha\beta} N^{\alpha\beta} + \rho \bar{f}^3 = 0, \qquad (2.128)$$

$$M^{(N)\alpha\beta}{}_{|\alpha} - b^\beta_\alpha M^{(N)\alpha 3} + \rho \bar{l}^{(N)\beta} = m^{(N)\beta} \ , \ (N = 1, 2, \ldots), \qquad (2.129)$$

$$M^{(N)\alpha 3}{}_{|\alpha} + b_{\alpha\beta} M^{(N)\alpha\beta} + \rho \bar{l}^{(N)3} = m^{(N)3} \ , \ (N = 1, 2, \ldots), \qquad (2.130)$$

where we have used the notation $N^{\alpha\beta} = M^{(0)\alpha\beta}$ and $N^{\alpha 3} = M^{(0)\alpha 3}$.

In a similar manner the component forms of equations (2.124) can be shown to be

$$N'^{\beta\alpha} = N'^{\alpha\beta} = N^{\alpha\beta} - \sum_{N=1}^{\infty} \left(m^{(N)\alpha} d_{(N)}{}^\beta + M^{(N)\gamma\alpha} \lambda_{(N)}{}^\beta{}_\gamma \right) \qquad (2.131)$$

$$N^{\alpha 3} + \sum_{N=1}^{\infty} \left(m^{(N)3} d_{(N)}{}^{\alpha} - m^{(N)\alpha} d_{(N)}{}^{3} \right) + \sum_{N=1}^{\infty} \left(M^{(N)\gamma 3} \lambda_{(N)}{}^{\alpha}{}_{\gamma} - M^{(N)\gamma\alpha} \lambda_{(N)}{}^{3}{}_{\gamma} \right) = 0, \tag{2.132}$$

and

$$M'^{(n)\alpha\beta} = M'^{(n)\beta\alpha} = M^{(n)\alpha\beta} - \sum_{N=1}^{\infty} \left(\frac{N}{N+n} m^{(N+n)\alpha} d_{(N)}{}^{\beta} + M^{(N+n)\gamma\alpha} \lambda_{(N)}{}^{\beta}{}_{\gamma} \right), (n = 1, 2, \ldots), \tag{2.133}$$

$$M^{(n)\alpha 3} + \sum_{N=1}^{\infty} \frac{N}{N+n} \left(m^{(N+n)3} d_{(N)}{}^{\alpha} - m^{(N+n)\alpha} d_{(N)}{}^{3} \right) + \sum_{N=1}^{\infty} \left(M^{(N+n)\gamma 3} \lambda_{(N)}{}^{\alpha}{}_{\gamma} - M^{(N+n)\gamma\alpha} \lambda_{(N)}{}^{3}{}_{\gamma} \right) = 0, (n = 1, 2 \ldots), \tag{2.134}$$

where we have defined symmetric tensors $N'^{\alpha\beta}$ and $M'^{(n)\alpha\beta}$ in terms of asymmetric tensor components.

Next we wish to proceed with the linearization of the general field equations and in order to do this we need to expand all of the terms appearing in the field equations as power series in a small parameter ϵ. Thus we write

$$\mathbf{r} = \mathbf{R} + \epsilon \mathbf{u} + O\left(\epsilon^2\right) \quad , \quad \mathbf{u} = u^i A_i, \tag{2.135}$$

which implies

$$\mathbf{a}_{\alpha} = \mathbf{A}_{\alpha} + \epsilon \mathbf{u}_{,\alpha} + O\left(\epsilon^2\right), \tag{2.136}$$

and leads to the results

$$\begin{aligned} a_{\alpha\beta} &= A_{\alpha\beta} + O(\epsilon), \\ b_{\alpha\beta} &= B_{\alpha\beta} + O(\epsilon). \end{aligned} \tag{2.137}$$

We assume that in the initial configuration the continuum is stress-free. Consequently in the complete three-dimensional linearized theory the stress tensor σ^{ij} and its derivatives

will be $O(\epsilon)$. It follows from the definitions (2.102) and (2.112) that the vector fields $\mathbf{N}^{\alpha}$, $\mathbf{M}^{(N)\alpha}$, $\mathbf{m}^{(N)}$ $(N \geq 1)$ and their tensor components as well as their derivatives with respect to the surface co-ordinates are all $O(\epsilon)$. Thus, we define new variables through

$$\tilde{N}^{\alpha i} = \epsilon N^{\alpha i} \ , \ \tilde{M}^{(N)\alpha i} = \epsilon M^{(N)\alpha i} \ , \ \tilde{m}^{(N)i} = \epsilon m^{(N)i}. \tag{2.138}$$

Consistent with the above assumptions we write

$$\tilde{f}_i = \epsilon \bar{F}_i + O(\epsilon) \ , \ \tilde{l}_i = \epsilon \bar{L}_i + O(\epsilon). \tag{2.139}$$

On substituting (2.137)–(2.139) into (2.127)–(2.130), the relevant linearized field equations become

$$\tilde{N}^{\alpha\beta}{}_{|\alpha} - B^{\beta}_{\alpha}\tilde{N}^{\alpha 3} + \rho_{\circ}\tilde{F}^{\beta} = 0, \tag{2.140}$$

$$\tilde{N}^{\alpha 3}{}_{|\alpha} + B_{\alpha\beta}\tilde{N}^{\alpha\beta} + \rho_{\circ}\tilde{F}^{3} = 0, \tag{2.141}$$

$$\tilde{M}^{(N)\alpha\beta}{}_{|\alpha} - B^{\beta}_{\alpha}\tilde{M}^{(N)\alpha 3} + \rho_{\circ}\tilde{L}^{(N)\beta} = \tilde{m}^{(N)\beta}, \tag{2.142}$$

$$\tilde{M}^{(N)\alpha 3}{}_{|\alpha} + B_{\alpha\beta}\tilde{M}^{(N)\alpha\beta} + \rho_{\circ}\tilde{L}^{(N)3} = \tilde{m}^{(N)3}. \tag{2.143}$$

where we have retained only leading order terms in ϵ.

For small deformations of the shell or plate we can also expand the components of the directors as power series in ϵ through

$$d_{(N)i} = D_{(N)i} + O(\epsilon), \tag{2.144}$$

where $D_{(N)i}$ are the values of $d_{(N)i}$ in the initial configuration. Using (2.144) we can now linearize the equations (2.131) to (2.134) obtaining

$$\tilde{N}'^{\alpha\beta} = \tilde{N}'^{\beta\alpha} = \tilde{N}^{\alpha\beta} - \sum_{N=1}^{\infty} \tilde{m}^{(N)\alpha} D_{(N)}{}^{\beta}, \tag{2.145}$$

$$\tilde{N}^{\alpha 3} + \sum_{N=1}^{\infty} \left(\tilde{m}^{(N)3} D_{(N)}{}^{\alpha} - \tilde{m}^{(N)\alpha} D_{(N)}{}^{3} \right) = 0, \tag{2.146}$$

$$\tilde{M}'^{(n)\alpha\beta} = \tilde{M}'^{(n)\beta\alpha} = \tilde{M}^{(n)\alpha\beta} - \sum_{N=1}^{\infty} \left(\frac{N}{N+n} \tilde{m}^{(N+n)\alpha} D_{(N)}{}^{\beta} \right), \tag{2.147}$$

$$\tilde{M}^{(n)\alpha 3} + \sum_{N=1}^{\infty} \left(\frac{N}{N+n} \tilde{m}^{(N+n)3} D_{(N)}{}^{\alpha} - \tilde{m}^{(N+n)\alpha} D_{(N)}{}^{3} \right) = 0. \tag{2.148}$$

In subsequent chapters of this thesis we will use the general linearized field equations which have been derived above.

Chapter 3

MATHEMATICAL MODEL OF A PLATE CONTAINING A WELD WITH INTERFACES NORMAL TO THE SURFACE OF THE PLATE

In this chapter we shall model the creep of an initially flat plate containing a weld region. For a ferritic material the weldment consists of four main regions, namely the parent material, low temperature heat affected zone or type IV region, the high temperature heat affected zone (HAZ) and the weld metal. Each of the regions has markedly different material properties , but these properties can be assumed to be constant in each of the respective zones. In this chapter we assume that each region is joined to the next by a plane interface normal to the central surface of the plate. The plate is subjected to constant uniaxial end loading. We wish to model the time to rupture and position of rupture of the specimen, and shall use the Cosserat theory of plates developed in chapter 2.

By using different welding techniques and heat treatments it is possible to vary the widths and creep strengths of the different zones, and so in our results we will investigate the changes in rupture time and position of rupture due to variations in the material parameters and zone widths. After the welding process has been completed there are normally residual stresses left in the weld. With correct post-weld heat treatment, however, these stresses can be eliminated and, hence, we shall ignore the presence of such stresses in our model.

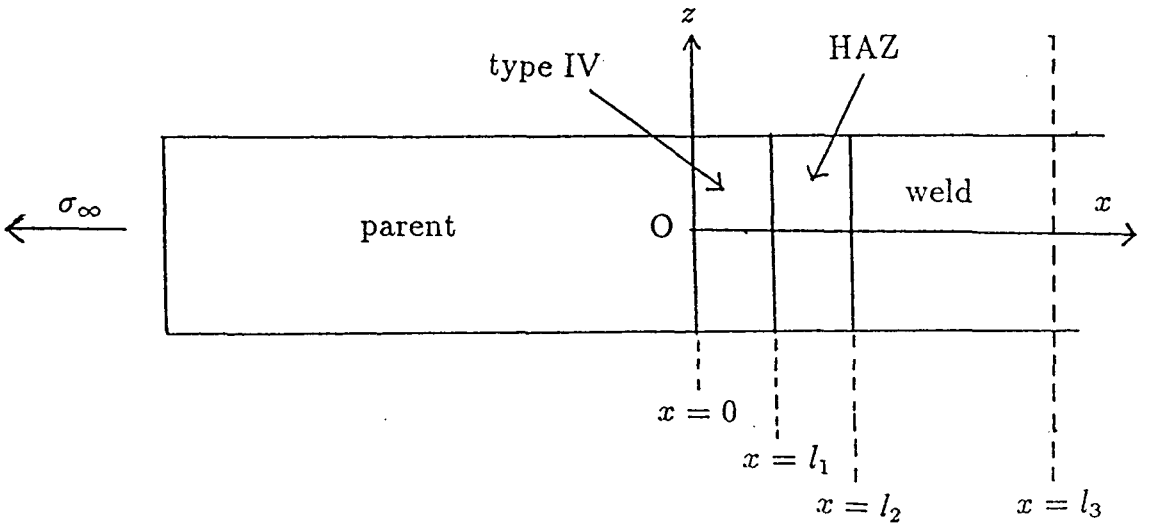

Figure 3.1: Diagram of a butt weld containing 4 zones.

3.1 Kinematics of the Plate.

In this section we follow closely the work of Hawkes (1989) and use the model for creep of a plate that proceeds directly from the three-dimensional constitutive equations.

In the model we use the Cartesian co-ordinates (x, y, z) defined as shown in Figure (3.1). The mid-surface of the plate $z = 0$ can now be identified with the Cosserat reference surface $\xi = 0$. To produce a simple model we shall only introduce a single director associated with each point of the surface, this director is initially assumed to be normal to the surface $z = 0$. We would expect that this model will be best when considering thin plates, but further comments will be made about this later in the thesis. Within this chapter we assume, therefore, that

$$\mathbf{d}_{(N)} \equiv \mathbf{D}_{(N)} \equiv 0 \ , \ N \geq 2. \tag{3.1}$$

Since we are now dealing with a single director we can write

$$\mathbf{d}_{(1)} = \mathbf{d} = (d_1, d_2, d_3)\,, \tag{3.2}$$

$$\mathbf{D}_{(1)} = \mathbf{D} = (0, 0, 1). \tag{3.3}$$

We can simplify the model further by considering only an infinite plate so that, by symmetry, there will be no y-dependence in the problem, that is

$$\frac{\partial}{\partial y} \equiv 0. \tag{3.4}$$

To specify the three-dimensional strain γ^*_{ij}, a displacement vector $\mathbf{u}(x,t)$ and a director $\delta(x,t)$ are associated with each point of the central surface of the plate, such that the three-dimensional displacement field $\mathbf{u}^*(x,z,t)$ is approximated by

$$\mathbf{u}^*(x,z,t) = \mathbf{u}(x,t) + z\boldsymbol{\delta}(x,t). \tag{3.5}$$

We also assume infinitesimal displacements, given by

$$\mathbf{p} = \mathbf{P} + \epsilon\mathbf{u}^* \quad , \quad \mathbf{u}^* = u^{*i}\mathbf{A}_i, \tag{3.6}$$

and infinitesimal director displacements

$$\mathbf{d} = \mathbf{D} + \epsilon\boldsymbol{\delta} \quad , \quad \boldsymbol{\delta} = \delta^i\mathbf{A}_i, \tag{3.7}$$

where $\mathbf{A}_i$ represents the initial value of the base vectors $\mathbf{a}_i$ associated with the reference surface $\xi = 0$.

Using the kinematic expressions defined by (2.71)–(2.83), in conjunction with equations (3.5) to (3.7), we can show that the linearized expressions for the three-dimensional strain tensor of the initially flat plate are

$$\gamma^*_{\alpha\beta} = \epsilon\left[\frac{1}{2}\left(u_{\beta,\alpha} + u_{\alpha,\beta}\right) + \frac{1}{2}z\left(\delta_{\beta,\alpha} + \delta_{\alpha,\beta}\right)\right] + O\left(\epsilon^2\right), \tag{3.8}$$

$$\gamma^*_{\alpha 3} = \gamma^*_{3\alpha} = \epsilon\left[\frac{1}{2}\delta_\alpha + \frac{1}{2}z\delta_{3,\alpha}\right] + O\left(\epsilon^2\right), \tag{3.9}$$

$$\gamma^*_{33} = \epsilon\delta_3 + O\left(\epsilon^2\right). \tag{3.10}$$

We can simplify our variables further by noting that for the case of initially flat plates, the linearized kinematic variables separate into two groups, namely

$$\begin{aligned} E &= \{u_\alpha, \delta_3, \varrho_{\alpha\beta}, \gamma_3, \kappa_{\alpha 3}\}, \\ F &= \{u_3, \delta_\alpha, \kappa_{\alpha\beta}, \gamma_\alpha\}. \end{aligned} \tag{3.11}$$

The displacements u_α, δ_3 in set E characterize the extensional motion of the plate, whereas u_3 and δ_α in set F characterize the flexural motion of the plate. In this chapter we wish to model an initially flat plate under uniaxial tension and since there will then be no bending of the plate we can set all flexural variables identically equal to zero.

Furthermore, taking the leading order term of each expression in equations (3.8) to (3.10) and setting $\epsilon = 1$, with no loss of generality, and then differentiating with respect to time, we obtain the following expressions for the linearized strain-rates of the initially flat plate under simple uniaxial tension, in terms of variables associated with the motion of the Cosserat surface $z = 0$:

$$\dot{\gamma}^*_{\alpha\beta} = \varrho_{\alpha\beta,t}, \tag{3.12}$$

$$\dot{\gamma}^*_{\alpha 3} = \frac{1}{2} z \delta_{3,\alpha t}, \tag{3.13}$$

$$\dot{\gamma}^*_{33} = \delta_{3,t}. \tag{3.14}$$

3.2 Stress Equations for the Plate.

In our model we assume that the three-dimensional stress tensor can be approximated by truncated power series of the form

$$\begin{aligned} \sigma_{\alpha\beta} &= a_{\alpha\beta} + z b_{\alpha\beta} + O\left(z^2\right), \\ \sigma_{\alpha 3} &= a_{\alpha 3} + z b_{\alpha 3} + O\left(z^2\right), \\ \sigma_{33} &= a_{33} + O\left(z\right). \end{aligned} \tag{3.15}$$

It is possible to include higher order powers of z in the above expressions, but this would also require us to include extra directors in the general theory leading to a more complicated model. Hawkes (1989) has found solutions using a three-director model for a simpler weldment under uniaxial tension, but his results are little different from those found using his simpler single director model.

In the general theory two-dimensional 'generalised' forces and moments are defined for initially flat plates by

$$\begin{aligned} N_{\alpha\beta} &= \int_{-\frac{h}{2}}^{\frac{h}{2}} \sigma_{\alpha\beta}\, dz \quad , \quad M_{(\alpha\beta)} = \int_{-\frac{h}{2}}^{\frac{h}{2}} \sigma_{\alpha\beta}\, z\, dz, \\ m_{\alpha} &= \int_{-\frac{h}{2}}^{\frac{h}{2}} \sigma_{3\alpha}\, dz \quad , \quad m_{3} = \int_{-\frac{h}{2}}^{\frac{h}{2}} \sigma_{33}\, dz, \\ M_{\alpha 3} &= \int_{-\frac{h}{2}}^{\frac{h}{2}} \sigma_{\alpha 3}\, z\, dz, \end{aligned} \tag{3.16}$$

where $M_{(\alpha\beta)}$ denotes the symmetric part of $M_{\alpha\beta}$ and h is the thickness of the plate. On substituting from (3.15) into (3.16) and integrating through the plate, it is easily shown that

$$\begin{aligned} a_{\alpha\beta} &= \frac{N_{\alpha\beta}}{h} \quad , \quad b_{\alpha\beta} = \frac{12}{h^3} M_{(\alpha\beta)}, \\ a_{\alpha 3} &= \frac{m_{\alpha}}{h} \quad , \quad b_{\alpha 3} = \frac{12}{h^3} M_{\alpha 3}, \\ a_{33} &= \frac{m_3}{h}. \end{aligned} \tag{3.17}$$

Nicol (1985) notes that we can split the stress variables into two separate sets, analogous to the situation for the strain variables described in section §3.1. For the initially flat plate under uniaxial tension all the bending variables, namely $M_{(\alpha\beta)}$ and m_{α}, are identically zero. Hence we deduce that the final expressions for the components of the three-dimensional stress tensor, using (3.17) in (3.15), are

$$\sigma_{\alpha\beta} \;=\; \frac{N_{\alpha\beta}}{h} + O\left(z^2\right),$$

$$\begin{aligned} \sigma_{\alpha 3} &= \frac{12}{h^3} M_{\alpha 3}\, z + O\left(z^2\right), \\ \sigma_{33} &= \frac{m_3}{h} + O\left(z\right). \end{aligned} \tag{3.18}$$

Having obtained the stress and strain variables relevant to an initially flat plate under uniaxial tension we shall next derive the governing system of partial differential equations.

To begin the derivation we shall use the expressions (3.18) to obtain some results that are required for latter use. From (3.18) and (2.47) the only non-zero components of the stress deviator tensor s_{ij} are

$$\begin{aligned} s_{11} &= \frac{2}{3}\frac{N_{11}}{h} - \frac{1}{3}\frac{N_{22}}{h} - \frac{1}{3}\frac{m_3}{h}, \\ s_{22} &= \frac{2}{3}\frac{N_{22}}{h} - \frac{1}{3}\frac{N_{11}}{h} - \frac{1}{3}\frac{m_3}{h}, \\ s_{33} &= \frac{2}{3}\frac{m_3}{h} - \frac{1}{3}\frac{N_{11}}{h} - \frac{1}{3}\frac{N_{22}}{h}, \end{aligned} \tag{3.19}$$

and

$$s_{13} = \frac{12}{h^3} M_{13} z.$$

Using (3.19) in (2.46) we can express the equivalent stress σ^* in terms of the two-dimensional generalised stresses, to leading order, as

$$(\sigma^*)^2 = \frac{1}{h^2}\left({N_{11}}^2 + {N_{22}}^2 + {m_3}^2 - N_{11}N_{22} - N_{11}m_3 - N_{22}m_3 + \frac{432}{h^4}{M_{13}}^2 z^2\right). \tag{3.20}$$

Using the expressions (3.12)–(3.14), (3.19) and (3.20) in equation (2.44) we obtain

$$\varrho_{11,t} = \frac{A}{2h}\frac{(\sigma^*)^{n-1}}{\psi^p}\left(2N_{11} - N_{22} - m_3\right), \tag{3.21}$$

$$\varrho_{22,t} = \frac{A}{2h}\frac{(\sigma^*)^{n-1}}{\psi^p}\left(-N_{11} + 2N_{22} - m_3\right), \tag{3.22}$$

$$\delta_{3,t} = \frac{A}{2h}\frac{(\sigma^*)^{n-1}}{\psi^p}\left(-N_{11} - N_{22} + 2m_3\right), \tag{3.23}$$

$$\delta_{3,xt} = \frac{36A}{h^3}\frac{(\sigma^*)^{n-1}}{\psi^p} M_{13}. \tag{3.24}$$

The plane strain condition implies that

$$\varrho_{22,t} = 0 \tag{3.25}$$

and so, with the use of (3.22) and (3.25) for a non-trivial solution we require that

$$N_{22} = \frac{1}{2}(N_{11} + m_3). \tag{3.26}$$

Using (3.26) to eliminate N_{22} from (3.21) and (3.23) then leads to the equations

$$\varrho_{11,t} = \frac{3}{4}\frac{A}{h}\frac{(\sigma^*)^{n-1}}{\psi^p}(N_{11} - m_3), \tag{3.27}$$

$$\delta_{3,t} = \frac{3}{4}\frac{A}{h}\frac{(\sigma^*)^{n-1}}{\psi^p}(-N_{11} + m_3). \tag{3.28}$$

Quoting directly from Hawkes (1989), the incompressibility condition for an initially flat plate, with a single director associated with each point on the reference surface $z = 0$, is

$$\varrho_{11,t} + \delta_{3,t} = 0. \tag{3.29}$$

We observe that equations (3.27) to (3.28) satisfy the incompressibility condition (3.29).

Next we must express σ^* in terms of the two-dimensional generalised stresses. On using (3.26) and (3.20), it follows that

$$\sigma^* = \left[\frac{3}{4h^2}\left((N_{11} - m_3)^2 + \frac{576}{h^4}{M_{13}}^2 z^2\right)\right]^{\frac{1}{2}}. \tag{3.30}$$

Assuming that $N_{11} \neq m_3$ and

$$\left|\frac{576{M_{13}}^2 z^2}{h^4(N_{11} - m_3)^2}\right| < 1, \tag{3.31}$$

which will certainly be true close to the surface $z = 0$, then to a first approximation

$$(\sigma^*)^{n-1} = \left(\frac{3}{4h^2}\right)^{\frac{n-1}{2}}(N_{11} - m_3)^{n-1}. \tag{3.32}$$

This value for σ^* can now be substituted into equations (3.24), (3.27), (3.28) and (2.45) to yield the partial differential equations

$$\delta_{3,t} = -A\left(\frac{1}{h}\right)^n \left(\frac{3}{4}\right)^{\frac{n+1}{2}} \frac{(N_{11}-m_3)^n}{\psi^p} = -\varrho_{11,t}, \tag{3.33}$$

$$\delta_{3,xt} = 36A\left(\frac{1}{h}\right)^{n+2} \left(\frac{3}{4}\right)^{\frac{n-1}{2}} \frac{(N_{11}-m_3)^{n-1}}{\psi^p} M_{13}, \tag{3.34}$$

and

$$\psi_{,t} = -B\left(\frac{3}{4}\right)^{\frac{m}{2}} \left(\frac{1}{h}\right)^m \frac{(N_{11}-m_3)^m}{\psi^q}. \tag{3.35}$$

Finally to complete the set of differential equations we need the equilibrium equations. For the case of the initially flat plate, all curvature terms are identically zero and hence assuming that there are no body forces acting on the plate i.e. $\tilde{\mathbf{F}} \equiv \tilde{\mathbf{L}}^{(N)} \equiv 0$, then the field equations, (2.140)–(2.143), with a single director reduce to

$$N_{11,x} = 0, \tag{3.36}$$

and

$$M_{13,x} = m_3. \tag{3.37}$$

We observe that in the present co-ordinate system, contravariant and covariant tensors are equivalent and so we can raise or lower the indices of tensor components trivially.

It follows immediately from equation (3.36) that

$$N_{11} = N(t), \tag{3.38}$$

and as we are assuming that the stress at the ends of the plate is constant (σ_∞), we obtain

$$N_{11} = N_\infty = \sigma_\infty h. \tag{3.39}$$

The system of partial differential equations (3.33) to (3.35) and (3.37) can be non-dimensionalised using the following substitutions

$$\check{x} = \sqrt{48}\,\frac{x}{h} \;,\; \check{t} = \frac{t}{T} \;,\; \check{\psi} = \psi \;,\; \check{\delta}_3 = \delta_3,$$

$$\tilde{m}_3 = \frac{m_3}{N_\infty} \ , \ \tilde{M}_{13} = \frac{\sqrt{48}}{h}\frac{M_{13}}{N_\infty}, \tag{3.40}$$

$$\tilde{A} = T\left(\frac{N_\infty}{h}\right)^n \left(\frac{3}{4}\right)^{\frac{n+1}{2}} A \ , \ \tilde{B} = T\left(\frac{N_\infty}{h}\right)^m \left(\frac{3}{4}\right)^{\frac{m}{2}} B,$$

where T is a suitable time scale for the problem. The transformations (3.40) lead to

$$\tilde{\delta}_{3,\tilde{t}} = -\tilde{A}\frac{(1-\tilde{m}_3)^n}{\tilde{\psi}^p}, \tag{3.41}$$

$$\tilde{\delta}_{3,\tilde{x}\tilde{t}} = \tilde{A}\frac{(1-\tilde{m}_3)^{n-1}}{\tilde{\psi}^p}\tilde{M}_{13}, \tag{3.42}$$

$$\tilde{\psi}_{,\tilde{t}} = -\tilde{B}\frac{(1-\tilde{m}_3)^m}{\tilde{\psi}^q}, \tag{3.43}$$

$$\tilde{M}_{13,\tilde{x}} = \tilde{m}_3. \tag{3.44}$$

Before solving the differential equations it is necessary to state the appropriate boundary conditions and initial conditions.

3.3 Boundary Conditions.

The boundary conditions used here are identical to those adopted by Nicol (1985) and Hawkes (1989):

$$\text{(i) as } x \to -\infty, M_{13} \to 0, \tag{3.45}$$

$$\text{(ii) at } x = l_3, M_{13} = 0, \tag{3.46}$$

where l_3 is the position of the centre of the weld. The condition (3.45) comes from the constant uniaxial tension at infinity, whilst (3.46) is due to symmetry at the centre of the weld. We must also apply continuity conditions at each of the interfaces between the zones. These continuity conditions can either be derived by energy considerations or by the following argument. The material parameter $\tilde{A}(\tilde{x})$ is assumed to be continuous for all $\tilde{x}$, except for jump discontinuities at each of the interfaces. Hence all the variables

in the problem are either continuous everywhere or suffer jump discontinuities at each of the interfaces: the variables must be piecewise continuous. It follows that the right-hand sides of equations (3.41), (3.42) and (3.44) are piecewise continuous and hence their integrals with respect to $\tilde{x}$ will be continuous everywhere. Consequently, the first integral with respect to $\tilde{x}$ of the left-hand sides of the equations must be continuous everywhere and so at each of the interfaces

$$\tilde{\delta}_{3,\tilde{t}} \ , \ \tilde{M}_{13} \quad \text{are continuous.} \tag{3.47}$$

For completeness we remind ourselves of the initial condition and failure criterion (2.43), namely

$$\begin{aligned} \tilde{\psi} &= 1 \quad \text{at} \quad \tilde{t} = 0, \\ \tilde{\psi} &= 0 \quad \text{at} \quad \tilde{t} = \tilde{t}_r. \end{aligned} \tag{3.48}$$

Before solving the complete system numerically we shall obtain first a small time solution, which can be used as a check on the full numerical solution, and then an analytical solution for the strain-rates at time $t = 0$.

3.4 Small-Time Solution to the General System of Equations.

In this section we will obtain the small-time solution to the system of equations derived in section §3.3. To simplify the analysis we will only look at the simple case of the two zone weldment, containing the parent material and the weld metal only. A similar form for the solution would be appropriate for a four zone weldment, but the algebra would be more complex.

The general non-dimensional partial differential equations (3.41) to (3.44), repeated here for convenience, are

$$\delta_{3,t} \ = \ -A(1 - m_3)^n \, \psi^{-p}, \tag{3.49}$$

$$\delta_{3,xt} = A(1-m_3)^{n-1} M_{13}\, \psi^{-p}, \tag{3.50}$$

$$\psi_{,t} = -B(1-m_3)^{m}\, \psi^{-q}, \tag{3.51}$$

$$M_{13,x} = m_3, \tag{3.52}$$

where a comma followed by a subscript denotes partial differentiation with respect to that variable, and where we have omitted the ˜ for convenience. Equation (3.51) can be written

$$\left(\frac{\psi_{,t}\,\psi^{q}}{-B}\right)^{\frac{1}{m}} = (1-m_3)\,. \tag{3.53}$$

Since the variable ψ is monotonically decreasing from 1 to 0 (at failure), $\psi_{,t}$ is negative and hence, the term in brackets on the left-hand side of equation (3.53) is positive as required. We can now substitute for $(1-m_3)$ from (3.53) into the equations (3.49) and (3.50), to give

$$\delta_{3,t} = -A\left(\frac{\psi_{,t}}{-B}\right)^{\frac{n}{m}} \psi^{\frac{qn}{m}-p}, \tag{3.54}$$

and

$$\delta_{3,xt} = A\left(\frac{\psi_{,t}}{-B}\right)^{\frac{n-1}{m}} \psi^{\frac{q(n-1)}{m}-p} M_{13}. \tag{3.55}$$

On differentiating (3.54) with respect to x, assuming that A and B are constant within each region and eliminating $\delta_{3,xt}$ from (3.55), we deduce that

$$M_{13} = -\left(\frac{\psi_{,t}}{-B}\right)^{\frac{1}{m}} \frac{\psi^{\frac{q-m}{m}}}{\psi_{,t}} \left[\left(\frac{n}{m}\right)\psi_{,xt}\psi + \left(\frac{qn}{m}-p\right)\psi_{,x}\psi_{,t}\right]. \tag{3.56}$$

After differentiating equation (3.56) and substituting into equation (3.52), and then using (3.53), we finally get the third order non-linear partial differential equation for ψ

$$\left(\frac{\psi_{,t}}{-B}\right)^{\frac{1}{m}} \frac{\psi^{\frac{q}{m}-2}}{(\psi_{,t})^2}$$

$$\times \quad \left[\left\{\left(\frac{1}{m}-1\right)\psi_{,xt}\psi + \left(\frac{q}{m}-1\right)\psi_{,x}\psi_{,t}\right\}\left\{\left(\frac{n}{m}\right)\psi_{,xt}\psi + \left(\frac{qn}{m}-p\right)\psi_{,x}\psi_{,t}\right\}\right.$$

$$+ \quad \psi_{,t}\psi\left\{\left(\frac{n}{m}\right)\left(\psi_{,xxt}\psi + \psi_{,xt}\psi_{,x}\right) + \left(\frac{qn}{m} - p\right)\left(\psi_{,xx}\psi_{,t} + \psi_{,x}\psi_{,xt}\right)\right\}\Bigg]$$

$$= \quad \left(\frac{\psi_{,t}}{-B}\right)^{\frac{1}{m}}\psi^{\frac{q}{m}} - 1. \tag{3.57}$$

In order to obtain a small time solution for ψ we assume

$$\psi(x,t) = 1 - t^{\alpha}\psi_1(x) - t^{2\alpha}\psi_2(x) - \cdots, \tag{3.58}$$

where $\alpha > 0$, with derivatives

$$\begin{aligned}
\psi_{,t} &= -\alpha t^{\alpha-1}\psi_1 + O\left(t^{2\alpha-1}\right), \\
\psi_{,x} &= -t^{\alpha}\psi_{1,x} + O\left(t^{2\alpha}\right), \\
\psi_{,xt} &= -\alpha t^{\alpha-1}\psi_{1,x} + O\left(t^{2\alpha-1}\right), \\
\psi_{,xxt} &= -\alpha t^{\alpha-1}\psi_{1,xx} + O\left(t^{2\alpha-1}\right).
\end{aligned} \tag{3.59}$$

If we now substitute these expressions for the derivatives into equation (3.57) and retain the leading order terms only, then we obtain the equation

$$\left(\frac{-\alpha t^{\alpha-1}\psi_1}{-B}\right)^{\frac{1}{m}}\left(\frac{1}{-\alpha t^{\alpha-1}\psi_1}\right)^2\left[\left(\frac{1}{m} - 1\right)\left(-\alpha t^{\alpha-1}\psi_{1,x}\right)\left(\frac{n}{m}\right)\left(-\alpha t^{\alpha-1}\psi_{1,x}\right)\right.$$

$$\left. + \left(-\alpha t^{\alpha-1}\psi_1\right)\left(\frac{n}{m}\right)\left(-\alpha t^{\alpha-1}\psi_{1,xx}\right)\right] = \left(\frac{-\alpha t^{\alpha-1}\psi_1}{-B}\right)^{\frac{1}{m}} - 1. \tag{3.60}$$

Comparing powers of t in equation (3.60) it is clear that we require $\alpha = 1$, in which case the equation reduces to

$$\frac{n}{m}\left(\left(\frac{1}{m} - 1\right)\left(\psi_{1,x}\right)^2 + \psi_1\psi_{1,xx}\right) = {\psi_1}^2 - \left(\frac{B}{\psi_1}\right)^{\frac{1}{m}}(\psi_1)^2. \tag{3.61}$$

The small time behaviour for ψ can therefore be found by solving the ordinary differential equation (3.61) subject to certain boundary conditions which will be discussed later in this section.

The equation (3.61) can be considerably simplified by introducing a new variable through

$$u = (\psi_1)^w. \tag{3.62}$$

Differentiating the above equation with respect to x gives

$$u_{,x} = w(\psi_1)^{w-1}\psi_{1,x}, \tag{3.63}$$

$$u_{,xx} = w(\psi_1)^{w-2}\left[(w-1)\left(\psi_{1,x}\right)^2 + \psi_1\psi_{1,xx}\right], \tag{3.64}$$

and comparing with equation (3.61) suggests we choose $w = \frac{1}{m}$. With this choice and with the use of (3.63) and (3.64), equation (3.61) is transformed to

$$u_{,xx} - \frac{1}{n}u = -\frac{B^{\frac{1}{m}}}{n}. \tag{3.65}$$

The latter equation is clearly a second order linear equation for u with constant coefficients and so its general solution is easily seen to be

$$u(x) = k_1 e^{\frac{x}{\sqrt{n}}} + k_2 e^{-\frac{x}{\sqrt{n}}} + B^{\frac{1}{m}}. \tag{3.66}$$

3.4.1 Boundary Conditions.

To apply the boundary conditions to the above solution, it is necessary to rewrite conditions (3.45) and (3.46) in terms of u and its derivatives.

(i) As we get further from the weld, its influence on the damage rate should be negligible and hence the damage should become independent of x, i.e. we require

$$\psi_{,x} \to 0 \text{ as } x \to -\infty \text{ for all } t. \tag{3.67}$$

Since from (3.62)

$$\psi_1 = u^m, \tag{3.68}$$

on differentiating (3.68) and using $(3.59)_{(ii)}$, we obtain the condition

$$u^{m-1}u_{,x} \to 0 \text{ as } x \to -\infty. \tag{3.69}$$

(ii) From symmetry considerations we must have

$$\psi_{,x} = 0 \text{ at } x = l_3 \text{ for all } t, \tag{3.70}$$

where l_3 is the position of the centre of the weld. In a similar manner to the derivation of (3.69) we then deduce that

$$u^{m-1}u_{,x} = 0 \text{ at } x = l_3. \tag{3.71}$$

The conditions at the interface are that M_{13} and $\delta_{3,t}$ must be continuous. Using (3.54), (3.58) and (3.59) with $\alpha = 1$ it follows by consideration of the leading order term that the continuity of $\delta_{3,t}$ implies that

$$A\left(\frac{\psi_1}{B}\right)^{\frac{n}{m}} \text{ is continuous at } x = 0, \tag{3.72}$$

and in terms of u we therefore require that

$$A\frac{u^n}{B^{\frac{n}{m}}} \text{ is continuous at } x = 0. \tag{3.73}$$

Similarly with the use of (3.56), (3.58) and (3.59) with $\alpha = 1$, it follows that the continuity of M_{13} at $x = 0$ requires that

$$\frac{1}{B}\left(\frac{\psi_1}{B}\right)^{\frac{1}{m}-1}\left(\frac{n}{m}\right)\psi_{1,x} \text{ is continuous at } x = 0, \tag{3.74}$$

which is equivalent, on recalling (3.68), to imposing

$$n\frac{u_{,x}}{B^{\frac{1}{m}}} \text{ is continuous at } x = 0. \tag{3.75}$$

For the present problem we shall assume n and m are constant throughout the weldment and so (3.75) is equivalent to requiring

$$\frac{u_{,x}}{B^{\frac{1}{m}}} \text{ is continuous at } x = 0. \tag{3.76}$$

The transformed boundary conditions for the problem under discussion have now been determined and we now proceed to find the actual solution.

3.4.2 Analysis.

Recalling (3.66) the general solution is

$$u(x) = \begin{cases} {k_1}^{(\mathrm{p})} e^{\frac{x}{\sqrt{n}}} + {k_2}^{(\mathrm{p})} e^{-\frac{x}{\sqrt{n}}} + \left(B^{(\mathrm{p})}\right)^{\frac{1}{m}} & , x < 0 \\ {k_1}^{(\mathrm{w})} e^{\frac{x}{\sqrt{n}}} + {k_2}^{(\mathrm{w})} e^{-\frac{x}{\sqrt{n}}} + \left(B^{(\mathrm{w})}\right)^{\frac{1}{m}} & , 0 \leq x \leq l_3 \end{cases} \tag{3.77}$$

and the constants are now determined from application of the boundary conditions. Condition (3.69) requires that

$$\left({k_1}^{(\mathrm{p})} e^{\frac{x}{\sqrt{n}}} + {k_2}^{(\mathrm{p})} e^{-\frac{x}{\sqrt{n}}} + \left(B^{(\mathrm{p})}\right)^{\frac{1}{m}}\right)^{m-1} \left(\frac{{k_1}^{(\mathrm{p})}}{\sqrt{n}} e^{\frac{x}{\sqrt{n}}} - \frac{{k_2}^{(\mathrm{p})}}{\sqrt{n}} e^{-\frac{x}{\sqrt{n}}}\right) \to 0 \text{ as } x \to -\infty, \tag{3.78}$$

and so for a non-trivial solution

$${k_2}^{(\mathrm{p})} \equiv 0. \tag{3.79}$$

Applying the condition (3.71) to the general solution (3.77) leads to

$$\left({k_1}^{(\mathrm{w})} e^{\frac{l_3}{\sqrt{n}}} + {k_2}^{(\mathrm{w})} e^{-\frac{l_3}{\sqrt{n}}} + \left(B^{(\mathrm{w})}\right)^{\frac{1}{m}}\right)^{m-1} \left(\frac{{k_1}^{(\mathrm{w})}}{\sqrt{n}} e^{\frac{l_3}{\sqrt{n}}} - \frac{{k_2}^{(\mathrm{w})}}{\sqrt{n}} e^{-\frac{l_3}{\sqrt{n}}}\right) = 0, \tag{3.80}$$

and it follows that either

$${k_2}^{(\mathrm{w})} = e^{\frac{2l_3}{\sqrt{n}}} {k_1}^{(\mathrm{w})}, \tag{3.81}$$

or

$${k_1}^{(\mathrm{w})} e^{\frac{l_3}{\sqrt{n}}} + {k_2}^{(\mathrm{w})} e^{-\frac{l_3}{\sqrt{n}}} + \left(B^{(\mathrm{w})}\right)^{\frac{1}{m}} = 0. \tag{3.82}$$

If (3.82) were true then the linear term in the time series for ψ is identically zero at the centre of the weld. Hence, the centre of the weld remains undamaged over a much longer time-scale than other parts of weld metal, which is physically unrealistic. Therefore, we assume that (3.81) is the correct condition to apply.

Using equations (3.77) and (3.79) the continuity conditions (3.73) and (3.76) imply that

$$\frac{A^{(\mathrm{p})}}{(B^{(\mathrm{p})})^{\frac{n}{m}}}\left(k_1{}^{(\mathrm{p})}+B^{(\mathrm{p})\frac{1}{m}}\right)^n=\frac{A^{(\mathrm{w})}}{(B^{(\mathrm{w})})^{\frac{n}{m}}}\left(k_1{}^{(\mathrm{w})}+k_2{}^{(\mathrm{w})}+B^{(\mathrm{w})\frac{1}{m}}\right)^n, \tag{3.83}$$

and

$$\frac{k_1{}^{(\mathrm{p})}}{(B^{(\mathrm{p})})^{\frac{1}{m}}}=\frac{1}{(B^{(\mathrm{w})})^{\frac{1}{m}}}\left(k_1{}^{(\mathrm{w})}-k_2{}^{(\mathrm{w})}\right). \tag{3.84}$$

On solving the simultaneous equations (3.81), (3.83) and (3.84) we obtain

$$k_1{}^{(\mathrm{p})} = \frac{\left(B^{(\mathrm{p})}\right)^{\frac{1}{m}}\left(\left(A^{(\mathrm{w})}\right)^{\frac{1}{n}}-\left(A^{(\mathrm{p})}\right)^{\frac{1}{n}}\right)\left(1-e^{\frac{2l_3}{\sqrt{n}}}\right)}{(A^{(\mathrm{p})})^{\frac{1}{n}}\left(1-e^{\frac{2l_3}{\sqrt{n}}}\right)-(A^{(\mathrm{w})})^{\frac{1}{n}}\left(1+e^{\frac{2l_3}{\sqrt{n}}}\right)}, \tag{3.85}$$

$$k_1{}^{(\mathrm{w})} = \frac{\left(B^{(\mathrm{w})}\right)^{\frac{1}{m}}\left(\left(A^{(\mathrm{w})}\right)^{\frac{1}{n}}-\left(A^{(\mathrm{p})}\right)^{\frac{1}{n}}\right)}{(A^{(\mathrm{p})})^{\frac{1}{n}}\left(1-e^{\frac{2l_3}{\sqrt{n}}}\right)-(A^{(\mathrm{w})})^{\frac{1}{n}}\left(1+e^{\frac{2l_3}{\sqrt{n}}}\right)} \tag{3.86}$$

$$k_2{}^{(\mathrm{w})} = k_1{}^{(\mathrm{w})}e^{\frac{2l_3}{\sqrt{n}}}, \tag{3.87}$$

with the remaining constant $k_2{}^{(\mathrm{p})}$ satisfying

$$k_2{}^{(\mathrm{p})}=0, \tag{3.88}$$

(equation (3.79), repeated here for completeness).

Using equation (3.58) and (3.68) in conjunction with equations (3.66) and (3.85) to (3.88), the leading terms in the small time solution for the damage are

$$\psi(x,t)=\begin{cases} 1-tB^{(\mathrm{p})}\left(\kappa e^{\frac{x}{\sqrt{n}}}\left(1-e^{\frac{2l_3}{\sqrt{n}}}\right)+1\right)^m+O\left(t^2\right) & x<0 \\ 1-tB^{(\mathrm{w})}\left(\kappa e^{\frac{x}{\sqrt{n}}}+\kappa e^{\frac{(2l_3-x)}{\sqrt{n}}}+1\right)^m+O\left(t^2\right) & 0\le x\le l_3 \end{cases} \tag{3.89}$$

where

$$\kappa = \frac{\left(A^{(w)}\right)^{\frac{1}{n}} - \left(A^{(p)}\right)^{\frac{1}{n}}}{\left(A^{(p)}\right)^{\frac{1}{n}}\left(1 - e^{\frac{2l_3}{\sqrt{n}}}\right) - \left(A^{(w)}\right)^{\frac{1}{n}}\left(1 + e^{\frac{2l_3}{\sqrt{n}}}\right)}. \tag{3.90}$$

This solution can be used to determine the values of the damage at small times and provides a check on the accuracy of the numerical procedure used in obtaining the solution for ψ for all $t > 0$.

3.5 Analytical Solution for the Strain-Rates at $t = 0$.

With the mathematical model introduced §3.2 it is possible to obtain an analytical solution for the strain-rates in the virgin, undamaged state. No equivalent analytical solution can be found for the model developed by Nicol (1985), and so the model presented in section §3.2 does possess an attractive feature not present in Nicol's earlier model.

If we write equations (3.49), (3.50) and (3.52) for the situation at $t = 0$, and hence $\psi = 1$, we obtain the system of differential equations

$$\delta_{3,t} = -A(1 - m_3)^n, \tag{3.91}$$

$$\delta_{3,xt} = A(1 - m_3)^{n-1} M_{13}, \tag{3.92}$$

$$M_{13,x} = m_3, \tag{3.93}$$

remembering that these equations are all written in terms of non-dimensional variables. Differentiating (3.91) with respect to x leads to

$$\delta_{3,xt} = An(1 - m_3)^{n-1} m_{3,x}, \tag{3.94}$$

where it has been assumed that A remains constant in each zone, which is a reasonable approximation in reality. Eliminating $\delta_{3,xt}$ between (3.92) and (3.94) yields

$$m_{3,x} = \frac{M_{13}}{n}. \tag{3.95}$$

The equations (3.93) and (3.95) are a pair of ordinary differential equations in the variables M_{13} and m_3. If we write these as a single second order differential equation, we obtain

$$m_{3,xx} - \frac{m_3}{n} = 0, \tag{3.96}$$

which is easily solved for m_3 to yield

$$m_3 = \begin{cases} k_1 e^{\frac{x}{\sqrt{n}}} + k_2 e^{-\frac{x}{\sqrt{n}}} & x < 0, \\ k_3 e^{\frac{x}{\sqrt{n}}} + k_4 e^{-\frac{x}{\sqrt{n}}} & 0 \leq x \leq l_3, \end{cases} \tag{3.97}$$

where we have assumed that the weldment under discussion has the simple composition discussed in section §3.4 . Recalling (3.27), knowledge of m_3 clearly allows us to determine the strain-rate $\varrho_{11,t}$.

For the two zone weldment the boundary conditions to be applied are:-

$$\text{as } x \to -\infty, M_{13} \to 0 \Rightarrow m_{3,x} \to 0, \tag{3.98}$$

$$\text{at } x = l_3, M_{13} = 0 \Rightarrow m_{3,x} = 0 \tag{3.99}$$

$$\text{at } x = 0, M_{13} \text{ is continuous } \Rightarrow m_{3,x} \text{ is continuous }, \tag{3.100}$$

$$\text{at } x = 0, \delta_{3,t} \text{ is continuous } \Rightarrow A^{(i)}(1 - m_3)^n \text{ is continuous,} \tag{3.101}$$

where $A^{(i)}$ takes the value $A^{(\mathrm{p})}$ in the parent material and $A^{(\mathrm{w})}$ in the weld region.

Applying these boundary conditions to the solution (3.97) and solving the resulting system of simultaneous equations in k_1, k_2, k_3 and k_4, we obtain a solution for the strain-rate $\varrho_{11,t}$ in the form

$$\varrho_{11,t} = \begin{cases} A^{(\mathrm{p})}\left(1 - k_1 e^{\frac{x}{\sqrt{n}}} - k_2 e^{-\frac{x}{\sqrt{n}}}\right)^n & x < 0, \\ A^{(\mathrm{w})}\left(1 - k_3 e^{\frac{x}{\sqrt{n}}} - k_4 e^{-\frac{x}{\sqrt{n}}}\right)^n & 0 \leq x \leq l_3, \end{cases} \tag{3.102}$$

where

$$k_1 = \kappa\left(1 - e^{\frac{2l_3}{\sqrt{n}}}\right), \tag{3.103}$$

$$k_2 = 0, \tag{3.104}$$

$$k_3 = \kappa, \tag{3.105}$$

$$k_4 = \kappa e^{\frac{2l_3}{\sqrt{n}}}. \tag{3.106}$$

In the above κ is defined by

$$\kappa = \frac{A^{\frac{1}{n}} - 1}{A^{\frac{1}{n}}\left(1 + e^{\frac{2l_3}{\sqrt{n}}}\right) - \left(1 - e^{\frac{2l_3}{\sqrt{n}}}\right)}, \tag{3.107}$$

where

$$A = \frac{A^{(\mathrm{w})}}{A^{(\mathrm{p})}}. \tag{3.108}$$

A similar solution can be obtained for the strain-rate of a weldment containing four separate zones, by applying the continuity conditions (3.47) at each of the additional interfaces.

The four zone weldment is represented by Figure (3.1), where l_∞ is chosen such that the values of the variables M_{13} and m_3 at l_∞ are sufficiently close to their respective values as $x \to -\infty$.

In this case the general solution takes the form

$$\varrho_{11,t}(x) = \begin{cases} A^{(\mathrm{p})}\left(1 - k_1 e^{\frac{x}{\sqrt{n}}} - k_2 e^{-\frac{x}{\sqrt{n}}}\right)^n & , l_\infty \le x < 0, \\ A^{(\mathrm{iv})}\left(1 - k_3 e^{\frac{x}{\sqrt{n}}} - k_4 e^{-\frac{x}{\sqrt{n}}}\right)^n & , 0 < x \le l_1, \\ A^{(\mathrm{haz})}\left(1 - k_5 e^{\frac{x}{\sqrt{n}}} - k_6 e^{-\frac{x}{\sqrt{n}}}\right)^n & , l_1 < x \le l_2, \\ A^{(\mathrm{w})}\left(1 - k_7 e^{\frac{x}{\sqrt{n}}} - k_8 e^{-\frac{x}{\sqrt{n}}}\right)^n & , l_2 < x \le l_3. \end{cases} \tag{3.109}$$

Applying the boundary conditions and the continuity conditions, we find not unexpectedly that the constants k_i satisfy a complicated system of simultaneous equations

which can be represented in matrix form as

$$\mathrm{M}\,\mathrm{x} = \mathrm{b} \tag{3.110}$$

where

$$\mathrm{M} = \begin{bmatrix} e^{\frac{l_\infty}{\sqrt{n}}} & -e^{-\frac{l_\infty}{\sqrt{n}}} & 0 & 0 \\ 1 & -1 & -1 & 1 \\ -\left(A^{(\mathrm{p})}\right)^{\frac{1}{n}} & -\left(A^{(\mathrm{p})}\right)^{\frac{1}{n}} & \left(A^{(\mathrm{iv})}\right)^{\frac{1}{n}} & \left(A^{(\mathrm{iv})}\right)^{\frac{1}{n}} \\ 0 & 0 & e^{\frac{l_1}{\sqrt{n}}} & -e^{-\frac{l_1}{\sqrt{n}}} \\ 0 & 0 & -\left(A^{(\mathrm{iv})}\right)^{\frac{1}{n}} e^{\frac{l_1}{\sqrt{n}}} & -\left(A^{(\mathrm{iv})}\right)^{\frac{1}{n}} e^{-\frac{l_1}{\sqrt{n}}} \\ 0 & 0 & 0 & 0 \\ 0 & 0 & 0 & 0 \\ 0 & 0 & 0 & 0 \end{bmatrix}$$

$$\begin{bmatrix} 0 & 0 & 0 & 0 \\ 0 & 0 & 0 & 0 \\ 0 & 0 & 0 & 0 \\ -e^{\frac{l_1}{\sqrt{n}}} & e^{-\frac{l_1}{\sqrt{n}}} & 0 & 0 \\ \left(A^{(\mathrm{haz})}\right)^{\frac{1}{n}} e^{\frac{l_1}{\sqrt{n}}} & \left(A^{(\mathrm{haz})}\right)^{\frac{1}{n}} e^{-\frac{l_1}{\sqrt{n}}} & 0 & 0 \\ e^{\frac{l_2}{\sqrt{n}}} & -e^{-\frac{l_2}{\sqrt{n}}} & -e^{\frac{l_2}{\sqrt{n}}} & e^{-\frac{l_2}{\sqrt{n}}} \\ -\left(A^{(\mathrm{haz})}\right)^{\frac{1}{n}} e^{\frac{l_2}{\sqrt{n}}} & -\left(A^{(\mathrm{haz})}\right)^{\frac{1}{n}} e^{-\frac{l_2}{\sqrt{n}}} & \left(A^{(\mathrm{w})}\right)^{\frac{1}{n}} e^{\frac{l_2}{\sqrt{n}}} & \left(A^{(\mathrm{w})}\right)^{\frac{1}{n}} e^{-\frac{l_2}{\sqrt{n}}} \\ 0 & 0 & e^{\frac{l_3}{\sqrt{n}}} & -e^{-\frac{l_3}{\sqrt{n}}} \end{bmatrix} \tag{3.111}$$

$$\mathrm{x}^{\mathrm{T}} = \left(k_1,\ k_2,\ k_3,\ k_4,\ k_5,\ k_6,\ k_7,\ k_8 \right), \tag{3.112}$$

$$\mathrm{b}^{\mathrm{T}} = \left(0,\ 0,\ \left(A^{(\mathrm{iv})}\right)^{\frac{1}{n}} - \left(A^{(\mathrm{p})}\right)^{\frac{1}{n}},\ 0, \right.$$

$$\left. \left(A^{(\mathrm{haz})}\right)^{\frac{1}{n}} - \left(A^{(\mathrm{iv})}\right)^{\frac{1}{n}},\ 0,\ \left(A^{(\mathrm{w})}\right)^{\frac{1}{n}} - \left(A^{(\mathrm{haz})}\right)^{\frac{1}{n}}, 0) \right). \tag{3.113}$$

This system can be solved on a computer using Gaussian elimination and back substitution with a relatively simple algorithm. The results will be shown graphically, and

discussed later in this chapter. First we shall discuss the numerical method used to obtain the solution to the full problem.

3.6 Numerical Method.

Before discussing the numerical procedure used to solve the system of partial differential equations (3.41) to (3.44), for the weldment containing four zones, it will be prudent to identify some simplifications of the material parameters, consistent with type IV cracking. Experimental data suggests that in the low stress regime ($\leq$100 MPa) it is reasonable to assume that

$$n^{(\mathrm{p})} = n^{(\mathrm{iv})} = n^{(\mathrm{haz})} = n^{(\mathrm{w})} = 4, \tag{3.114}$$

$$m^{(\mathrm{p})} = m^{(\mathrm{iv})} = m^{(\mathrm{haz})} = m^{(\mathrm{w})} = 4, \tag{3.115}$$

$$p^{(\mathrm{p})} = p^{(\mathrm{iv})} = p^{(\mathrm{haz})} = p^{(\mathrm{w})} = 4, \tag{3.116}$$

$$q^{(\mathrm{p})} = q^{(\mathrm{iv})} = q^{(\mathrm{w})} = 4, \tag{3.117}$$

and

$$q^{(\mathrm{haz})} = 7. \tag{3.118}$$

These assumptions simplify the problem considerably, but it should be noted that they are not necessary in order to obtain a numerical solution. In the algebra that follows we set, $p = m = n$, then equations (3.41), (3.42) and (3.44) can be written as

$$\delta_{3,t} = -A\left(\frac{1-m_3}{\psi}\right)^n, \tag{3.119}$$

$$\delta_{3,xt} = A\frac{(1-m_3)^{n-1}}{\psi^n}M_{13}, \tag{3.120}$$

$$M_{13,x} = m_3. \tag{3.121}$$

On eliminating δ_3 and m_3 from the above equations we derive the ordinary differential equation

$$\psi M_{13,xx} - \psi_{,x} M_{13,x} - \frac{\psi}{n} M_{13} = -\psi_{,x}. \tag{3.122}$$

In addition, with the aid of (3.121), the damage evolution equation (3.43) can be expressed as

$$\psi_{,t} = -\frac{B\left(1 - M_{13,x}\right)^n}{\psi^q}, \tag{3.123}$$

which for the purpose of our numerical calculations can be more conveniently written as

$$\left(\psi^{q+1}\right)_{,t} = -B\left(1+q\right)\left(1 - M_{13,x}\right)^n. \tag{3.124}$$

The algorithm for the numerical procedure is as follows;

Step(1) Initialise Variables: At $t = 0$ the weldment is undamaged and hence $\psi = 1$ everywhere, which can then be used in the next step of the algorithm.

Step(2) Solve the Ordinary Differential Equation: The ordinary differential equation (3.122) can be solved using a suitable finite difference scheme, subject to the applied boundary conditions (3.45) and (3.46). Using the method of central differences the various derivatives in (3.122) are represented by

$$M_{13,xx} = \frac{M^j_{i+1} - 2M^j_i + M^j_{i-1}}{\left(\Delta x\right)^2}, \tag{3.125}$$

$$M_{13,x} = \frac{M^j_{i+1} - M^j_{i-1}}{2\left(\Delta x\right)}, \tag{3.126}$$

and

$$\psi_{,x} = \frac{\psi^j_{i+1} - \psi^j_{i-1}}{2\left(\Delta x\right)}, \tag{3.127}$$

where M^j_i represents the value of M_{13} at the i^{th} node at the j^{th} time step. Substituting (3.125)–(3.127) into (3.122) we obtain the algebraic equation

$$\left(\psi^j_i - \frac{\psi^j_{i+1}}{4} + \frac{\psi^j_{i-1}}{4}\right) M^j_{i+1} + \left(-2\psi^j_i - \frac{\left(\Delta x\right)^2}{n}\psi^j_i\right) M^j_i$$

$$+ \quad \left(\psi_i^j + \frac{\psi_{i+1}^j}{4} - \frac{\psi_{i-1}^j}{4}\right) M_{i-1}^j = -\frac{(\Delta x)}{2}\left(\psi_{i+1}^j - \psi_{i-1}^j\right), i = 1 \ldots 4N, \quad (3.128)$$

If each region has $N+1$ nodes $(x_i, i = 0, \ldots N)$ then (3.128) is satisfied at every node. This requires the introduction of two imaginary nodes for each region, one associated with the first node and the other linked with the last node of each respective region. Thus we now have a system of $4N + 4$ algebraic equations in $4N + 12$ unknowns. To complete the system, the remaining 8 equations arise from the boundary and continuity conditions.

At both $x = l_\infty$ and $x = l_3$, $M_{13} = 0$ and $\psi_{,x} = 0$ and hence (3.122) implies that

$$\text{at } x = l_\infty \text{ and } x = l_3, M_{13,xx} = 0 \quad (3.129)$$

Using the finite difference formulæ it follows that

$$M_{-1}^{(\mathrm{p})j} = M_1^{(\mathrm{p})j}, \quad (3.130)$$

$$M_{N+1}^{(\mathrm{w})j} = M_{N-1}^{(\mathrm{w})j}. \quad (3.131)$$

For the continuity conditions, assume that at the interface between the parent material and the type IV region the imaginary node associated with the parent material has an M_{13} value represented by $M_{I+1}^{(\mathrm{p})j}$, similarly the imaginary node associated with the type IV region has an M_{13} value given by $M_{I-1}^{(\mathrm{iv})j}$. To begin with the two regions can be thought of as being separate , and hence the values at the nodes in each region satisfy the algebraic equation (3.128), i.e.

$$\left(\psi_I^{(\mathrm{p})} - \frac{\psi_{I+1}^{(\mathrm{p})}}{4} + \frac{\psi_{I-1}^{(\mathrm{p})}}{4}\right) M_{I+1}^{(\mathrm{p})} + \left(-2\psi_I^{(\mathrm{p})} - \frac{\left(\Delta x^{(\mathrm{p})}\right)^2}{n}\psi_I^{(\mathrm{p})}\right) M_I^{(\mathrm{p})}$$

$$+ \quad \left(\psi_I^{(\mathrm{p})} + \frac{\psi_{I+1}^{(\mathrm{p})}}{4} - \frac{\psi_{I-1}^{(\mathrm{p})}}{4}\right) M_{I-1}^{(\mathrm{p})} = -\frac{\left(\Delta x^{(\mathrm{p})}\right)}{2}\left(\psi_{I+1}^{(\mathrm{p})} - \psi_{I-1}^{(\mathrm{p})}\right), \quad (3.132)$$

and

$$\left(\psi_I^{(\mathrm{iv})} - \frac{\psi_{I+1}^{(\mathrm{iv})}}{4} + \frac{\psi_{I-1}^{(\mathrm{iv})}}{4}\right) M_{I+1}^{(\mathrm{iv})} + \left(-2\psi_I^{(\mathrm{iv})} - \frac{\left(\Delta x^{(\mathrm{iv})}\right)^2}{n}\psi_I^{(\mathrm{iv})}\right) M_I^{(\mathrm{iv})}$$

$$+\quad\left(\psi_I^{(\mathrm{iv})}+\frac{\psi_{I+1}^{(\mathrm{iv})}}{4}-\frac{\psi_{I-1}^{(\mathrm{iv})}}{4}\right)M_{I-1}^{(\mathrm{iv})}=-\frac{\left(\Delta x^{(\mathrm{iv})}\right)}{2}\left(\psi_{I+1}^{(\mathrm{iv})}-\psi_{I-1}^{(\mathrm{iv})}\right),\qquad(3.133)$$

where we are at the j^{th} time step but have removed the superscript j to improve legibility. The symbols $\Delta x^{(\mathrm{p})}$ and $\Delta x^{(\mathrm{iv})}$ represent the step-sizes in the parent and type IV regions respectively .

The continuity conditions $(3.47)_{(\mathrm{i})(\mathrm{ii})}$ with equations (3.119), (3.121) and the expressions (3.126) lead to

$$M_I^{(\mathrm{p})}=M_I^{(\mathrm{iv})},\qquad(3.134)$$

and

$$\frac{\left(A^{(\mathrm{p})}\right)^{\frac{1}{n}}}{\psi_I^{(\mathrm{p})}}\left(1-\frac{M_{I+1}^{(\mathrm{p})}}{2\left(\Delta x^{(\mathrm{p})}\right)}+\frac{M_{I-1}^{(\mathrm{p})}}{2\left(\Delta x^{(\mathrm{p})}\right)}\right)=\frac{\left(A^{(\mathrm{iv})}\right)^{\frac{1}{n}}}{\psi_I^{(\mathrm{iv})}}\left(1-\frac{M_{I+1}^{(\mathrm{iv})}}{2\left(\Delta x^{(\mathrm{iv})}\right)}+\frac{M_{I-1}^{(\mathrm{iv})}}{2\left(\Delta x^{(\mathrm{iv})}\right)}\right).\qquad(3.135)$$

The equations (3.132) to (3.135) can now be used to eliminate $M_{I+1}^{(\mathrm{p})}$ and $M_{I-1}^{(\mathrm{iv})}$, to leave a single algebraic equation that must be satisfied at the interface:

$$\frac{\left(A^{(\mathrm{iv})}\right)^{\frac{1}{n}}}{2\left(\Delta x^{(\mathrm{iv})}\right)\psi_I^{(\mathrm{iv})}}\left[1+\left(\frac{4\psi_I^{(\mathrm{iv})}-\psi_{I+1}^{(\mathrm{iv})}+\psi_{I-1}^{(\mathrm{iv})}}{4\psi_I^{(\mathrm{iv})}+\psi_{I+1}^{(\mathrm{iv})}-\psi_{I-1}^{(\mathrm{iv})}}\right)\right]M_{I+1}$$

$$+\left[-\frac{\left(A^{(\mathrm{p})}\right)^{\frac{1}{n}}}{\left(\Delta x^{(\mathrm{p})}\right)}\left(\frac{4+(2/n)\left(\Delta x^{(\mathrm{p})}\right)^2}{4\psi_I^{(\mathrm{p})}-\psi_{I+1}^{(\mathrm{p})}+\psi_{I-1}^{(\mathrm{p})}}\right)-\frac{\left(A^{(\mathrm{iv})}\right)^{\frac{1}{n}}}{\left(\Delta x^{(\mathrm{iv})}\right)}\left(\frac{4+(2/n)\left(\Delta x^{(\mathrm{iv})}\right)^2}{4\psi_I^{(\mathrm{iv})}+\psi_{I+1}^{(\mathrm{iv})}-\psi_{I-1}^{(\mathrm{iv})}}\right)\right]M_I$$

$$+\frac{\left(A^{(\mathrm{p})}\right)^{\frac{1}{n}}}{2\left(\Delta x^{(\mathrm{p})}\right)\psi_I^{(\mathrm{p})}}\left[1+\left(\frac{4\psi_I^{(\mathrm{p})}+\psi_{I+1}^{(\mathrm{p})}-\psi_{I-1}^{(\mathrm{p})}}{4\psi_I^{(\mathrm{p})}-\psi_{I+1}^{(\mathrm{p})}+\psi_{I-1}^{(\mathrm{p})}}\right)\right]M_{I-1}$$

$$=\frac{\left(A^{(\mathrm{iv})}\right)^{\frac{1}{n}}}{\psi_I^{(\mathrm{iv})}}\left(1-\left(\frac{\psi_{I+1}^{(\mathrm{iv})}-\psi_{I-1}^{(\mathrm{iv})}}{4\psi_I^{(\mathrm{iv})}+\psi_{I+1}^{(\mathrm{iv})}-\psi_{I-1}^{(\mathrm{iv})}}\right)\right)-\frac{\left(A^{(\mathrm{p})}\right)^{\frac{1}{n}}}{\psi_I^{(\mathrm{p})}}\left(1+\left(\frac{\psi_{I+1}^{(\mathrm{p})}-\psi_{I-1}^{(\mathrm{p})}}{4\psi_I^{(\mathrm{p})}-\psi_{I+1}^{(\mathrm{p})}+\psi_{I-1}^{(\mathrm{p})}}\right)\right).\qquad(3.136)$$

Due to the discontinuity of ψ at the interface we need to know both $\psi_I^{(\mathrm{p})}$ and $\psi_I^{(\mathrm{iv})}$, the values of ψ associated with the parent material and type IV region respectively. We

shall assume also that before updating M_{13} at each time-step the values of ψ are known everywhere.

The equations (3.128) with (3.130), (3.131) and the analogous equations to (3.136) for the type IV/HAZ interface and HAZ/weld interface form a system of $4N+1$ linear equations for the unknown values of M_{13} at each node, which can be written in matrix form as

$$\mathbf{Am} = \mathbf{b}, \tag{3.137}$$

where $\mathbf{A}$ is a tri-diagonal $(4N+1)\times(4N+1)$ matrix. The system (3.137) was solved, using Gaussian elimination and partial pivoting, to provide the updated value of M_{13} at each node.

Step(3) March Forward in Time: It is now possible to march forward in time using the calculated values of M_{13} and equation (3.124). The latter equation in difference form becomes

$$\frac{\left(\psi_i^{j+1}\right)^{q+1} - \left(\psi_i^{j}\right)^{q+1}}{\Delta t} = -B\,(q+1)\left(1-\left(\frac{M_{i+1}^{j}-M_{i-1}^{j}}{2\,(\Delta x)}\right)\right)^{n}. \tag{3.138}$$

Step(4): Steps (2) and (3) are repeated in turn until

$$\left(\psi_i^{j+1}\right)^{q+1} \leq 0, \tag{3.139}$$

at some position x_i. If the inequality (3.139) is satisfied at more than one value of x, then the step-size Δt is reduced and new values for ψ are calculated. This procedure of reducing Δt is repeated until the failure criterion (3.139) is satisfied uniquely.

The robustness of the numerical solution was checked by altering the size of the time step, and by varying the number of nodes in each region from 20 to 100. Both of these checks produced a negligible variation in the position of rupture and the rupture time. At small times , there was also good agreement between solutions found using the above numerical scheme and the small time solution derived in section §3.4. It seems, therefore,

that the numerical scheme developed is satisfactory, and the coding has been carried out accurately.

3.7 Results.

Before discussing the results it is convenient to specify the widths of each region by introducing the non-dimensional variables;

$$x^{(\mathrm{iv})} = \frac{l_1}{h}, \tag{3.140}$$

$$x^{(\mathrm{haz})} = \left(\frac{l_2 - l_1}{h}\right), \tag{3.141}$$

$$x^{(\mathrm{w})} = \left(\frac{l_3 - l_2}{h}\right), \tag{3.142}$$

where h represents the thickness of the plate.

All of the above widths will be varied in the results to be presented, and hence we can observe the effects of narrowing or widening the various regions on the position of rupture and the time to rupture. Another property that can be changed is the relative hardness (or softness) of each region to that of the parent material, through altering the ratios

$$\frac{A^{(\mathrm{iv})}}{A^{(\mathrm{p})}}, \quad \frac{A^{(\mathrm{haz})}}{A^{(\mathrm{p})}}, \quad \frac{A^{(\mathrm{w})}}{A^{(\mathrm{p})}}.$$

If the indices n and m satisfy (3.114) and (3.115) and time is measured in hours then the experimental data indicates that for a typical weldment that leads to type IV cracking

$$\begin{aligned} A^{(\mathrm{p})} &= 3.2 \times 10^{-15}, \\ B^{(\mathrm{p})} &= 3.8 \times 10^{-14}, \\ B^{(\mathrm{iv})} &= 1.8 \times 10^{-11}, \\ B^{(\mathrm{haz})} &= 1.5 \times 19^{-14}, \end{aligned} \tag{3.143}$$

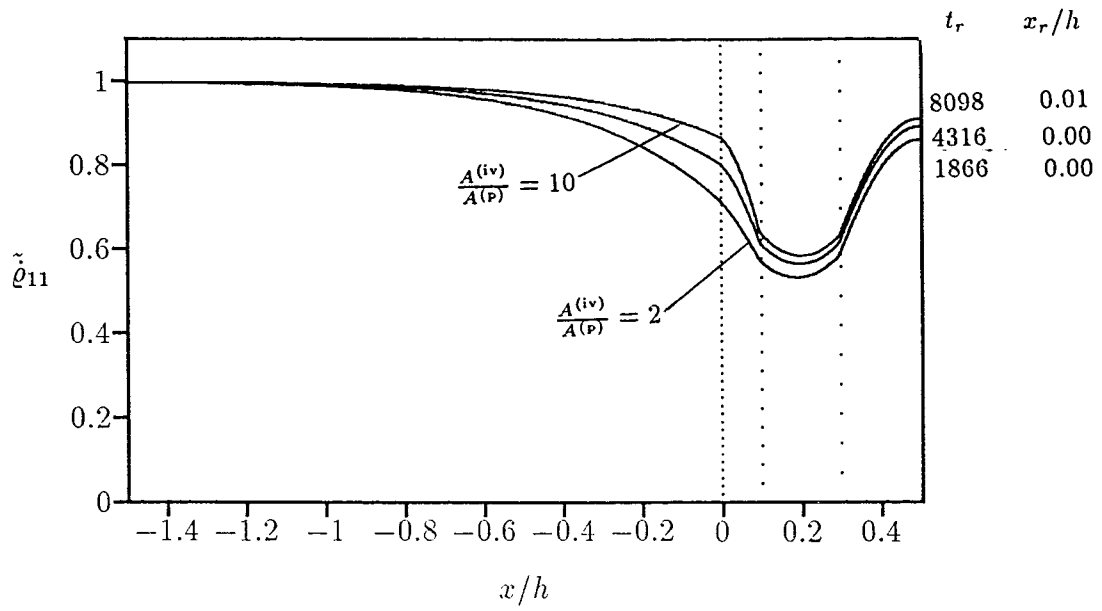

Figure 3.2: Strain-rates for various values of $A^{(\mathrm{iv})}/A^{(\mathrm{p})}$ with $x^{(\mathrm{iv})} = 0.1$

$$B^{(\mathrm{w})} = 2.2 \times 10^{-13}.$$

These figures were obtained by Powergen from their long-term creep experiments. A large number of solutions were found using the numerical scheme for a variety of values for the remaining parameters, and some of these are discussed below, where in each of the Figures (3.2) to (3.10) the non-dimensional strain-rate $\hat{\varrho}_{11,\hat{t}}$ is plotted on the y-axis and the x-axis represents the non-dimensional position x/h.

In Figures (3.2) to (3.4) we can observe the effects of varying the width and strength of the type IV region. In each of the three figures the ratio $A^{(\mathrm{iv})}/A^{(\mathrm{p})}$ takes the values 10, 5 and 2 respectively. In all the displayed results, however, the widths and relative strengths of the HAZ and weld region are kept constant at $x^{(\mathrm{haz})} = 0.2$, $x^{(\mathrm{w})} = 0.2$, $A^{(\mathrm{haz})}/A^{(\mathrm{p})} = 0.1$ and $A^{(\mathrm{w})}/A^{(\mathrm{p})} = 3$. The only parameter that changes from figure to figure is $x^{(\mathrm{iv})}$, which takes the values

- Figure (3.2), $x^{(\mathrm{iv})} = 0.1$.

- Figure (3.3), $x^{(\mathrm{iv})} = 0.2$.

- Figure (3.4), $x^{(\mathrm{iv})} = 0.5$.

The numbers on the right-hand side of each graph show the rupture time in hours (in the first column) and the non-dimensional position of rupture (in the second column).

To interpret the results it is useful to note that due to the choice of the values of the material parameters, the evolution equation can be written in the form

$$\psi_{,t} = -\left(\frac{B}{A}\right) \varrho_{11,t} \frac{1}{\psi^{k}} \tag{3.144}$$

where $k = 3$ within the heat affected zone and $k = 0$ in all the other regions. Note from the values (3.143) that because $B^{(\mathrm{iv})}$ is very much greater than B in any other region it is not surprising that the weld usually ruptures in the type IV region. This result is not unexpected since all the material parameters were taken from experiments related to type IV cracking.

From Figure (3.2) we see that the strong heat affected zone, restricts the strain-rate at $t = 0$, even when the type IV region is very weak $\left(A^{(\mathrm{iv})}/A^{(\mathrm{p})} = 10\right)$. So, for a thin type IV region the HAZ (Heat Affected Zone) is the dominant zone. In particular, the results show that the variation in the relative strength of the type IV region by a factor of 5 produces only a small variation in the initial value of the strain-rate $\varrho_{11,t}$. Equation (3.144) then suggests that (at $t = 0$) the magnitude of the damage rate $\psi_{,t}$ will decrease and hence the time to rupture will increase as $A^{(\mathrm{iv})}/A^{(\mathrm{p})}$ increases and the material gets weaker. The figures on the right-hand side of the graph confirm this trend. This behaviour is most surprising however and so it will be considered in more detail in section §3.8.

It should also be noted that in Figure (3.2) the position of rupture is at, or very close to, the interface between the parent material and the type IV region, which is the position of maximum strain-rate within this region at $t = 0$.

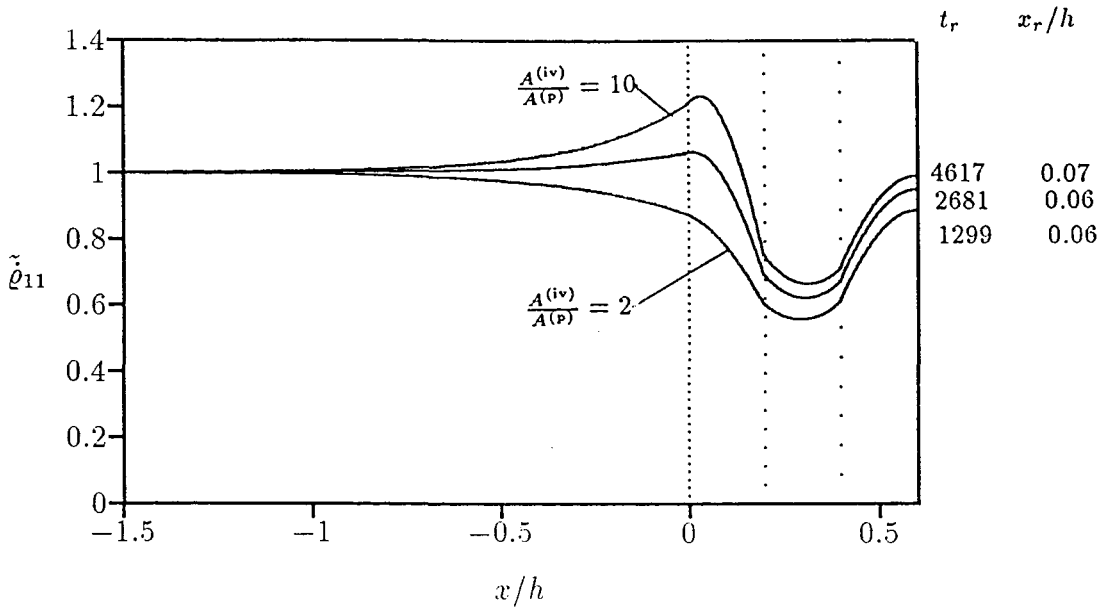

Figure 3.3: Strain-rates for various values of $A^{(iv)}/A^{(p)}$ with $x^{(iv)} = 0.2$

When the width of the type IV region is increased we observe from Figure (3.3) that the HAZ now has much less effect on restricting the initial strain-rate in the type IV region. Since the type IV region is very much weaker than the parent material, the strain-rate becomes larger and hence there is a decrease in rupture time compared with the analogous cases for the thinner type IV region shown in Figure (3.2). We observe again, however, that the increase in strain-rate as the material gets weaker is not so great as the factor by which the material weakens and so this produces a decrease in the magnitude of the rate of damage as the ratio $A^{(iv)}/A^{(p)}$ changes from 2 to 10, with a consequential increase in the time to rupture.

The results for a very wide type IV region confirm the same trend with the rupture time decreasing as the type IV material gets stronger. There is a considerable decrease in the rupture time for the wider zone $\left(x^{(iv)} = 0.5\right)$ compared to a thin zone of the same strength. We finally observe from Figure (3.4) that, not unexpectedly, the position of rupture tends to move towards the centre of the type IV region, the position of maximum

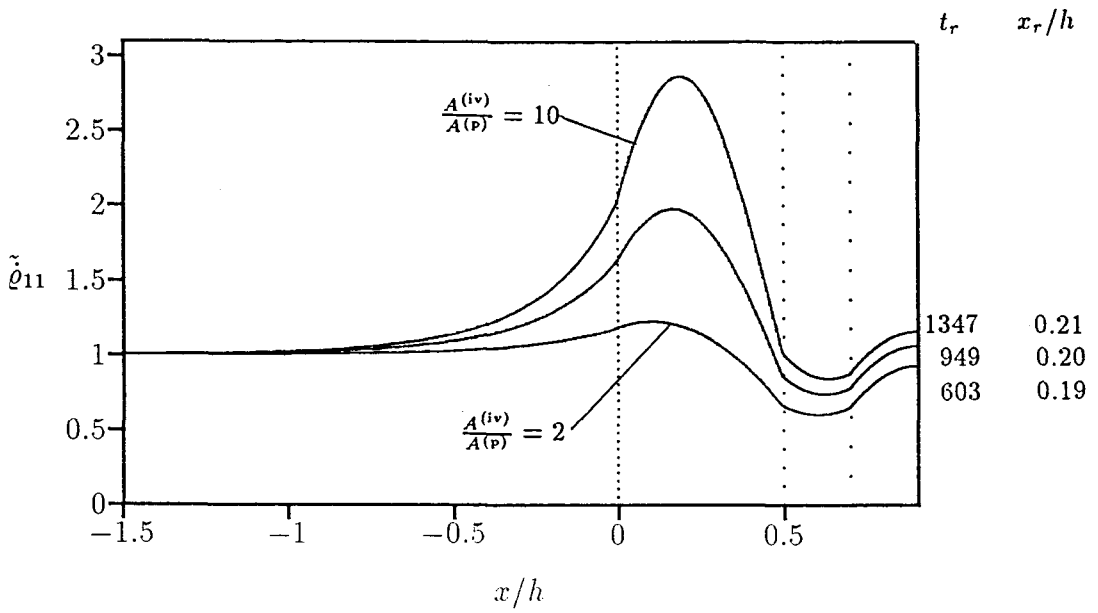

Figure 3.4: strain-rates for various values of $A^{(\mathrm{iv})}/A^{(\mathrm{p})}$ with $x^{(\mathrm{iv})} = 0.5$

strain-rate at $t = 0$.

We shall now consider varying the properties of the HAZ, the results of which are shown in Figures (3.5) to (3.7). We wish again to keep the other material properties of the type IV region and weld metal constant, so we retain the 'standard' values of $A^{(\mathrm{iv})}/A^{(\mathrm{p})} = 10$, $A^{(\mathrm{w})}/A^{(\mathrm{p})} = 3$, with the widths $x^{(\mathrm{iv})}$, $x^{(\mathrm{w})}$ being kept constant at 0.1 and 0.2 respectively. In all three figures the ratio $A^{(\mathrm{haz})}/A^{(\mathrm{p})}$ takes the values 1, 0.1 and 0.01, and the only difference in the values of the parameters used in obtaining the graphs concerns $x^{(\mathrm{haz})}$, which has the values:

- Figure (3.5), $x^{(\mathrm{haz})} = 0.05$,
- Figure (3.6), $x^{(\mathrm{haz})} = 0.2$,
- Figure (3.7), $x^{(\mathrm{haz})} = 0.5$.

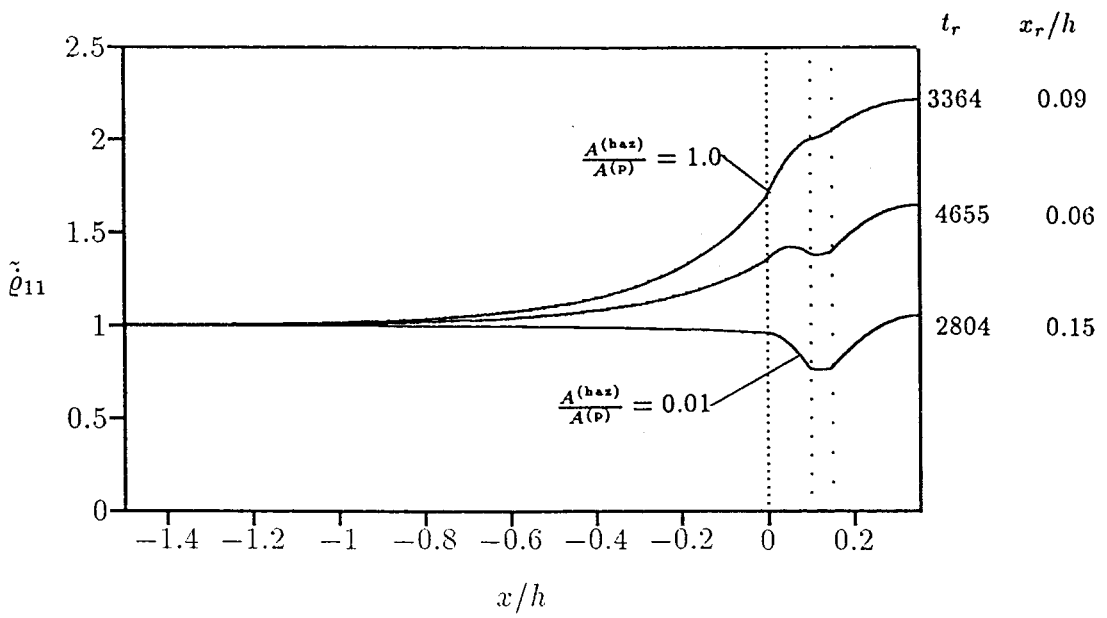

Figure 3.5: strain-rates for various values of $A^{(\mathrm{haz})}/A^{(\mathrm{p})}$ with $x^{(\mathrm{haz})} = 0.05$

We see in Figure (3.5) that as the HAZ gets stronger, from $A^{(\mathrm{haz})}/A^{(\mathrm{p})} = 1$ to $A^{(\mathrm{haz})}/A^{(\mathrm{p})} = 0.1$ the values of the initial strain-rate in each zone are lowered and the time to rupture is longer. This result appears at first sight to contradict the situation discussed above. However, we should emphasize that here we are varying the material properties of the HAZ and are keeping all material properties constant in the type IV region. Since the rupture occurs in the latter region it is only the effect on the strain-rate in the type IV region caused by varying the properties of the HAZ that determines the variation in failure time.

For the final curve in Figure (3.5), when the HAZ has been strengthened by another factor of 10, such that $A^{(\mathrm{haz})}/A^{(\mathrm{p})} = 0.01$, we observe surprisingly that the time to rupture actually decreases, and rupture now occurs at the interface between the HAZ and weld metal. This change in rupture position arises because in the situation under discussion

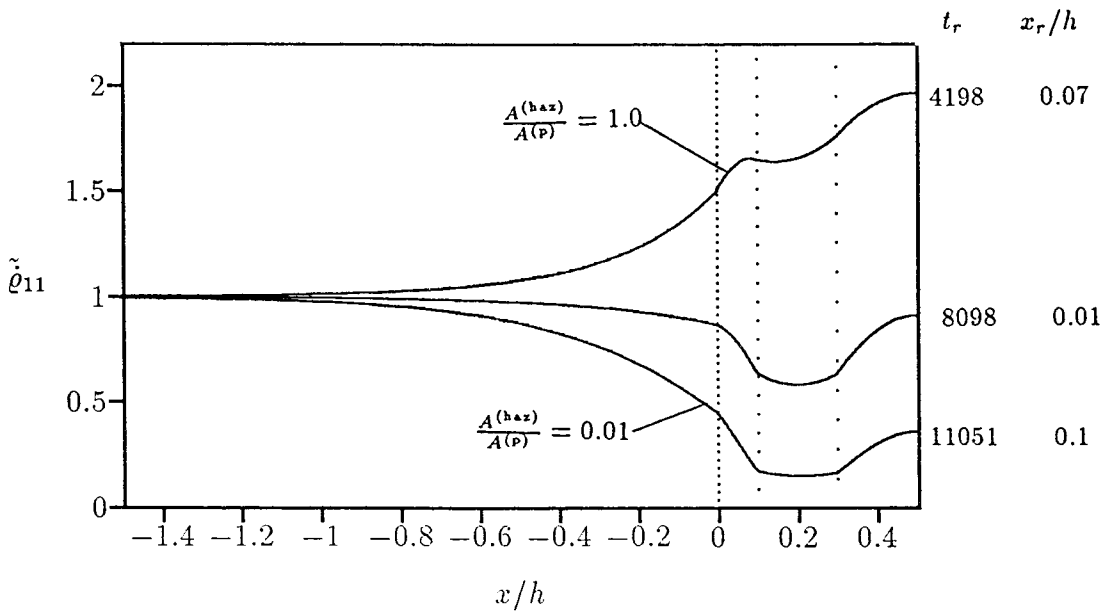

Figure 3.6: strain-rates for various values of $A^{(\mathrm{haz})}/A^{(\mathrm{p})}$ with $x^{(\mathrm{haz})} = 0.2$

the values of both

$$\frac{B^{(\mathrm{iv})}}{A^{(\mathrm{iv})}}\varrho_{11,t} \text{ and } \frac{B^{(\mathrm{haz})}}{A^{(\mathrm{haz})}}\varrho_{11,t},$$

in the type IV region and HAZ are comparable, and it is the presence of the ψ^3 term in equation (3.144) for the HAZ that causes the material to rupture in this zone.

In Figure (3.6) we display results for a wider HAZ with $x^{(\mathrm{haz})} = 0.2$. The results in Figure (3.6) show that all strengthenings of the HAZ lead to decreases in the strain-rates at $t = 0$ and increases in the times to rupture. The position of rupture switches from being inside the type IV region for the top two curves , to being at the interface between the type IV region and the HAZ for the final curve , with $A^{(\mathrm{haz})}/A^{(\mathrm{p})} = 0.01$. The reason for the switch is similar to that discussed in the previous paragraph but now the maximum value of the strain-rate within the HAZ is attained at its interface with the type IV region.

Results for an even wider HAZ $\left(x^{(\mathrm{haz})} = 0.5\right)$ are shown in Figure (3.7). In this figure the initial strain-rates are reduced even more and there is a subsequent increase in the

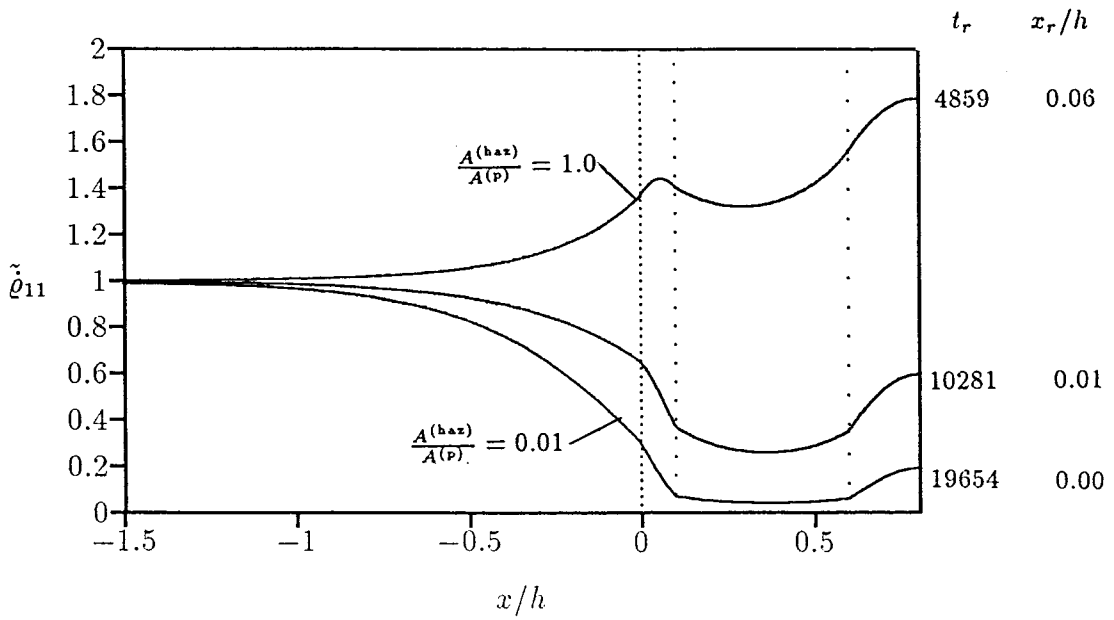

Figure 3.7: strain-rates for various values of $A^{(\mathrm{haz})}/A^{(\mathrm{p})}$ with $x^{(\mathrm{haz})} = 0.5$

rupture times. We observe that the position of rupture remains in the type IV region at the position of the maximum strain-rate (at $t = 0$).

In the penultimate group of results in this section we investigate how the rupture time changes when we vary the widths and properties of the weld metal. In all the Figures (3.8) to (3.10), we choose $A^{(\mathrm{iv})}/A^{(\mathrm{p})} = 10$, $A^{(\mathrm{haz})}/A^{(\mathrm{p})} = 0.1$, with the widths of these regions being $x^{(\mathrm{iv})} = 0.1$ and $x^{(\mathrm{haz})} = 0.2$. In each of the figures, $A^{(\mathrm{w})}/A^{(\mathrm{p})}$ takes the values 30, 3 and 0.3 respectively, but the values of $x^{(\mathrm{w})}$ varies as follows:-

- Figure (3.8), $x^{(\mathrm{w})} = 0.05$,
- Figure (3.9), $x^{(\mathrm{w})} = 0.2$,
- Figure (3.10), $x^{(\mathrm{w})} = 0.5$.

We note from Figure (3.8) that for a narrow weld region, the dominant feature of the complete weldment is the strength of the HAZ, which reduces the initial strain-rate

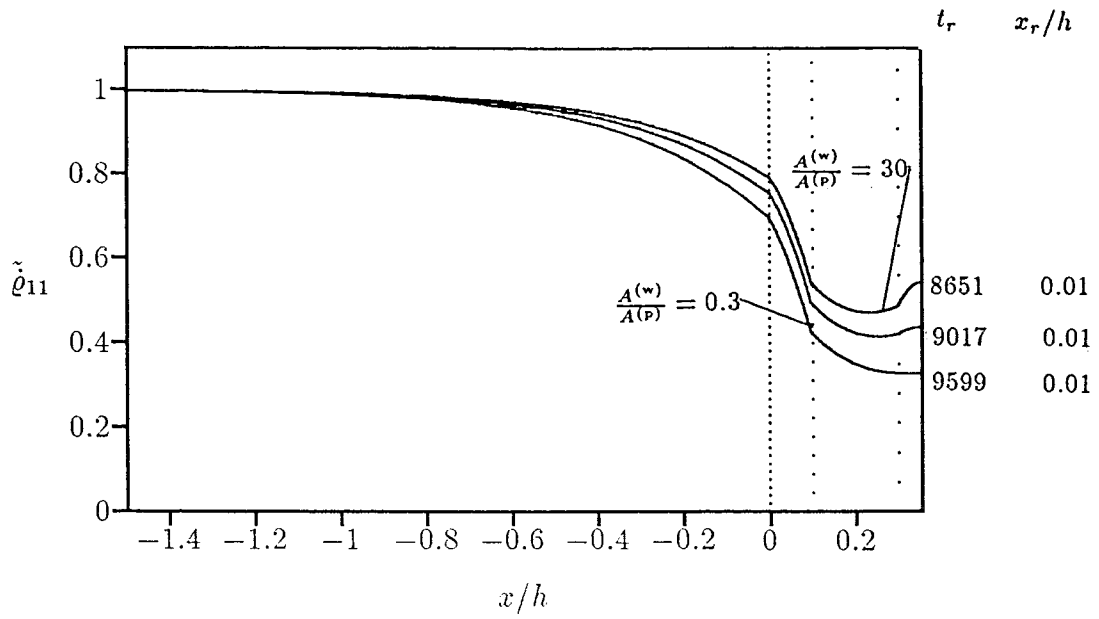

Figure 3.8: strain-rates for various values of $A^{(w)}/A^{(p)}$ with $x^{(w)} = 0.05$

dramatically. Moreover, since the width of the weld metal is very small, there is little opportunity for the strain-rate to increase in this region, even when the weld metal is very weak $\left(A^{(w)}/A^{(p)} = 30\right)$. Varying the strength of the weld, therefore, leads to little variation in the rupture time when the weld is narrow. Rupture still occurs in the type IV region.

If the width of the weld region is increased to $x^{(w)} = 0.2$ and $x^{(w)} = 0.5$ (Figures (3.9) and (3.10) respectively) we observe that, the strain-rate increases significantly, especially when the weld metal is very weak. However, even this large increase has only a minimal effect on the rupture time and, in the case of the strong weld material, there is virtually no change to the rupture time by widening the weld region. In both these situations, the changes in rupture time are small because $B^{(w)}$ is three orders of magnitude smaller than $B^{(iv)}$ (see (3.143)) and the large changes in strain-rate in the weld region are not sufficiently large to alter the overall rupture behaviour of the weldment.

In the final set of plots Figure (3.11), we examine the development of the strain-rate

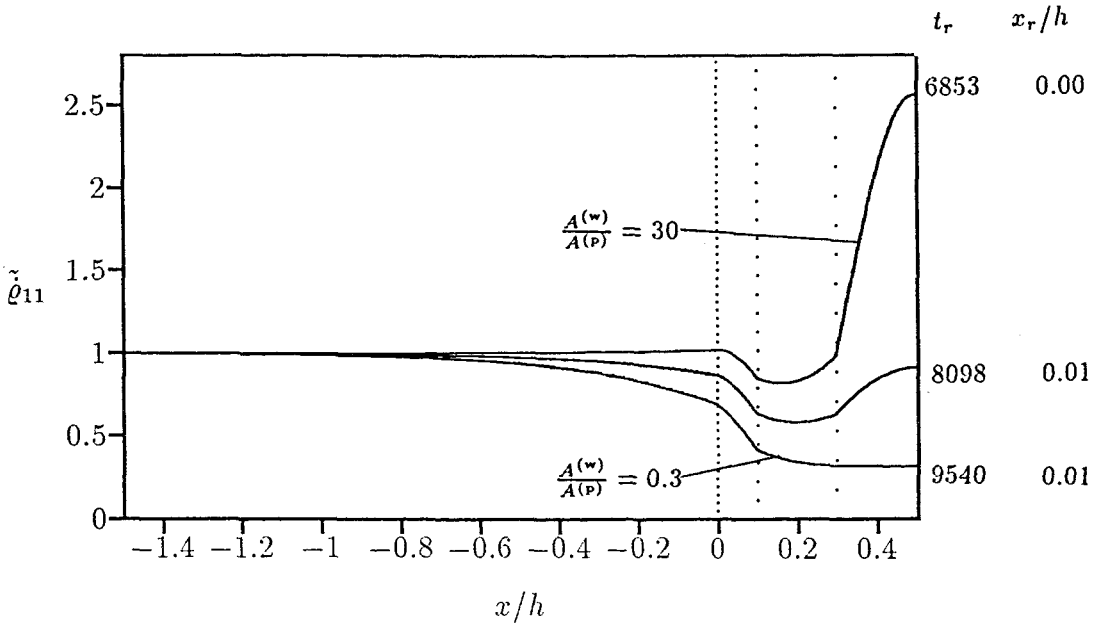

Figure 3.9: strain-rates for various values of $A^{(w)}/A^{(p)}$ with $x^{(w)} = 0.2$

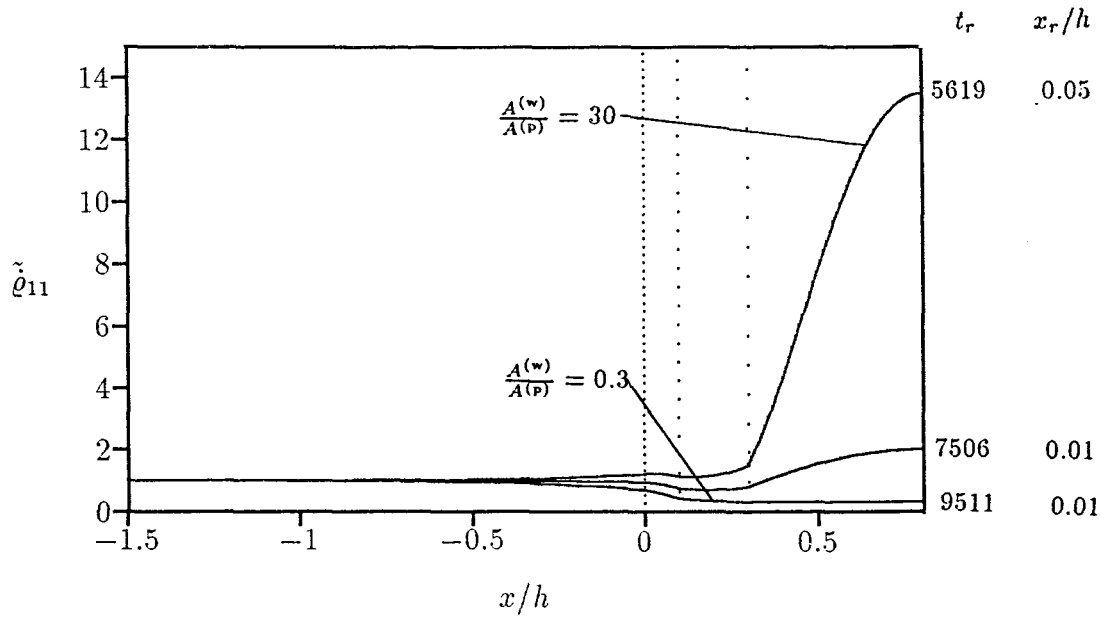

Figure 3.10: strain-rates for various values of $A^{(w)}/A^{(p)}$ with $x^{(w)} = 0.5$

at particular stages during the lifetime of the weld. The parameters chosen for the weld

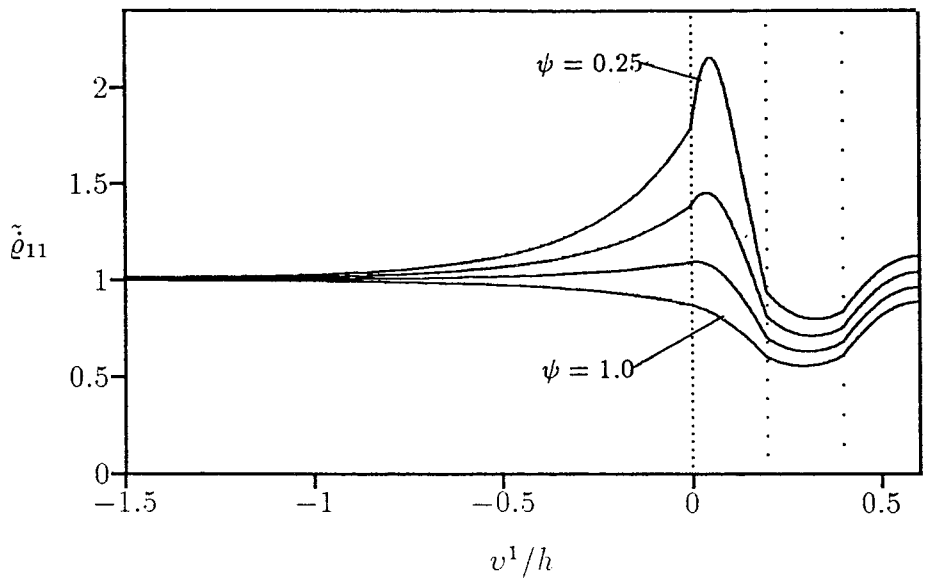

Figure 3.11: strain-rates at different stages of a weld's lifetime

are those represented in Figure (3.3) with $A^{(\mathrm{iv})}/A^{(\mathrm{p})} = 2$. It is not obvious from the graph of the initial strain-rates that the position of rupture will occur within the type IV region. In Figure (3.11) we plot the strain rates when the minimum value of ψ at some position in the weldment is ψ=1.0, 0.75, 0.5 and 0.25 respectively. We observe that although initially the position of maximum strain-rate in the type IV region is at the interface between the parent material and the type IV region, it subsequently moves to a location inside the type IV region.

3.8 Discussion of the Variation of the Rupture Times.

As noted in section §3.7, in the paragraph with discussion of Figure (3.2), when varying the material properties of the type IV region we were surprised to see that as the material gets softer the time to rupture increases, contrary to intuition which suggests that the rupture time should increase when the strength of the material increases. Recalling the

assumptions that were made for our material parameters, we note that the ratio $A^{(\mathrm{iv})}/A^{(\mathrm{p})}$ was allowed to take the values 10, 5 and 2 respectively, but the evolution parameter $B^{(\mathrm{iv})}$ was kept constant at 1.8×10^{-11}. Since both A and B are 'strength-dependent' parameters, however, it seems unrealistic to change one without some variation in the other. How changes in A and B should be connected is not obvious, but some indication can be found as follows.

In the simplest possible uniaxial damage model, we have

$$\varepsilon_{,t} = A\sigma^n \quad , \quad \psi_{,t} = -B\sigma^n. \tag{3.145}$$

If the stress, σ, is constant everywhere, then from $(3.145)_{(ii)}$

$$t_r = \frac{1}{B\sigma^n}, \tag{3.146}$$

where t_r represents the rupture time of the specimen. Experimentally it is found that

$$\varepsilon_{,t}\, t_r \approx constant, \tag{3.147}$$

and so from (3.145) and (3.147) it follows that

$$\frac{A}{B} \approx constant. \tag{3.148}$$

In practice it is found that the product $\varepsilon_{,t}\, t_r$ does vary a little as A is changed, and so we need to estimate this variation. As A increases the material becomes more ductile, both in terms of the rupture ductility and through the product $\varepsilon_{,t}\, t_r$ increasing. Hence, if A increases then A/B must increase slightly, which means that any changes in A must be greater, but only slightly greater than the corresponding changes in B.

To incorporate this effect into our model we assume that B is changed by a proportion p, of the change in A, i.e.

$$\frac{B - B_\circ}{B_\circ} = p\left(\frac{A - A_\circ}{A_\circ}\right). \tag{3.149}$$

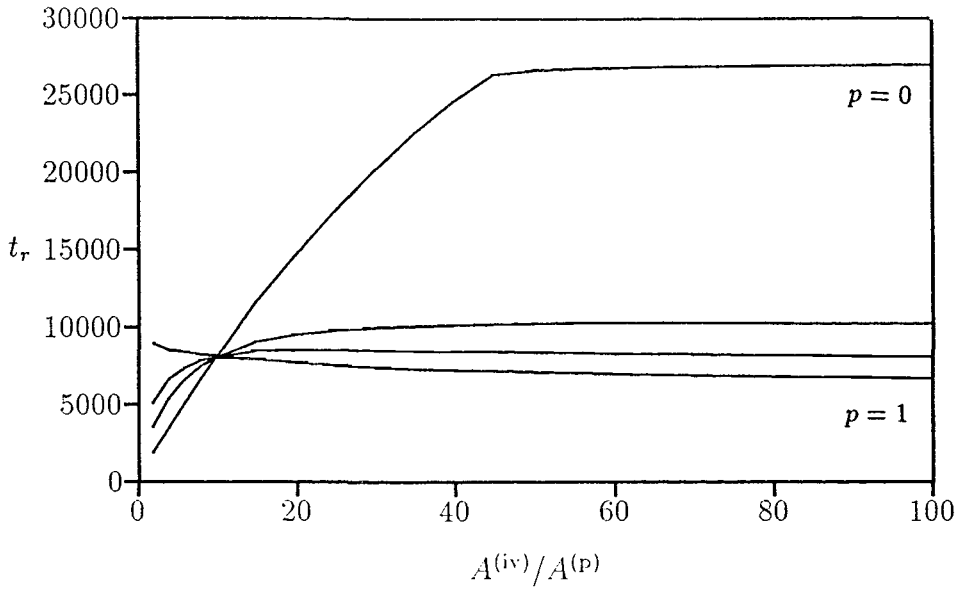

Figure 3.12: Effect of p on rupture times, with $x^{(iv)} = 0.1$

where B_o is the 'standard value' for the evolution parameter B as stated in (3.143) and A_o is the 'standard value' of the strength ratio $A^{(iv)}/A^{(p)}$. By varying the parameter p, between 0 and 1, we can observe the effect on the rupture times caused by this variation in ductility.

Figures (3.12) and (3.13) show what effect the variation in p has on the time to rupture. To obtain the graphs shown in Figure (3.12) we assume that $A^{(haz)}/A^{(p)} = 0.1$, $A^{(w)}/A^{(p)} = 3$, $x^{(iv)} = 0.1$, $x^{(haz)} = 0.2$ and $x^{(w)} = 0.2$. The ratio $A^{(iv)}/A^{(p)}$ is varied between 2 and 100, and $B^{(iv)}$ is changed according to the equation (3.149) with p taking the values 0, 0.6, 0.8 and 1.0 respectively. We see that the time to rupture varies considerably, and depending on the choice of p the rupture time can increase or decrease. Experimental results suggest that p is most likely to lie near the upper limit of its permissible range, $0 \leq p \leq 1$, in which case a weakening of the type IV region does not produce the significant increase in rupture time discussed earlier.

To obtain the results shown in Figure (3.13), the width of the type IV region has

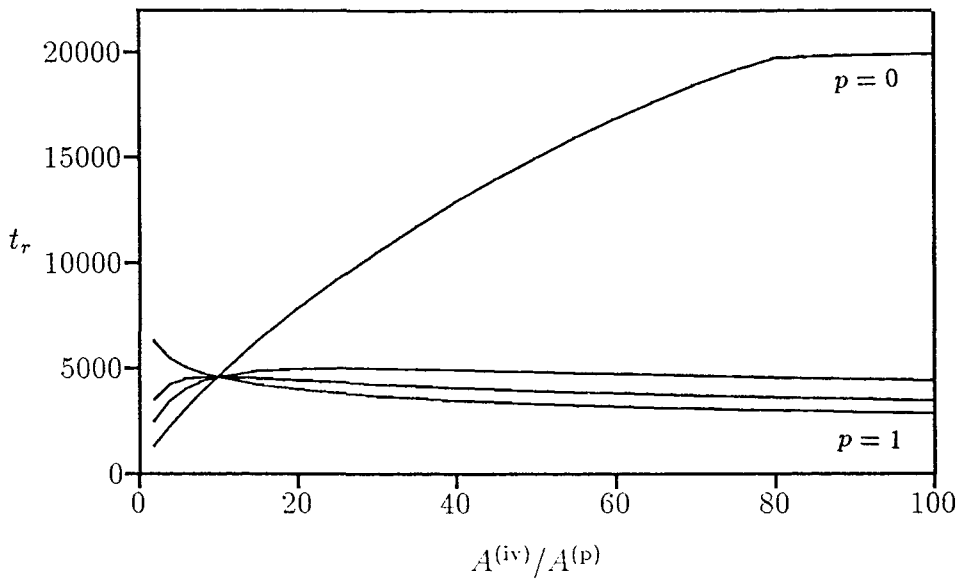

Figure 3.13: Effect of p on rupture times, with $x^{(iv)} = 0.2$

been doubled $\left(x^{(iv)} = 0.2\right)$, with all the other parameters retaining the values stated in the previous paragraph. The ratio $A^{(iv)}/A^{(p)}$ is again varied between 2 and 100. With $x^{(iv)} = 0.2$ now, the strain-rate within the type IV region will be increased with a consequential decrease in rupture time. Comparing Figure (3.13) with Figure (3.12) shows that for all values of p $(0 \leq p \leq 1)$, the rupture time will be less for the wider type IV region than for the corresponding narrow one. It is also evident from Figure (3.13) that as the material gets weaker, the sensitivity of the rupture time to the chosen value of p decreases.

3.9 An Alternative Evolution Model.

It has been suggested that the evolution equation (2.45) is not the most appropriate equation to model the damage associated with most types of materials, and a more suitable model requires in the damage evolution equation some combination of the maximum

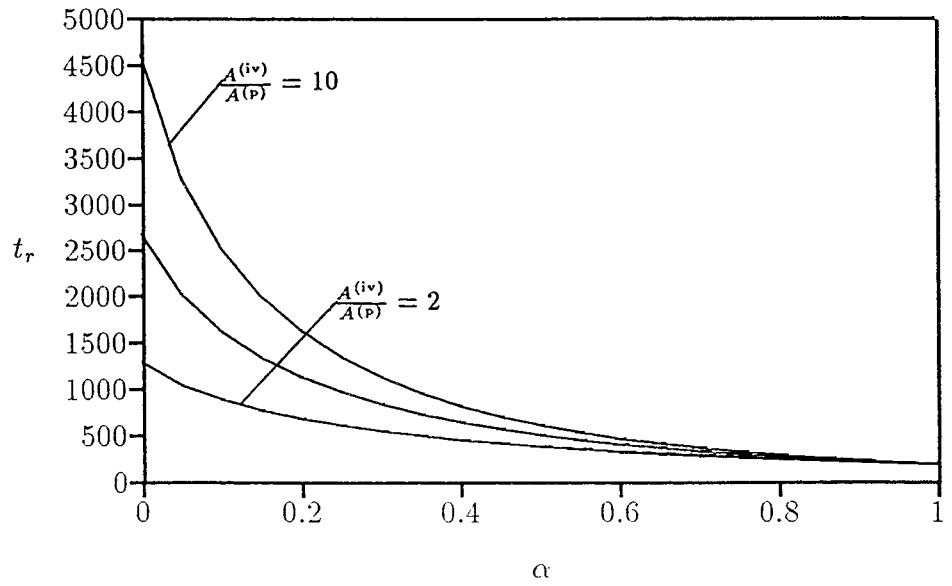

Figure 3.14: Variation in lifetimes using Hayhurst's evolution equation

principal stress $\sigma_{\max}$ and Von Mises equivalent stress σ^*, defined by (2.46) and (2.47). Hayhurst (1983) suggests that the evolution equation should take the form

$$\psi_{,t} = -\frac{B(\alpha\sigma_{\max} + (1-\alpha)\,\sigma^*)^m}{\psi^q}, \tag{3.150}$$

where α is a material dependent parameter. The equation (3.150) can be introduced into the numerical procedure with little alteration to the code.

Figure (3.14) shows the effect on the rupture time t_r due to the variation of the material parameter α, when the material parameters take the values $A^{(\mathrm{haz})}/A^{(\mathrm{p})} = 0.1$, $A^{(\mathrm{w})}/A^{(\mathrm{p})} = 3$, and the widths of the regions satisfy $x^{(\mathrm{iv})} = x^{(\mathrm{haz})} = x^{(\mathrm{w})} = 0.2$. The strength ratio of the type IV region $A^{(\mathrm{iv})}/A^{(\mathrm{p})}$ takes the values 10, 5 and 2 respectively in the three displayed graphs, but no change is made to the value of $B^{(\mathrm{iv})}$.

From Figure (3.14) we observe the convergence of the three graphs to a single value of the rupture time as $\alpha \to 1$. This result is expected since the maximum principal stress is N_{11} and from equation (3.39) $N_{11} = N_\infty$. Therefore, with the evolution equation

dependent only on N_∞ we will obtain a single rupture time regardless of the value of $A^{(\mathrm{iv})}/A^{(\mathrm{p})}$. If we had changed the evolution parameter $B^{(\mathrm{iv})}$ as discussed in §3.8, we would have observed three separate limits for the rupture time as $\alpha \to 1$, relating to each value of $A^{(\mathrm{iv})}/A^{(\mathrm{p})}$. It should be noted from Figure (3.14) that the introduction of this alternative evolution equation has dramatic effects on the time to rupture of the weldment.

Chapter 4

MATHEMATICAL MODEL OF A WELD WITH ZERO SHEAR STRESS ON THE TOP AND BOTTOM SURFACES

In previous work Hawkes (1989) and Nicol (1985) modelled the creep of a weld under simple uniaxial tension, by assuming that the three dimensional stress can be expressed as a linear expression in ξ, where ξ represents the co-ordinate normal to the reference surface of the plate. However, this assumption leads to the plate being subjected to a non-zero shear stress at the top and bottom surfaces of the plate and a more realistic model would be to introduce a stress distribution in the material such that there would be zero shear stress on the outer surfaces. The system can be modelled in this way by the introduction of a cubic expression in ξ for the stress components, but for a consistent theory it is then necessary to increase the number of directors. The derivation in this section is somewhat similar to chapter 5 of Hawkes' thesis.

4.1 Geometry of the Plate.

Introduce curvilinear co-ordinates (v^1, v^2, ξ) in the body. Let the position vector of some point on the central surface $\mathcal{S}$ of the plate, lying between the inner and outer surfaces of the plate, be $\mathbf{r}$. Referred to some fixed origin O, $\mathbf{r}$ has cartesian co-ordinates (x, y, z) given by

$$\mathbf{r} = x\mathbf{i} + y\mathbf{j} + z\mathbf{k}. \tag{4.1}$$

The curvilinear co-ordinates in the body need to be introduced such that the two-

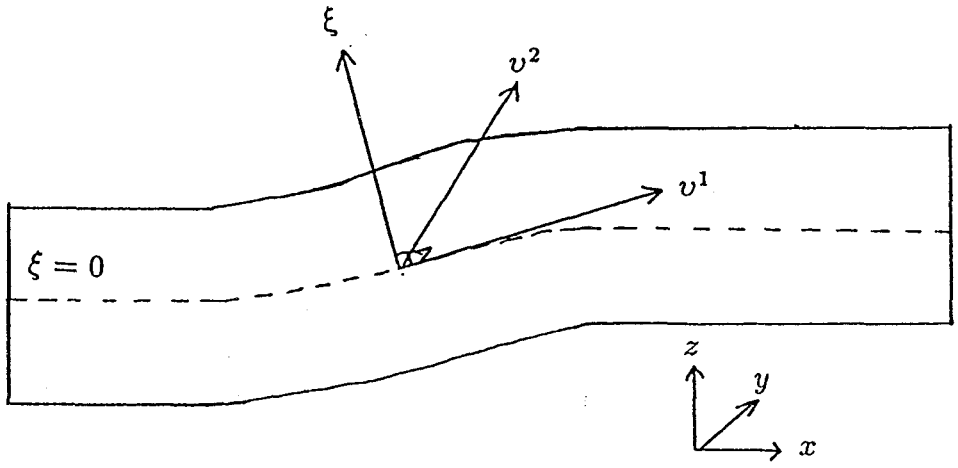

Figure 4.1: Geometry of a plate at time t

dimensional Cosserat surface lies strictly between the lower and upper surfaces of the plate and is given by

$$\xi = 0. \tag{4.2}$$

Let $f(v^1, t)$ be the position along the x-axis corresponding to a position v^1 along the v^1-axis. Also let $h(v^1, t)$ be the position along the z-axis corresponding to a position v^1, along the v^1-axis. The co-ordinate system can now be defined with the aid of Figure (4.1).

Suppose that v^2-axis lies parallel to j, in the plane of the (possibly deformed) Cosserat surface. Then let the v^1-axis be perpendicular to the v^2-axis such that it too lies in the plane of the Cosserat surface $\mathcal{S}$. Finally the ξ-axis lies in the direction of the outward facing normal to the surface, such that (v^1, v^2, ξ) form a right-handed co-ordinate system. With these definitions we obtain

$$x = f\left(v^1, t\right),$$

$$y = v^2, \tag{4.3}$$

$$z = h\left(v^1, t\right),$$

and hence the position vector $\mathbf{r}$ can be expressed in terms of the new convected co-ordinates, using equations (4.1) and (4.3), by

$$\mathbf{r} = f\left(v^1, t\right)\mathbf{i} + v^1\mathbf{j} + h\left(v^1, t\right)\mathbf{k}. \tag{4.4}$$

If $\mathbf{R}$ represents the position vector at $t = 0$, then it is clear that for an initially flat plate

$$\mathbf{R}\left(v^1, v^2\right) = \mathbf{r}\left(v^1, v^2, 0\right) = v^1\mathbf{i} + v^2\mathbf{j}, \tag{4.5}$$

and therefore at $t = 0$, we can identify v^1, v^2 with x and y respectively.

Assuming that the displacement of the Cosserat surface from its initial position is small, we can introduce a small parameter ϵ. Then, $f\left(v^1, t\right)$ and $h\left(v^1, t\right)$ can be expanded as series in ϵ about their initial values and the linearised version of (4.4) can be expressed as

$$\mathbf{r} = \left(v^1 + \epsilon f_1\left(v^1, t\right)\right)\mathbf{i} + v^2\mathbf{j} + \left(\epsilon h_1\left(v^1, t\right)\right)\mathbf{k}. \tag{4.6}$$

We observe that for (4.6) to reduce to (4.5) at $t = 0$ we require that

$$f_1\left(v^1, 0\right) = h_1\left(v^1, 0\right) = 0. \tag{4.7}$$

Using equation $(2.25)_{(i)}$ and (4.6), the linearized base vectors on the surface can be written

$$\mathbf{a}_1 = \left(1 + \epsilon f_{1,1}\right)\mathbf{i} + \left(\epsilon h_{1,1}\right)\mathbf{k}, \tag{4.8}$$

$$\mathbf{a}_2 = \mathbf{j}, \tag{4.9}$$

where $_{,1}$ represents differentiation with respect to the material co-ordinate v^1 and likewise $_{,2}$ represents differentiation with respect to the material co-ordinate v^2. With the aid of

equations (2.26), (4.8) and (4.9) the unit normal vector to the surface can be calculated to be

$$\mathrm{a}_3 = \left(-\epsilon h_{1,1}\right)\mathrm{i} + \mathrm{k}. \tag{4.10}$$

It should be noted that in the above expressions for a_i, terms of $O(\epsilon^2)$ and higher are ignored. From equations (2.29) and (4.8) to (4.9) the components $a_{\alpha\beta}$ can be calculated:

$$\begin{aligned} a_{11} &= 1 + 2\epsilon f_{1,1} + O\left(\epsilon^2\right), \\ a_{12} &= a_{21} = 0, \\ a_{22} &= 1. \end{aligned} \tag{4.11}$$

It will be useful to calculate the (contravariant) reciprocal base vectors a^α, but first the matrix $(a_{\alpha\beta})$ must be inverted to obtain, correct to first order in ϵ,

$$\left(a^{\alpha\beta}\right) = \begin{pmatrix} 1 - 2\epsilon f_{1,1} & 0 \\ 0 & 1 \end{pmatrix}. \tag{4.12}$$

Hence, on using (2.30), the contravariant base vectors, again neglecting terms of $O(\epsilon^2)$, become

$$\mathrm{a}^1 = \left(1 - \epsilon f_{1,1}\right)\mathrm{i} + \left(\epsilon h_{1,1}\right)\mathrm{k}, \tag{4.13}$$

$$\mathrm{a}^2 = \mathrm{j}, \tag{4.14}$$

from which it can be deduced that a^3, defined by

$$\mathrm{a}^3 = \frac{\mathrm{a}^1 \times \mathrm{a}^2}{|\mathrm{a}^1 \times \mathrm{a}^2|}, \tag{4.15}$$

can be expressed

$$\mathrm{a}^3 = \mathrm{a}_3 = \left(-\epsilon h_{1,1}\right)\mathrm{i} + \mathrm{k}. \tag{4.16}$$

It is important, for later use, to invert the base vectors and derive expressions for i, j and k in terms of the covariant and contravariant base vectors respectively. Performing the relevant algebra we obtain, correct to first order

$$\begin{aligned} \mathrm{i} &= \left(1 - \epsilon f_{1,1}\right) \mathrm{a}_1 - \left(\epsilon h_{1,1}\right) \mathrm{a}_3, \\ \mathrm{j} &= \mathrm{a}_2, \\ \mathrm{k} &= \left(\epsilon h_{1,1}\right) \mathrm{a}_1 + \mathrm{a}_3. \end{aligned} \tag{4.17}$$

Similarly in terms of the contravariant base vectors we have

$$\begin{aligned} \mathrm{i} &= \left(1 + \epsilon f_{1,1}\right) \mathrm{a}^1 - \left(\epsilon h_{1,1}\right) \mathrm{a}^3, \\ \mathrm{j} &= \mathrm{a}^2, \\ \mathrm{k} &= \left(\epsilon h_{1,1}\right) \mathrm{a}^1 + \mathrm{a}^3. \end{aligned} \tag{4.18}$$

From the definitions of the Christoffel symbols (2.36) and the expressions (4.8), (4.9), and (4.13)–(4.16), the only non-zero component can be shown to be

$$\Gamma^1_{11} = \epsilon f_{1,11} + O\left(\epsilon^2\right). \tag{4.19}$$

Similarly , to first order, the only non-zero components of the second fundamental form $b_{\alpha\beta}$, defined by (2.33), are

$$b_{11} = \epsilon h_{1,11} = b^1_1. \tag{4.20}$$

If $B_{\alpha\beta}$ are the values of $b_{\alpha\beta}$ in the initial configuration then it follows immediately using (4.7) that

$$B_{\alpha\beta} = 0, \tag{4.21}$$

as required for an initially flat plate.

Before deriving the required kinematic results, we should point out that in this section we have considered a model for a semi-infinite plate which is initially flat but has a central

surface which may deform with time. This basic geometry is similar to that employed later in this thesis in the model for the 'V-shaped' weld.

4.2 Kinematic Results.

For a consistent theory including the more general expressions for the stress components $\sigma^{\alpha\beta}$ it is necessary to include at least three directors. Hence, it is assumed that the position vector p, of the deformed plate is given by

$$\mathrm{p} = \mathrm{r} + \sum_{N=1}^{3} \xi^N \mathrm{d}_{(N)}. \tag{4.22}$$

On differentiating (4.22) we obtain

$$\mathrm{g}_\alpha = \mathrm{a}_\alpha + \sum_{N=1}^{3} \xi^N \mathrm{d}_{(N),\alpha}, \tag{4.23}$$

$$\mathrm{g}_3 = \sum_{N=1}^{3} N\xi^{N-1} \mathrm{d}_{(N)}. \tag{4.24}$$

Since we are assuming small deformation, it is possible to expand the directors about their original values which, in terms of their components, take the form

$$d_{(N)i} = D_{(N)i} + \epsilon\delta_{(N)i} + O\left(\epsilon^2\right). \tag{4.25}$$

It should be noted that the initial values of the director components are

$$\begin{aligned} D_{(N)\gamma} &= D_{(N)}{}^{\gamma} = 0 \ , \quad N = 1,2,3 \ , \\ D_{(1)3} &= D_{(1)}{}^{3} = 1 \ , \\ D_{(N)3} &= D_{(N)}{}^{3} = 0 \ , \quad N = 2,3 \ , \end{aligned} \tag{4.26}$$

as this defines with (2.62) every point within the plate at $t = 0$. In this work we also assume the plane strain condition, which in turn implies that there is no variation of

quantities in the v^2 direction. Hence, we can assume that

$$d_{(N)2} = constant = 0 \ , \quad N = 1, 2, 3. \tag{4.27}$$

With the above assumptions it follows from (4.23) and (4.24) that

$$\begin{aligned} \mathrm{g}_1 &= \left[1 + \epsilon\left(f_{1,1} + \xi\left[\delta_{(1)1_{,1}} - h_{1,11}\right] + \xi^2\delta_{(2)1_{,1}} + \xi^3\delta_{(3)1_{,1}}\right)\right]\mathrm{i} \\ &\quad + \left[\epsilon\left(h_{1,1} + \xi\delta_{(1)3_{,1}} + \xi^2\delta_{(2)3_{,1}} + \xi^3\delta_{(3)3_{,1}}\right)\right]\mathrm{k}, \end{aligned} \tag{4.28}$$

$$\mathrm{g}_2 = \mathrm{j}, \tag{4.29}$$

$$\begin{aligned} \mathrm{g}_3 &= \left[\epsilon\left(\delta_{(1)1} - h_{1,1} + 2\xi\delta_{(2)1} + 3\xi^2\delta_{(3)1}\right)\right]\mathrm{i}, \\ &\quad + \left[1 + \epsilon\left(\delta_{(1)3} + 2\xi\delta_{(2)3} + 3\xi^2\delta_{(3)3}\right)\right]\mathrm{k}. \end{aligned} \tag{4.30}$$

The kinematic variables $\varrho_{\alpha\beta}$, $\kappa_{(N)\alpha\beta}$, $\kappa_{(N)\alpha 3}$ and $\gamma_{(N)i}$, defined by (2.71) to (2.73), have time derivatives

$$\dot{\varrho}_{11} = \epsilon\dot{f}_{1,1}, \tag{4.31}$$

$$\dot{\varrho}_{12} = \dot{\varrho}_{21} = \dot{\varrho}_{22} = 0, \tag{4.32}$$

$$\dot{\kappa}_{(1)11} = \epsilon\left(\dot{\delta}_{(1)1_{,1}} - \dot{h}_{1,11}\right), \tag{4.33}$$

$$\dot{\kappa}_{(2)11} = \epsilon\dot{\delta}_{(2)1_{,1}}, \tag{4.34}$$

$$\dot{\kappa}_{(3)11} = \epsilon\dot{\delta}_{(3)1_{,1}}, \tag{4.35}$$

$$\dot{\kappa}_{(N)12} = \dot{\kappa}_{(N)21} = \dot{\kappa}_{(N)22} = 0, \tag{4.36}$$

$$\dot{\kappa}_{(N)13} = \epsilon\dot{\delta}_{(N)3_{,1}}, \tag{4.37}$$

$$\dot{\kappa}_{(N)23} = 0, \tag{4.38}$$

$$\dot{\gamma}_{(N)1} = \epsilon\dot{\delta}_{(N)1}, \tag{4.39}$$

$$\dot{\gamma}_{(N)2} = 0, \tag{4.40}$$

$$\dot{\gamma}_{(N)3} = \epsilon\dot{\delta}_{(N)3}. \tag{4.41}$$

To complete the set of the kinematic results we can use equations (4.28) to (4.30) with $(2.14)_{(ii)}$ to calculate components g_{ij}:

$$g_{11} = 1 + 2\epsilon\left(f_{1,1} + \xi\left[\delta_{(1)1_{,1}} - h_{1,11}\right] + \xi^2\left[\delta_{(2)1_{,1}}\right] + \xi^3\left[\delta_{(3)1_{,1}}\right]\right), \tag{4.42}$$

$$g_{12} = g_{21} = 0, \tag{4.43}$$

$$g_{22} = 1, \tag{4.44}$$

$$g_{23} = g_{32} = 0, \tag{4.45}$$

$$g_{13} = g_{13} = \epsilon\left(\delta_{(1)1} + \xi\left[2\delta_{(2)1} + \delta_{(1)3_{,1}}\right] + \xi^2\left[3\delta_{(3)1} + \delta_{(2)3_{,1}}\right] + \xi^3\left[\delta_{(3)3_{,1}}\right]\right), \tag{4.46}$$

$$g_{33} = 1 + 2\epsilon\left(\delta_{(1)3} + \xi\left[2\delta_{(2)3}\right] + \xi^2\left[3\delta_{(3)3}\right]\right), \tag{4.47}$$

again neglecting terms of $O(\epsilon^2)$. It is now possible to calculate the components of the three dimensional strain-rate $\dot{\gamma}^*_{ij}$ either by substituting (4.42)–(4.47) into the equation (2.80) and differentiating with respect to time or, alternatively, by substituting the kinematic results (4.31) to (4.41) directly into the expressions (2.81)–(2.83). Either method leads to the results

$$\dot{\gamma}^*_{11} = \epsilon\left(\dot{f}_{1,1} + \xi\left[\dot{\delta}_{(1)1_{,1}} - \dot{h}_{1,11}\right] + \xi^2\left[\dot{\delta}_{(2)1_{,1}}\right] + \xi^3\left[\dot{\delta}_{(3)1_{,1}}\right]\right), \tag{4.48}$$

$$\dot{\gamma}^*_{12} = \dot{\gamma}^*_{21} = \dot{\gamma}^*_{22} = \dot{\gamma}^*_{23} = \dot{\gamma}^*_{32} = 0, \tag{4.49}$$

$$\dot{\gamma}^*_{13} = \frac{\epsilon}{2}\left(\dot{\delta}_{(1)1} + \xi\left[2\dot{\delta}_{(2)1} + \dot{\delta}_{(1)3_{,1}}\right] + \xi^2\left[3\dot{\delta}_{(3)1} + \dot{\delta}_{(2)3_{,1}}\right] + \xi^3\left[\dot{\delta}_{(3)3_{,1}}\right]\right), \tag{4.50}$$

$$\dot{\gamma}^*_{33} = \epsilon\left(\dot{\delta}_{(1)3} + \xi\left[2\dot{\delta}_{(2)3}\right] + \xi^2\left[3\dot{\delta}_{(3)3}\right]\right). \tag{4.51}$$

4.3 Calculation of the Two-Dimensional Stress Components.

Next we must introduce the two-dimensional generalised stress measures appropriate to the Cosserat theory with three directors. It can be shown by using the definitions (2.90) in the expressions (2.102) and (2.112) that the two-dimensional stress measures are related to the components of the three-dimensional stress tensor σ^{ij} through the expressions

$$\mathbf{N}^{\alpha} a^{\frac{1}{2}} = \int_{-\frac{h}{2}}^{\frac{h}{2}} g^{\frac{1}{2}} \sigma^{\alpha j} \mathbf{g}_j \, d\xi, \tag{4.52}$$

$$\mathbf{M}^{(N)\alpha} a^{\frac{1}{2}} = \int_{-\frac{h}{2}}^{\frac{h}{2}} g^{\frac{1}{2}} \xi^N \sigma^{\alpha j} \mathbf{g}_j \, d\xi, \tag{4.53}$$

$$\mathbf{m}^{(N)} a^{\frac{1}{2}} = N \int_{-\frac{h}{2}}^{\frac{h}{2}} g^{\frac{1}{2}} \xi^{N-1} \sigma^{3j} \mathbf{g}_j \, d\xi \ , \ (N = 1, 2, 3). \tag{4.54}$$

Taking the dot product of (4.52) to (4.54) with the contravariant base vectors $\mathbf{a}^i$ yields the equations linking the components of the two-dimensional stress measures to the three-dimensional stress tensor through

$$N^{\alpha i} a^{\frac{1}{2}} = \int_{-\frac{h}{2}}^{\frac{h}{2}} g^{\frac{1}{2}} \sigma^{\alpha j} \left(\mathbf{g}_j \cdot \mathbf{a}^i \right) d\xi, \tag{4.55}$$

$$M^{(N)\alpha i} a^{\frac{1}{2}} = \int_{-\frac{h}{2}}^{\frac{h}{2}} g^{\frac{1}{2}} \xi^N \sigma^{\alpha j} \left(\mathbf{g}_j \cdot \mathbf{a}^i \right) d\xi, \tag{4.56}$$

$$m^{(N)i} a^{\frac{1}{2}} = N \int_{-\frac{h}{2}}^{\frac{h}{2}} g^{\frac{1}{2}} \xi^{N-1} \sigma^{3j} \left(\mathbf{g}_j \cdot \mathbf{a}^i \right) d\xi \ , \ (N = 1, 2, 3). \tag{4.57}$$

The above equations can be simplified by assuming that the expected small deformations are associated with small three-dimensional stresses and hence with small generalised two-dimensional stresses. These assumptions suggest that we redefine our stress variables by

$$\sigma^{ij} = \epsilon \tilde{\sigma}^{ij} \ , \ N^{\alpha i} = \epsilon \tilde{N}^{\alpha i} \ , \ M^{(N)\alpha i} = \epsilon \tilde{M}^{(N)\alpha i} \ , \ m^{(N)i} = \epsilon \tilde{m}^{(N)i}. \tag{4.58}$$

It follows then that we only require the leading order terms in the expressions for $a^{\frac{1}{2}}$, $g^{\frac{1}{2}}$

and $(\mathbf{g}_j \cdot \mathbf{a}^i)$. From (4.8), (4.9), (4.28) to (4.30) and (4.42) to (4.47) we can deduce that

$$a^{\frac{1}{2}} = 1 + O(\epsilon), \tag{4.59}$$

$$g^{\frac{1}{2}} = 1 + O(\epsilon), \tag{4.60}$$

$$\mathbf{g}^j \cdot \mathbf{a}_i = \delta^i_j + O(\epsilon). \tag{4.61}$$

With the simplifications (4.59) to (4.61), the definitions (4.55) to (4.57) become

$$\tilde{N}^{\alpha i} = \int_{-\frac{h}{2}}^{\frac{h}{2}} \tilde{\sigma}^{\alpha i} d\xi, \tag{4.62}$$

$$\tilde{M}^{(N)\alpha i} = \int_{-\frac{h}{2}}^{\frac{h}{2}} \xi^N \tilde{\sigma}^{\alpha i} d\xi, \tag{4.63}$$

$$\tilde{m}^{(N)i} = N \int_{-\frac{h}{2}}^{\frac{h}{2}} \xi^{N-1} \tilde{\sigma}^{3i} d\xi \quad , \quad (N = 1, 2, 3). \tag{4.64}$$

In future we shall ignore the $\tilde{}$ and for simplicity we have set $\epsilon = 1$, with no loss of generality.

We now wish to represent the three-dimensional stress components by power series in ξ, and in this chapter assume

$$\sigma^{\alpha i} = a^{\alpha i} + b^{\alpha i}\xi + c^{\alpha i}\xi^2 + d^{\alpha i}\xi^3 + O\left(\xi^4\right), \tag{4.65}$$

$$\sigma^{3i} = a^{3i} + b^{3i}\xi + c^{3i}\xi^2 + O\left(\xi^3\right). \tag{4.66}$$

Once again it is convenient to use a model in which the polynomial for σ^{3i} has order one less than the polynomial for $\sigma^{\alpha i}$. Substituting (4.65)–(4.66) into (4.62)–(4.64) and solving the resulting set of simultaneous equations for a^{ij}, b^{ij}, c^{ij} and $d^{\alpha i}$ leads to the results

$$a^{\alpha i} = \frac{9}{4h} N^{\alpha i} - \frac{15}{h^3} M^{(2)\alpha i}, \tag{4.67}$$

$$b^{\alpha i} = \frac{75}{h^3} M^{(1)\alpha i} - \frac{420}{h^5} M^{(3)\alpha i}, \tag{4.68}$$

$$c^{\alpha i} = -\frac{15}{h^3}N^{\alpha i} + \frac{180}{h^5}M^{(2)\alpha i}, \tag{4.69}$$

$$d^{\alpha i} = -\frac{420}{h^5}M^{(1)\alpha i} + \frac{2800}{h^7}M^{(3)\alpha i}, \tag{4.70}$$

$$a^{3i} = \frac{9}{4h}m^{(1)i} - \frac{5}{h^3}m^{(3)i}, \tag{4.71}$$

$$b^{3i} = \frac{6}{h^3}m^{(2)i}, \tag{4.72}$$

$$c^{3i} = -\frac{15}{h^3}m^{(1)i} + \frac{60}{h^5}m^{(3)i}. \tag{4.73}$$

The plate is under simple uniaxial tension, which causes no bending of the central surface, and so all stress and strain terms relating to flexural motion are identically zero:

$$\dot{\kappa}_{(1)\alpha\beta} = \dot{\kappa}_{(3)\alpha\beta} = \dot{\kappa}_{(2)\alpha 3} = \dot{\gamma}_{(1)\alpha} = \dot{\gamma}_{(3)\alpha} = \dot{\gamma}_{(2)3} = 0, \tag{4.74}$$

$$N^{\alpha 3} = M^{(1)\alpha\beta} = M^{(3)\alpha\beta} = M^{(2)\alpha 3} = m^{(1)\alpha} = m^{(3)\alpha} = m^{(2)3} = 0. \tag{4.75}$$

In addition there will be no torsional effects and the associated stresses can be assumed to be zero, that is

$$N^{12} = N^{21} = M^{(N)12} = M^{(N)21} = 0. \tag{4.76}$$

Finally, we observe that the plane strain condition implies that there is no variation of stress within planes normal to the v^2-direction and so we can take

$$M^{(N)23} = m^{(N)2} = 0 \tag{4.77}$$

It is important to point out that it is not essential to make the above assumptions at this stage, since the statements (4.74) to (4.77) would all follow naturally from the theory. However by introducing the results now the algebra that follows is considerably simplified.

With the simplifications (4.74) to (4.77) and substituting the values a^{ij}, b^{ij}, c^{ij} and $d^{\alpha i}$ from (4.67)–(4.73) into (4.65)–(4.66) we obtain the explicit definitions for the components of the three-dimensional stress tensor in terms of the non-zero components of

two-dimensional generalised stresses to be

$$\sigma^{11} = \frac{9}{4h}N^{11} - \frac{15}{h^3}M^{(2)11} + \xi^2\left(-\frac{15}{h^3}N^{11} + \frac{180}{h^5}M^{(2)11}\right), \tag{4.78}$$

$$\sigma^{12} = \sigma^{21} = 0, \tag{4.79}$$

$$\sigma^{22} = \frac{9}{4h}N^{22} - \frac{15}{h^3}M^{(2)22} + \xi^2\left(-\frac{15}{h^3}N^{22} + \frac{180}{h^5}M^{(2)22}\right), \tag{4.80}$$

$$\sigma^{23} = \sigma^{32} = 0, \tag{4.81}$$

$$\sigma^{13} = \xi\left(\frac{75}{h^3}M^{(1)13} - \frac{420}{h^5}M^{(3)13}\right) + \xi^2\left(-\frac{420}{h^5}M^{(1)13} + \frac{2800}{h^7}M^{(3)13}\right), \tag{4.82}$$

$$\sigma^{31} = \xi\left(\frac{6}{h^3}m^{(2)1}\right) \tag{4.83}$$

$$\sigma^{33} = \frac{9}{4h}m^{(1)3} - \frac{5}{h^3}m^{(3)3} + \xi^2\left(-\frac{15}{h^3}m^{(1)3} + \frac{60}{h^5}m^{(3)3}\right). \tag{4.84}$$

The method used to derive the constitutive equations in the following sections is different to that employed in chapter 3 of this thesis. The method we use below was first suggested by Nicol (1985) and was developed further by Hawkes (1989) in chapters 5 and 6 of his thesis.

4.4 Derivation of the Constitutive Equations.

Before presenting the derivation of the multi-axial form of Norton's Law for general tensors in any co-ordinate system, and the corresponding generalised form of Norton's Law used in Cosserat theory, we need to discuss briefly the concept of physical tensors.

4.4.1 Physical Tensors.

For an extended discussion on the physical components of tensors the reader is referred to the text by Eringen (1967) and, in particular, to the article by Truesdell (1953) in which he defines physical components of tensors in non-orthogonal co-ordinate systems. It is necessary to know relationships between the contravariant and covariant components of

a tensor and the components used in mathematical physics, since tensor components will often not have the same physical dimension as the vector field to which they belong.

The right physical components of a second order tensor can be defined as

$$a_{<ij>} = \sqrt{\frac{g_{ii}}{g_{jj}}} a^i{}_j \quad \text{(unsummed)}, \tag{4.85}$$

and for the left physical components

$${}_{<ij>}a = \sqrt{\frac{g_{ii}}{g_{jj}}} a_j{}^i \quad \text{(unsummed)}. \tag{4.86}$$

It is clear from (4.85) and (4.86) that there is a relationship between left and right physical components of a mixed tensor $a^i{}_j$ such that

$${}_{<ij>}a = \sqrt{\frac{g_{ii}g_{ll}}{g_{jj}g_{kk}}} g_{jk} g^{il} a_{<kl>} \quad (i,j \text{ unsummed}). \tag{4.87}$$

It then follows that in an orthogonal co-ordinate system the left physical components of a tensor field equal the right physical components and both are given by

$${}_{<ij>}a = a_{<ij>} = \sqrt{\frac{g_{ii}}{g_{jj}}} a^i{}_j = \sqrt{\frac{g_{jj}}{g_{ii}}} a_i{}^j = \sqrt{g_{ii}g_{jj}}\, a^{ij} \quad (i,j \text{ unsummed}). \tag{4.88}$$

4.4.2 Derivation of the Kachanov-Rabotnov Equations.

To derive the multi-axial form of the Kachanov-Rabotnov equations, we first state the five postulates generally used (see Odqvist (1974) for more details). The five postulates are:

1. The material is incompressible.

2. The creep rate is independent of superimposed hydrostatic pressure.

3. A flow potential exists.

4. The material is isotropic (which implies the co-axiality of the stress and strain-rate tensors).

5. The Kachanov-Rabotnov equations hold in the special case of uniaxial stress.

Hayhurst (1983) adds that we must also assume that the influence of continuum damage on the creep deformation rate is scalar in character.

In a general co-ordinate system the stress deviator tensor can be defined in terms of right physical tensors through

$$s_{<ij>} = \sigma_{<ij>} - \frac{1}{3}\delta_{<ij>}\sigma_{<kk>}. \tag{4.89}$$

Then, using (4.85), the stress deviator tensor can be written as a mixed mode tensor

$$s^i{}_j = \sigma^i{}_j - \frac{1}{3}\delta^i{}_j\sigma^k_k. \tag{4.90}$$

The rate of dissipation $\dot{W}$ is a scalar invariant and hence can be written in terms of the physical components of the stress and strain rate tensors through

$$\dot{W} = \sigma_{<ij>}\dot{\gamma}^*_{<ji>} = \sigma^i{}_j\dot{\gamma}^{*j}{}_i. \tag{4.91}$$

By varying the dissipation $\dot{W}$, while keeping the strain-rate tensor constant, we obtain

$$\delta\dot{W} = \delta s^i{}_j\dot{\gamma}^{*j}_i, \tag{4.92}$$

where we have used (4.89) and the incompressibility equation. It follows immediately that

$$\dot{\gamma}^{*j}{}_i = \frac{\partial\dot{W}}{\partial s^i{}_j}. \tag{4.93}$$

One of the postulates introduced at the beginning of this section was that $\dot{W}$ is a flow potential, i.e. it is dependent on some scalar function σ^* of the components of the stress deviator tensor only. In general $\dot{W}$ will depend on the three invariants of the stress

tensor. The first invariant is identically zero, however, and Johnson (1951) has shown that the dependence on the third invariant is negligible. Hence, $\dot{W}$ will depend only on the second invariant σ^*, which may be written in terms of the physical components of the stress deviator tensor as

$$(\sigma^*)^2 = \frac{3}{2} s_{<kl>} s_{<lk>} = \frac{3}{2} s^k{}_l s^l{}_k. \tag{4.94}$$

Carrying out the differentiation in (4.93), we obtain

$$\begin{aligned} \dot{\gamma}^{*j}{}_i &= \frac{d\dot{W}}{d\sigma^*} \frac{\partial \sigma^*}{\partial s^i{}_j} = \frac{d\dot{W}}{d\sigma^*} \frac{1}{2\sigma^*} \frac{\partial (\sigma^*)^2}{\partial s^i{}_j}, \\ &= \frac{1}{2\sigma^*} \frac{d\dot{W}}{d\sigma^*} \frac{3}{2} \left(s^k{}_l \frac{\partial s^l{}_k}{\partial s^i{}_j} + s^l{}_k \frac{\partial s^k{}_l}{\partial s^i{}_j} \right), \end{aligned} \tag{4.95}$$

using equation (4.94). The dummy variables k and l can be swapped in the final term of (4.95) to reduce equation (4.95) to

$$\dot{\gamma}^{*j}{}_i = \frac{3}{2\sigma^*} \frac{d\dot{W}}{d\sigma^*} s^k{}_l \frac{\partial s^l{}_k}{\partial s^i{}_j}. \tag{4.96}$$

On introducing the mixed mode form of the Kronecker delta tensor

$$\delta^l_k = \begin{cases} 1, & l = k, \\ 0, & l \neq k, \end{cases} \tag{4.97}$$

we can reduce equation (4.96) to

$$\dot{\gamma}^{*j}{}_i = \frac{3}{2\sigma^*} \frac{d\dot{W}}{d\sigma^*} s^k{}_l \, \delta^l_i \, \delta^j_k = \frac{3}{2\sigma^*} \frac{d\dot{W}}{d\sigma^*} s^j{}_i. \tag{4.98}$$

A necessary requirement for equation (4.98) is that it reduces in the uniaxial case to the mixed tensor form of the Kachanov-Rabotnov equation, that is

$$\dot{\gamma}^*{}_1{}^1 = A \frac{(\sigma^1{}_1)^n}{\psi^p}. \tag{4.99}$$

For a uniaxial stress

$$s^1{}_1 = \frac{2}{3}\sigma^1{}_1 = \frac{2}{3}\sigma^*, \tag{4.100}$$

hence on comparing (4.98) and (4.99) we deduce that

$$\frac{d\dot{W}}{d\sigma^*} = A\frac{(\sigma^*)^n}{\psi^p}. \tag{4.101}$$

On substituting the result (4.101) into equation (4.98) we determine the mixed mode form of one of the Kachanov-Rabotnov equations as

$$\dot{\gamma}^{*i}{}_j = \frac{3}{2}A\frac{(\sigma^*)^{n-1}}{\psi^p}s^i{}_j. \tag{4.102}$$

The second Kachanov-Rabotnov equation has the simple form

$$\dot{\psi} = -B\frac{(\sigma^*)^m}{\psi^q}. \tag{4.103}$$

Next, we wish to apply the multi-axial constitutive equations (4.102) and (4.103) to problems in Cosserat shell theory. Nicol (1985) generalised the multi-axial form of Norton's Law (equation (4.102) with $\psi = 1$) for the case of a single director and a plate that is initially flat. Hawkes (1989) extended this work to include three directors and general tensors. The derivation presented here will generalise both these earlier approaches and will include the basic concepts of continuum damage mechanics.

The constitutive equations must be derived in forms that are invariant under rigid body transformations. This requires that the equations must be written in terms of variables which are invariant under rigid body transformations. Naghdi (1972) notes that the variables

$$N'^{\alpha\beta}, M^{(N)\alpha i}, m^{(N)i}, \dot{\varrho}_{\alpha\beta}, \dot{\kappa}_{(N)\alpha i}, \dot{\gamma}_{(N)i}, \tag{4.104}$$

where we have defined

$$N'^{\alpha\beta} = N'^{\beta\alpha} = N^{\alpha\beta} - \sum_{N=1}^{\infty}\left(m^{(N)\alpha}d_{(N)}{}^{\beta} + M^{(N)\gamma\alpha}\lambda_{(N)}{}^{\beta}_{\gamma}\right), \tag{4.105}$$

are all invariant under rigid body transformations and hence constitute a suitable set of variables with which to derive the constitutive equations.

The sets of generalised stresses and strains, Ψ and Φ respectively are defined by

$$\begin{aligned} \Psi &= \left(N'^{\alpha\beta}, M^{(N)\alpha i}, m^{(N)i}\right), \\ \Phi &= \left(\varrho_{\alpha\beta}, \kappa_{(N)\alpha i}, \gamma_{(N)i}\right). \end{aligned} \tag{4.106}$$

We define a flow potential f by

$$\Psi \cdot \dot{\Phi} = f, \tag{4.107}$$

from which we can deduce that

$$\dot{\Phi} = \frac{\partial f}{\partial \Psi}. \tag{4.108}$$

We introduce an invariant analogous to σ^*, through

$$(N^*)^2 = h \int_\alpha^\beta (\sigma^*)^2 \, d\xi, \tag{4.109}$$

where the values of α and β can be calculated using (2.58) and (2.59).

Assuming that the flow potential is a function of N^* only and performing the differentiation in (4.108) we obtain

$$\dot{\Phi} = \frac{df}{dN^*}\frac{\partial N^*}{\partial \Psi} = \frac{1}{2N^*}\frac{df}{dN^*}\frac{\partial (N^*)^2}{\partial \Psi}. \tag{4.110}$$

It is necessary that the Kachanov-Rabotnov equations reduce for the simple case of uniaxial tension to

$$\dot{\varrho}_{11} = A\left(\frac{N^{11}}{\sigma_c h}\right)^n \frac{1}{\psi^p}, \tag{4.111}$$

and

$$\dot{\psi} = -B\left(\frac{N^{11}}{\sigma_c h}\right)^m \frac{1}{\psi^q}, \tag{4.112}$$

where σ_c is any constant value of stress.

Under simple uniaxial tension, we have $N^* = N^{11}$ and hence comparing (4.110) and (4.111) we deduce that

$$\frac{df}{dN^*} = A\left(\frac{N^*}{\sigma_c h}\right)^n \frac{1}{\psi^p}. \tag{4.113}$$

Finally substituting the result (4.113) into (4.110) we obtain the generalised form of the Kachanov-Rabotnov equations, appropriate for use in a Cosserat shell theory, to be

$$\dot{\Phi} = \frac{A}{2\sigma_c h}\left(\frac{N^*}{\sigma_c h}\right)^{n-1} \frac{1}{\psi^p} \frac{\partial (N^*)^2}{\partial \Psi}, \tag{4.114}$$

and

$$\dot{\psi} = -B\left(\frac{N^*}{\sigma_c h}\right)^m \frac{1}{\psi^q}. \tag{4.115}$$

Before continuing with the analysis to obtain an appropriate model for an initially flat plate, with zero stress on the top and bottom surfaces of the plate, we wish to examine briefly the continuity equation associated with the problem under discussion.

4.5 Continuity Equations.

The equations of continuity are given by

$$\nabla \cdot \mathbf{v}^* = \frac{1}{\sqrt{g}} \frac{\partial}{\partial v^k} \left(\sqrt{g} v^{*k}\right) = 0, \tag{4.116}$$

where

$$\mathbf{v}^* = \dot{\mathbf{r}} + \sum_{N=1}^{3} \xi^N \dot{\mathbf{d}}_{(N)}, \tag{4.117}$$

the superposed dot representing differentiation with respect to time. On using (4.6), (4.25) and (4.26) in (4.117), we obtain

$$\mathbf{v}^* = \epsilon \left[\left(\dot{f}_1 + \xi^2 \dot{\delta}_{(2)1}\right)\mathbf{i} + \left(\dot{h}_1 + \xi \dot{\delta}_{(1)3} + \xi^3 \dot{\delta}_{(3)3}\right)\mathbf{k}\right]. \tag{4.118}$$

By observing from (4.17) that to leading order the base vectors $\mathbf{a}_1$ and $\mathbf{a}_3$ are identical to $\mathbf{i}$ and $\mathbf{k}$ respectively, then the components of the velocity are given by

$$v^{*1} = \dot{f}_1 + \xi^2 \dot{\delta}_{(2)1}, \tag{4.119}$$

$$v^{*2} = 0, \tag{4.120}$$

$$v^{*3} = \dot{h}_1 + \xi \dot{\delta}_{(1)3} + \xi^3 \dot{\delta}_{(3)3}. \tag{4.121}$$

Substituting equations (4.119) to (4.121) into the continuity equation (4.116) we obtain

$$\dot{f}_{1,1} + \xi^2 \dot{\delta}_{(2)1_{,1}} + \dot{\delta}_{(1)3} + 3\xi^2 \dot{\delta}_{(3)3} = 0. \tag{4.122}$$

On integrating equation (4.122) through the plate with respect to ξ, between the limits $-\frac{h}{2} \leq \xi \leq \frac{h}{2}$, we obtain the continuity equation as

$$\dot{f}_{1,1} + \dot{\delta}_{(1)3} + \frac{h^2}{12}\left(\dot{\delta}_{(2)1_{,1}} + 3\dot{\delta}_{(3)3}\right) = 0. \tag{4.123}$$

4.6 Analysis.

As stated in the introduction to this chapter, we wish to impose the condition that the three-dimensional stress tensor defined by (4.78) to (4.84) is identically zero on the top and bottom surfaces of the plate, that is

$$\sigma^{13}|_{\xi=\pm\frac{h}{2}} = \sigma^{31}|_{\xi=\pm\frac{h}{2}} = 0. \tag{4.124}$$

Clearly for the condition (4.124) to hold then we must require that

$$M^{(3)13} = \frac{3h^2}{28} M^{(1)13}, \tag{4.125}$$

It is also necessary that the three-dimensional stress tensor is symmetrical for all ξ, which from (4.82) to (4.83) would lead to the relationships

$$M^{(3)13} = \frac{3h^2}{20} M^{(1)13}, \tag{4.126}$$

and

$$m^{(2)1} = 2M^{(1)13}. \tag{4.127}$$

We now observe that conditions (4.125) and (4.126) are only satisfied if $M^{(1)13} = M^{(3)13} = 0$. Using these results it can be shown that the model collapses so we must relax one of our constraints. The aim of this chapter is to produce a model of a weld with a zero stress distribution on the top and bottom surfaces of the plate and so it seems sensible that the constraint on the symmetry of the stress will have to be amended.

As an alternative constraint we require that the difference between σ^{13} and σ^{31} when integrated through the plate between the limits $\frac{h}{2}$ and $-\frac{h}{2}$ is zero. This requires examination of

$$\int_{-\frac{h}{2}}^{\frac{h}{2}} \left(\sigma^{13} - \sigma^{31}\right) \xi \, d\xi = 0, \tag{4.128}$$

which leads again to the condition (4.127). Thus we wish to modify the Von Mises equivalent stress by

$$(\sigma_1^*)^2 = (\sigma^*)^2 + \lambda_1 \left(\sigma^{13} - \sigma^{31}\right) \xi + \lambda_2 \left(\sigma^{13}|_{\xi=\frac{h}{2}}\right), \tag{4.129}$$

where λ_1 and λ_2 are two Lagrange multipliers. From (4.129), redefine N^* through the integral

$$(N^*)^2 = h \int_{-\frac{h}{2}}^{\frac{h}{2}} (\sigma_1^*)^2 d\xi. \tag{4.130}$$

On substituting the expressions (4.78) to (4.84) for the three-dimensional stress tensor in terms of the two-dimensional generalised stresses into (4.129), using (4.94) and noting the equivalence of contravariant and covariant tensors in the present co-ordinate system we obtain, after performing the integration (4.130),

$$\begin{aligned}
(N^*)^2 &= \frac{9}{4}\left(N^{11}\right)^2 + \frac{9}{4}\left(N^{22}\right)^2 + \frac{9}{4}\left(N^{11}N^{22}\right) + \frac{180}{h^4}\left(M^{(2)11}\right)^2 + \frac{180}{h^4}\left(M^{(2)22}\right)^2 \\
&- \frac{180}{h^4}\left(M^{(2)11}M^{(2)22}\right) + \frac{9}{4}\left(m^{(1)3}\right)^2 - \frac{9}{4}\left(N^{11}m^{(1)3}\right) - \frac{9}{4}\left(N^{22}m^{(1)3}\right) \\
&+ \frac{15}{h^2}\left(M^{(2)11}m^{(1)3}\right) - \frac{30}{h^2}\left(N^{11}M^{(2)11}\right) + \frac{15}{h^2}\left(N^{22}M^{(2)11}\right) + \frac{15}{h^2}\left(m^{(1)3}M^{(2)22}\right)
\end{aligned}$$

$$
\begin{aligned}
&+ \frac{5}{h^2}\left(N^{11}m^{(3)3}\right) + \frac{15}{h^2}\left(N^{11}M^{(2)22}\right) - \frac{30}{h^2}\left(N^{22}M^{(2)22}\right) - \frac{10}{h^2}\left(m^{(1)3}m^{(3)3}\right) \\
&+ \frac{5}{h^2}\left(N^{22}m^{(3)3}\right) - \frac{60}{h^4}\left(M^{(2)22}m^{(3)3}\right) + \frac{20}{h^4}\left(m^{(3)3}\right)^2 - \frac{60}{h^4}\left(M^{(2)11}m^{(3)3}\right) \\
&+ \frac{225}{2h^2}\left(M^{(1)13}\right)^2 - \frac{1260}{h^4}\left(M^{(1)13}M^{(3)13}\right) + \frac{4200}{h^6}\left(M^{(3)13}\right)^2 + \frac{9}{2h^2}\left(m^{(2)1}\right)^2 \\
&+ \lambda_1 h\left(2M^{(1)13} - m^{(2)1}\right) + \lambda_2\left(3M^{(1)13} - \frac{28}{h^2}M^{(3)13}\right). \qquad (4.131)
\end{aligned}
$$

Provided that (4.125) and (4.127) hold, then the terms involving the Lagrange multipliers in (4.131) are identically zero.

We can now apply the constitutive equations derived in section §4.4, by using (4.131) in (4.114) with the expressions for the kinematic variables given by (4.31) to (4.41). Neglecting terms of $O(\epsilon^2)$, we obtain the following system of equations

$$
\begin{aligned}
\dot{f}_{1,1} &= \frac{A}{2\sigma_c h}\left(\frac{N^*}{\sigma_c h}\right)^{n-1}\frac{1}{\psi^p}\left(\frac{9}{2}N^{11} - \frac{9}{4}N^{22} - \frac{9}{4}m^{(1)3}\right. \\
&- \left.\frac{30}{h^2}M^{(2)11} + \frac{5}{h^2}m^{(3)3} + \frac{15}{h^2}M^{(2)22}\right), \qquad (4.132) \\
0 &= \frac{A}{2\sigma_c h}\left(\frac{N^*}{\sigma_c h}\right)^{n-1}\frac{1}{\psi^p}\left(\frac{9}{2}N^{22} - \frac{9}{4}N^{11} - \frac{9}{4}m^{(1)3}\right. \\
&+ \left.\frac{15}{h^2}M^{(2)11} - \frac{30}{h^2}M^{(2)22} + \frac{5}{h^2}m^{(3)3}\right), \qquad (4.133) \\
\dot{\delta}_{(2)1,1} &= \frac{A}{2\sigma_c h}\left(\frac{N^*}{\sigma_c h}\right)^{n-1}\frac{1}{\psi^p}\left(\frac{360}{h^4}M^{(2)11} - \frac{180}{h^4}M^{(2)22} + \frac{15}{h^2}m^{(1)3}\right. \\
&- \left.\frac{30}{h^2}N^{11} + \frac{15}{h^2}N^{22} - \frac{60}{h^4}m^{(3)3}\right), \qquad (4.134) \\
0 &= \frac{A}{2\sigma_c h}\left(\frac{N^*}{\sigma_c h}\right)^{n-1}\frac{1}{\psi^p}\left(\frac{360}{h^4}M^{(2)22} - \frac{180}{h^4}M^{(2)11} + \frac{15}{h^2}m^{(1)3}\right. \\
&+ \left.\frac{15}{h^2}N^{11} - \frac{30}{h^2}N^{22} - \frac{60}{h^4}m^{(3)3}\right), \qquad (4.135) \\
\dot{\delta}_{(1)3,1} &= \frac{A}{2\sigma_c h}\left(\frac{N^*}{\sigma_c h}\right)^{n-1}\frac{1}{\psi^p}\left(\frac{225}{h^2}M^{(1)13} - \frac{1260}{h^4}M^{(3)13} + 2\lambda_1 h + 3\lambda_2\right), \qquad (4.136)
\end{aligned}
$$

$$\dot{\delta}_{(3)3,1} = \frac{A}{2\sigma_c h}\left(\frac{N^*}{\sigma_c h}\right)^{n-1}\frac{1}{\psi^p}\left(-\frac{1260}{h^4}M^{(1)13}+\frac{8400}{h^6}M^{(3)13}-\frac{28}{h^2}\lambda_2\right), \quad (4.137)$$

$$\dot{\delta}_{(1)3} = \frac{A}{2\sigma_c h}\left(\frac{N^*}{\sigma_c h}\right)^{n-1}\frac{1}{\psi^p}\left(\frac{9}{2}m^{(1)3}-\frac{9}{4}N^{11}-\frac{9}{4}N^{22}\right.$$
$$\left. + \frac{15}{h^2}M^{(2)11}+\frac{15}{h^2}M^{(2)22}-\frac{10}{h^2}m^{(3)3}\right), \quad (4.138)$$

$$\dot{\delta}_{(2)1} = \frac{A}{2\sigma_c h}\left(\frac{N^*}{\sigma_c h}\right)^{n-1}\frac{1}{\psi^p}\left(\frac{9}{h^2}m^{(2)1}-\lambda_1 h\right), \quad (4.139)$$

$$\dot{\delta}_{(3)3} = \frac{A}{2\sigma_c h}\left(\frac{N^*}{\sigma_c h}\right)^{n-1}\frac{1}{\psi^p}\left(\frac{5}{h^2}N^{11}-\frac{10}{h^2}m^{(1)3}+\frac{5}{h^2}N^{22}\right.$$
$$\left. - \frac{60}{h^4}M^{(2)22}+\frac{40}{h^4}m^{(3)3}-\frac{60}{h^4}M^{(2)11}\right). \quad (4.140)$$

Observe from equations (4.132) to (4.140) that the displacement of the central surface $h_1(v^1,t)$ has disappeared from the problem. This is due to the central surface remaining flat for all time t.

It can be shown from equations (4.133) and (4.135) that

$$N^{22} = \frac{1}{2}\left(N^{11}+m^{(1)3}\right), \quad (4.141)$$

and

$$M^{(2)22} = \frac{1}{2}M^{(2)11}+\frac{1}{6}m^{(3)3}. \quad (4.142)$$

Hence, with the aid of results (4.141) and (4.142), N^{22} and $M^{(2)22}$ can be eliminated from the remaining differential equations (4.132), (4.134), (4.138) and (4.140) to give

$$\dot{f}_{1,1} = \frac{A}{2\sigma_c h}\left(\frac{N^*}{\sigma_c h}\right)^{n-1}\frac{1}{\psi^p}\left(\frac{27}{8}N^{11}-\frac{27}{8}m^{(1)3}-\frac{45}{2h^2}M^{(2)11}+\frac{15}{2h^2}m^{(3)3}\right), \quad (4.143)$$

$$\dot{\delta}_{(2)1,1} = \frac{A}{2\sigma_c h}\left(\frac{N^*}{\sigma_c h}\right)^{n-1}\frac{1}{\psi^p}\left(\frac{270}{h^4}M^{(2)11}-\frac{90}{h^4}m^{(3)3}-\frac{45}{2h^2}N^{11}+\frac{45}{2h^2}m^{(1)3}\right), \quad (4.144)$$

$$\dot{\delta}_{(1)3} = \frac{A}{2\sigma_c h}\left(\frac{N^*}{\sigma_c h}\right)^{n-1}\frac{1}{\psi^p}\left(\frac{27}{8}m^{(1)3}-\frac{27}{8}N^{11}+\frac{45}{2h^2}M^{(2)11}-\frac{15}{2h^2}m^{(3)3}\right), \quad (4.145)$$

$$\dot{\delta}_{(3)3} = \frac{A}{2\sigma_c h}\left(\frac{N^*}{\sigma_c h}\right)^{n-1}\frac{1}{\psi^p}\left(\frac{15}{2h^2}N^{11}-\frac{15}{2h^2}m^{(1)3}-\frac{90}{h^4}M^{(2)11}+\frac{30}{h^4}m^{(3)3}\right). \quad (4.146)$$

It is trivial to show that (4.143) to (4.146) satisfy the continuity equation (4.123).

From (2.140) to (2.143) the field equations for an initially flat plate, with no body forces, corresponding to a three director model are

$$N^{11}{}_{,1} = 0, \tag{4.147}$$

$$M^{(2)11}{}_{,1} = m^{(2)1}, \tag{4.148}$$

$$M^{(1)13}{}_{,1} = m^{(1)3}, \tag{4.149}$$

$$M^{(3)13}{}_{,1} = m^{(3)3}. \tag{4.150}$$

To complete the system we also have the evolution equation given by (4.103).

The Lagrange multipliers can be eliminated from the system using (4.137) and (4.139) and on applying the constraints (4.125) and (4.127) the system reduces to

$$\begin{aligned} \dot{f}_{1,1} = -\dot{\delta}_{(1)3} &= \frac{A}{2\sigma_c h}\left(\frac{N^*}{\sigma_c h}\right)^{n-1}\frac{1}{\psi^p}\left(\frac{27}{8}N^{11}\right. \\ &- \left.\frac{18}{7}m^{(1)3} - \frac{45}{2h^2}M^{(2)11}\right), \end{aligned} \tag{4.151}$$

$$\begin{aligned} \dot{\delta}_{(2)1}{}_{,1} = -3\dot{\delta}_{(3)3} &= \frac{A}{2\sigma_c h}\left(\frac{N^*}{\sigma_c h}\right)^{n-1}\frac{1}{\psi^p}\left(\frac{270}{h^4}M^{(2)11}\right. \\ &+ \left.\frac{90}{7h^2}m^{(1)3} - \frac{45}{2h^2}N^{11}\right), \end{aligned} \tag{4.152}$$

$$\dot{\delta}_{(1)3}{}_{,1} + \frac{3h^2}{28}\dot{\delta}_{(3)3}{}_{,1} = \frac{A}{2\sigma_c h}\left(\frac{N^*}{\sigma_c h}\right)^{n-1}\frac{1}{\psi^p}\left(\frac{612}{7h^2}M^{(1)13}\right) - 2\dot{\delta}_{(2)1}, \tag{4.153}$$

$$N^{11}{}_{,1} = 0, \tag{4.154}$$

$$M^{(2)11}{}_{,1} = 2M^{(1)13}, \tag{4.155}$$

$$M^{(1)13}{}_{,1} = m^{(1)3}. \tag{4.156}$$

Equations (4.151) and (4.152) can be used to eliminate $m^{(1)3}$ from the system and hence obtain a relationship between $\dot{\delta}_{(1)3}$ and $\dot{\delta}_{(3)3}$.

$$\dot{\delta}_{(3)3} = \frac{A}{2\sigma_c h}\left(\frac{N^*}{\sigma_c h}\right)^{n-1}\frac{1}{\psi^p}\left(\frac{15}{8h^2}N^{11} - \frac{105}{2h^4}M^{(2)11}\right) - \frac{5}{3h^2}\dot{\delta}_{(1)3}. \tag{4.157}$$

Differentiating (4.157) with respect to v^1 and using the equations (4.154) and (4.155) yields the final system of differential equations

$$\begin{aligned}
\dot{\delta}_{(1)3,1} &= \frac{A}{2\sigma_c h}\left(\frac{N^*}{\sigma_c h}\right)^{n-1}\frac{1}{\psi^p}\left(\frac{2763}{23h^2}M^{(1)13} - \left((n-1)\left(\frac{N^*{}_{,1}}{N^*}\right) - p\left(\frac{\psi_{,1}}{\psi}\right)\right)\right. \\
&\times \left.\left(\frac{45}{184}N^{11} - \frac{315}{46h^2}M^{(2)11}\right)\right) - \frac{56}{23}\dot{\delta}_{(2)1}, \qquad (4.158)\\
\dot{\delta}_{(2)1,1} &= \frac{A}{2\sigma_c h}\left(\frac{N^*}{\sigma_c h}\right)^{n-1}\frac{1}{\psi^p}\left(\frac{315}{2h^4}M^{(2)11} - \frac{45}{18h^2}N^{11}\right) + \frac{5}{h^2}\dot{\delta}_{(1)3}, \qquad (4.159)\\
M^{(2)11}{}_{,1} &= 2M^{(1)13}, \qquad (4.160)\\
M^{(1)13}{}_{,1} &= \frac{2\sigma_c h}{A}\left(\frac{\sigma_c h}{N^*}\right)^{n-1}\psi^p\left(\frac{7}{18}\dot{\delta}_{(1)3}\right) + \frac{21}{16}N^{11} - \frac{35}{4h^2}M^{(2)11}, \qquad (4.161)\\
N^{11}{}_{,1} &= 0. \qquad (4.162)
\end{aligned}$$

Equation (4.162) implies that $N^{11} = N^\infty$, which can then be used to simplify the forms of the other equations (4.158) to (4.161) through the use of new dimensionless variables defined by

$$\begin{aligned}
&\tilde{\dot{\delta}}_{(1)3} = \frac{2\sigma_c h}{A^{(\mathrm{p})}}\frac{\dot{\delta}_{(1)3}}{N^\infty}\ ,\ \tilde{N}^* = \frac{N^*}{N^\infty}\ ,\ \tilde{M}^{(1)13} = \frac{M^{(1)13}}{N^\infty h},\\
&\tilde{\dot{\delta}}_{(2)1} = \frac{2\sigma_c h^2}{A^{(\mathrm{p})}N^\infty}\dot{\delta}_{(2)1}\ ,\ \tilde{M}^{(2)11} = \frac{M^{(2)11}}{N^\infty h^2}\ ,\ \tilde{v}^1 = \frac{v^1}{h}, \qquad (4.163)\\
&\tilde{A} = \frac{A}{A^{(\mathrm{p})}}\left(\frac{N^\infty}{\sigma_c h}\right)^{n-1}\ ,\ \tilde{\psi} = \psi\ ,\ \tilde{B} = T\left(\frac{N^\infty}{\sigma_c h}\right)^m B\ ,\ \tilde{t} = \frac{t}{T},
\end{aligned}$$

where $A^{(\mathrm{p})}$ represents the value of the parameter A in the parent material. The ratio $A/A^{(\mathrm{p})}$ is introduced so that the problem is rescaled and hence only the relative creep strengths in each region are required.

4.7 Boundary Conditions.

We wish to specify the boundary conditions as $v^1 \to -\infty$ and at $v^1 = l_3$ where l_3 represents the position of the centre of the weld.

(1) It is clear that as $v^1 \to -\infty$ then the influence of the weld upon the stresses diminishes and hence as $v^1 \to -\infty$ we expect the plate to act as a homogeneous plate under simple uniaxial tension, where the applied three-dimensional stress components satisfy

$$\sigma^{11} = \sigma^{\infty} \quad , \quad \sigma^{13} = 0. \tag{4.164}$$

Using the definitions (4.62) and (4.64), conditions (4.164) lead to

$$N^{11} = \int_{-\frac{h}{2}}^{\frac{h}{2}} \sigma^{\infty} \, d\xi = \sigma^{\infty} h = N^{\infty}, \tag{4.165}$$

$$M^{(2)11} = \int_{-\frac{h}{2}}^{\frac{h}{2}} \sigma^{\infty} \xi^2 d\xi = \sigma^{\infty} \frac{h^3}{12}, \tag{4.166}$$

$$M^{(1)13} = 0. \tag{4.167}$$

When (4.166) to (4.167) are non-dimensionalised using (4.163) then as $\tilde{v}^1 \to -\infty$ we require

$$\tilde{M}^{(2)11} \to \frac{1}{12}, \tag{4.168}$$

$$\tilde{M}^{(1)13} \to 0. \tag{4.169}$$

(2) At $v^1 = l_3$, the centre of the weld, we observe that we have a position of symmetry. Hence, derivatives of the components of normal stress with respect to v^1 are identically zero there, as are the derivatives of the displacement with respect to v^1. This implies that at $v^1 = l_3$

$$N^{11}{}_{,1} = 0, \tag{4.170}$$

$$M^{(2)11}{}_{,1} = 0, \tag{4.171}$$

$$\dot{\delta}_{(1)3,1} = 0. \tag{4.172}$$

Condition (4.170) is identically satisfied by (4.162). The two conditions (4.171) and (4.172) together with (4.168) and (4.169) form the boundary conditions for the system of partial differential equations (4.115) and (4.158) to (4.161).

4.8 Continuity Conditions.

Next we must examine the continuity conditions to be applied at each of the interfaces. In this section we shall present two alternative approaches to obtaining the continuity conditions, the first is attributable to Naghdi (1972), and as such we shall use results from this piece of work freely without further justification. The second method was used by Hawkes (1989).

To obtain the continuity conditions we observe that in a mechanical system we require that the rate of work of the contact forces across each interface must be identically zero. The rate of work of the contact forces $\mathbf{N}^{\alpha}$ and $\mathbf{M}^{(N)\alpha}$ may be written

$$R_c = \int_{\partial\mathcal{P}} \left(\mathbf{N} \cdot \mathbf{v} + \sum_{N=1}^{\infty} \mathbf{M}^{(N)} \cdot \mathbf{w}_{(N)} \right) ds, \tag{4.173}$$

where $\partial\mathcal{P}$ is the boundary of part $\mathcal{P}$, of the body. For the case of only three directors (4.173) can be expressed in component form as

$$R_c = \int_{\partial\mathcal{P}} \mu_\alpha \left(N^{\alpha i} v_i + \sum_{N=1}^{3} M^{(N)\alpha i} w_{(N)i} \right) ds, \tag{4.174}$$

where μ_α is the unit normal to the boundary curve $\partial\mathcal{P}$. For the case of an initially flat plate we obtain from Naghdi (1972) that

$$\begin{aligned} \mu_1 &= 1, \\ \mu_2 &= 0. \end{aligned} \tag{4.175}$$

Thus the mechanical rate of work of the contact forces reduces to

$$R_c = \int_{\partial\mathcal{P}} \left(N^{1i} v_i + \sum_{N=1}^{3} M^{(N)1i} w_{(N)i} \right) ds. \tag{4.176}$$

It can be shown from (2.64), (4.6), (4.25) and (4.74) that the only non-zero components of the surface and director velocities are

$$v_1 = \epsilon \dot{f}_1, \tag{4.177}$$

$$w_{(2)1} = \epsilon\dot{\delta}_{(2)1}, \tag{4.178}$$

$$w_{(1)3} = \epsilon\dot{\delta}_{(1)3}, \tag{4.179}$$

$$w_{(3)1} = \epsilon\dot{\delta}_{(3)3}, \tag{4.180}$$

and hence the expression for the rate of work becomes

$$R_c = \int_{\partial\mathcal{P}} \epsilon \left(N^{11}\dot{f}_1 + M^{(1)13}\dot{\delta}_{(1)3} + M^{(2)11}\dot{\delta}_{(2)1} + M^{(3)13}\dot{\delta}_{(3)3} \right) ds. \tag{4.181}$$

If, as an example, we concentrate on the interface between the parent material and the type IV region at $v^1 = 0$ then we require

$$\lim_{v^1 \to 0^-} R_c^{(\mathrm{p})} = \lim_{v^1 \to 0^+} R_c^{(\mathrm{iv})}, \tag{4.182}$$

where $R_c^{(\mathrm{p})}$ and $R_c^{(\mathrm{iv})}$ represent the rate of work in the parent material and type IV region respectively. By observing each term in the integrand of (4.181) in relation to the requirement (4.182) then, for the rate of work to be identically zero across the interface $v^1 = 0$, we require

$$\lim_{v^1 \to 0^-} N^{(\mathrm{p})11} = \lim_{v^1 \to 0^+} N^{(\mathrm{iv})11}, \tag{4.183}$$

$$\lim_{v^1 \to 0^-} \dot{\delta}_1^{(\mathrm{p})} = \lim_{v^1 \to 0^+} \dot{\delta}_1^{(\mathrm{iv})}, \tag{4.184}$$

The above conditions, with similar expressions for the other terms in the integrand implies that the variables

$$N^{11}, M^{(1)13}, M^{(2)11}, M^{(3)13}, \dot{f}_1, \dot{\delta}_{(1)3}, \dot{\delta}_{(2)1}, \dot{\delta}_{(3)3}, \tag{4.185}$$

are all continuous across this interface. Clearly some of these variables depend on the others and for our system, we need only require that

$$M^{(1)13}, M^{(2)11}, \dot{\delta}_{(1)3}, \dot{\delta}_{(2)1} \text{ are continuous at each interface.} \tag{4.186}$$

Alternatively we observe the differential equations (4.158) to (4.161) and note that all the variables on the right-hand side of equations (4.158) to (4.161) are continuous in each region. We also observe that A suffers a jump discontinuity at each interface only, which implies that the variables on the right-hand side of equations (4.158) to (4.161) are either continuous or suffer a jump discontinuity at each interface. This implies that the right-hand side of each differential equation is piecewise continuous and hence the left hand sides of the equations are piecewise continuous, which means that the integrals of the left-hand side of equations (4.158) to (4.161) are continuous everywhere. In particular

$$M^{(1)13}, M^{(2)11}, \dot{\delta}_{(1)3}, \dot{\delta}_{(2)1} \text{ are continuous at each interface.} \tag{4.187}$$

4.9 The Elastic Case, $n = 1$.

The constitutive equations simplify considerably for the 'elastic case' when $n = 1$, and we shall introduce this postulate for the remainder of this section. The non-dimensional form of the equations reduce to

$$\frac{\dot{\delta}_{(1)3,1}}{A} = \frac{1}{\psi^p}\left(\frac{2763}{23}M^{(1)13}\right) - \frac{56}{23}\frac{\dot{\delta}_{(2)1}}{A}, \tag{4.188}$$

$$\frac{\dot{\delta}_{(2)1,1}}{A} = \frac{1}{\psi^p}\left(\frac{315}{2}M^{(2)11} - \frac{45}{8}\right) + 5\frac{\dot{\delta}_{(1)3}}{A}, \tag{4.189}$$

$$M^{(2)11}{}_{,1} = 2M^{(1)13}, \tag{4.190}$$

$$M^{(1)13}{}_{,1} = \frac{7}{18}\psi^p\frac{\dot{\delta}_{(1)3}}{A} + \frac{21}{16} - \frac{35}{4}M^{(2)11}, \tag{4.191}$$

where for clarity we have omitted the $\hat{}$ from all non-dimensional variables.

This simplified set of equations is linear and so it is possible to obtain analytical solutions for the strain-rates at $t = 0$. If we set $\psi = 1$ (which is the appropriate value if the material is undamaged at $t = 0$) then the equations (4.188) to (4.191) can be written

in matrix form as

$$\mathbf{X}_{,1} = L\mathbf{X} + \mathbf{B}, \tag{4.192}$$

where

$$\mathbf{X}^T = \left(\frac{\dot{\delta}_{(1)3}}{A}, \frac{\dot{\delta}_{(2)1}}{A}, M^{(2)11}, M^{(1)13}\right), \tag{4.193}$$

$$\mathbf{B}^T = \left(0, -\frac{45}{8}, 0, \frac{21}{16}\right), \tag{4.194}$$

$$L = \begin{pmatrix} 0 & -\frac{56}{23} & 0 & \frac{2763}{23} \\ 5 & 0 & \frac{315}{2} & 0 \\ 0 & 0 & 0 & 2 \\ \frac{7}{18} & 0 & -\frac{35}{4} & 0 \end{pmatrix}. \tag{4.195}$$

Assuming that the solutions to the homogeneous equations

$$\mathbf{X}_{,1} - L\mathbf{X} = 0, \tag{4.196}$$

take the form

$$\mathbf{X} = \mathbf{C}e^{\lambda v^1}, \tag{4.197}$$

then substituting (4.197) into (4.196) gives

$$\mathbf{C}\lambda e^{\lambda v^1} - L\mathbf{C}e^{\lambda v^1} = 0. \tag{4.198}$$

Since

$$\forall v^1, \;\; e^{\lambda v^1} > 0 \text{ and } \mathbf{C} \neq 0, \tag{4.199}$$

it follows that non-trivial solutions of (4.196) exist only when

$$|L - \lambda I| = 0, \tag{4.200}$$

where in (4.200) I is the identity matrix of rank 4. For the matrix (4.195) the characteristic equation resulting from (4.200) is

$$23\lambda^4 - 392\lambda^2 + 11760 = 0, \tag{4.201}$$

which has the solutions

$$\begin{aligned} \lambda_1 &= -3.945 + 2.654\imath, \\ \lambda_2 &= -3.945 - 2.654\imath, \\ \lambda_3 &= 3.945 + 2.654\imath, \\ \lambda_4 &= 3.945 - 2.654\imath. \end{aligned} \tag{4.202}$$

The particular solution to equation (4.192) when $\mathbf{X}_{,1} = 0$ is

$$\mathbf{X}_p = -L^{-1}\mathbf{B}. \tag{4.203}$$

It is simple to show that

$$\mathbf{X}_p^T = \left(-\frac{3}{2}, 0, \frac{1}{12}, 0\right), \tag{4.204}$$

and so the general solution of (4.192) takes the form

$$\mathbf{X} = \sum_{i=1}^{4} a_i \, \mathbf{C}_i \, e^{\lambda_i v^1} + \mathbf{X}_p, \tag{4.205}$$

where $\mathbf{C}_i$ are the complex eigenvectors associated with each eigenvalue λ_i. The parameters a_i can take different values in each of the four regions of the weld. The values of the eigenvectors associated with each respective eigenvalue of (4.202) can be calculated to be

$$\begin{aligned} C_1^T &= (0.321 + 0.386\imath, 0.864, -0.011 + 0.002\imath, 0.02 - 0.02\imath), \\ C_2^T &= (-0.321 - 0.386\imath, 0.864, -0.011 - 0.002\imath, 0.02 + 0.02\imath), \\ C_3^T &= (0.321 + 0.386\imath, 0.864, 0.011 + 0.002\imath, -0.02 + 0.02\imath), \\ C_4^T &= (0.321 - 0.386\imath, 0.864, 0.011 - 0.002\imath, -0.02 - 0.02\imath). \end{aligned} \tag{4.206}$$

The values of the constants a_i are calculated with the use of the boundary conditions (4.168) to (4.169) and (4.171) to (4.172), and the continuity conditions (4.182).

4.10 Solution of the Boundary and Continuity Conditions.

It is now possible to determine the values of the coefficients $a_i^{(\mathrm{p})}, a_i^{(\mathrm{iv})}, a_i^{(\mathrm{haz})}$ and $a_i^{(\mathrm{w})} (i = 1 \ldots 4)$ in each of the respective zones. We note that C_{ij} denotes the j^{th} component of the eigenvector which corresponds to the i^{th} eigenvalue. The material quantity A takes the value 1 in the parent material and $A^{(\mathrm{iv})}, A^{(\mathrm{haz})}$ and $A^{(\mathrm{w})}$ in the other three regions, with an obvious identification. The boundary conditions imply:-

$$\text{as } v^1 \to -\infty \quad : \quad M^{(1)13} \to 0$$

$$\Rightarrow \quad a_1^{(\mathrm{p})} = 0, \tag{4.207}$$

$$\Rightarrow \quad a_2^{(\mathrm{p})} = 0, \tag{4.208}$$

$$\text{at } v^1 = 0 \quad : \quad \dot{\delta}_{(1)3} \text{ continuous}$$

$$\Rightarrow \quad \sum_{i=1}^{4} a_i^{(\mathrm{p})} C_{i1} - \frac{3}{2} = A^{(\mathrm{iv})} \left(\sum_{i=1}^{4} a_i^{(\mathrm{iv})} C_{i1} - \frac{3}{2} \right), \tag{4.209}$$

$$: \quad \dot{\delta}_{(2)1} \text{ continuous}$$

$$\Rightarrow \quad \sum_{i=1}^{4} a_i^{(\mathrm{p})} C_{i2} = A^{(\mathrm{iv})} \left(\sum_{i=1}^{4} a_i^{(\mathrm{iv})} C_{i2} \right), \tag{4.210}$$

$$: \quad M^{(2)11} \text{ continuous}$$

$$\Rightarrow \quad \sum_{i=1}^{4} a_i^{(\mathrm{p})} C_{i3} = \sum_{i=1}^{4} a_i^{(\mathrm{iv})} C_{i3}, \tag{4.211}$$

$$: \quad M^{(1)13} \text{ continuous}$$

$$\Rightarrow \quad \sum_{i=1}^{4} a_i^{(\mathrm{p})} C_{i4} = \sum_{i=1}^{4} a_i^{(\mathrm{iv})} C_{i4}, \tag{4.212}$$

$$\text{at } v^1 = l_1 \quad : \quad \dot{\delta}_{(1)3} \text{ continuous}$$

$$\Rightarrow \quad A^{(\mathrm{iv})} \left(\sum_{i=1}^{4} a_i^{(\mathrm{iv})} C_{i1} e^{\lambda_i l_1} - \frac{3}{2} \right)$$

$$= A^{(\mathrm{haz})} \left(\sum_{i=1}^{4} a_i^{(\mathrm{haz})} C_{i1} e^{\lambda_i l_1} - \frac{3}{2} \right), \tag{4.213}$$

$$: \quad \dot{\delta}_{(2)1} \text{ continuous}$$

$$\Rightarrow \quad A^{(\mathrm{iv})}\left(\sum_{i=1}^{4} a_i^{(\mathrm{iv})} C_{i2} e^{\lambda_i l_1}\right) = A^{(\mathrm{haz})}\left(\sum_{i=1}^{4} a_i^{(\mathrm{haz})} C_{i2} e^{\lambda_i l_1}\right), \tag{4.214}$$

: $M^{(2)11}$ continuous

$$\Rightarrow \quad \sum_{i=1}^{4} a_i^{(\mathrm{iv})} C_{i3} e^{\lambda_i l_1} = \sum_{i=1}^{4} a_i^{(\mathrm{haz})} C_{i3} e^{\lambda_i l_1}, \tag{4.215}$$

: $M^{(1)13}$ continuous

$$\Rightarrow \quad \sum_{i=1}^{4} a_i^{(\mathrm{iv})} C_{i4} e^{\lambda_i l_1} = \sum_{i=1}^{4} a_i^{(\mathrm{haz})} C_{i4} e^{\lambda_i l_1}, \tag{4.216}$$

at $v^1 = l_2$: $\dot{\delta}_{(1)3}$ continuous

$$\Rightarrow \quad A^{(\mathrm{haz})}\left(\sum_{i=1}^{4} a_i^{(\mathrm{haz})} C_{i1} e^{\lambda_i l_2} - \frac{3}{2}\right)$$

$$= A^{(\mathrm{w})}\left(\sum_{i=1}^{4} a_i^{(\mathrm{w})} C_{i1} e^{\lambda_i l_2} - \frac{3}{2}\right), \tag{4.217}$$

: $\dot{\delta}_{(2)1}$ continuous

$$\Rightarrow \quad A^{(\mathrm{haz})}\left(\sum_{i=1}^{4} a_i^{(\mathrm{haz})} C_{i2} e^{\lambda_i l_2}\right) = A^{(\mathrm{w})}\left(\sum_{i=1}^{4} a_i^{(\mathrm{w})} C_{i2} e^{\lambda_i l_2}\right), \tag{4.218}$$

: $M^{(2)11}$ continuous

$$\Rightarrow \quad \sum_{i=1}^{4} a_i^{(\mathrm{haz})} C_{i3} e^{\lambda_i l_2} = \sum_{i=1}^{4} a_i^{(\mathrm{w})} C_{i3} e^{\lambda_i l_2}, \tag{4.219}$$

: $M^{(1)13}$ continuous

$$\Rightarrow \quad \sum_{i=1}^{4} a_i^{(\mathrm{haz})} C_{i4} e^{\lambda_i l_2} = \sum_{i=1}^{4} a_i^{(\mathrm{w})} C_{i4} e^{\lambda_i l_2}, \tag{4.220}$$

at $v^1 = l_3$: $M^{(2)11}{}_{,1} = 0 \Rightarrow M^{(1)13} = 0$ (using (4.190)),

$$\Rightarrow \quad \sum_{i=1}^{4} a_i^{(\mathrm{w})} C_{i4} e^{\lambda_i l_3} = 0, \tag{4.221}$$

: $\dot{\delta}_{(1)3,1} = 0 \Rightarrow \dot{\delta}_{(2)1} = 0$ (using (4.188) and above),

$$= \quad \sum_{i=1}^{4} a_i^{(\mathrm{w})} C_{i2} e^{\lambda_i l_3} = 0. \tag{4.222}$$

The 16 simultaneous equations (4.207) to (4.222) can be solved to obtain the 16 unknown coefficients $a_i^{(\mathrm{p})}, a_i^{(\mathrm{iv})}, a_i^{(\mathrm{haz})}$ and $a_i^{(\mathrm{w})}$ $(i = 1 \ldots 4)$, and hence the general solution (4.205) can be determined.

4.11 Results.

In this section we shall present some results for the strain-rates at $t = 0$, using the analytical solutions obtained in the previous section. At the end of the section there will be a brief discussion about the implications of these results. As in section §3.7 we specify the widths of each region by introducing the non-dimensional variables;

$$x^{(\mathrm{iv})} = \frac{l_1}{h}, \tag{4.223}$$

$$x^{(\mathrm{haz})} = \left(\frac{l_2 - l_1}{h}\right), \tag{4.224}$$

$$x^{(\mathrm{w})} = \left(\frac{l_3 - l_2}{h}\right), \tag{4.225}$$

where h represents the thickness of the plate.

Since we are mainly concerned with the type IV region we shall confine our attention to the effect on the strain-rates over the whole weldment by varying the parameters associated with the type IV region, namely its width $x^{(\mathrm{iv})}$, and the relative strength of the type IV region, $A^{(\mathrm{iv})}/A^{(\mathrm{p})}$. The following figures have the non-dimensional strain-rate, $\tilde{\dot{\varrho}}_{11}$, at $t = 0$ plotted on the y-axis against the non-dimensional position v^1/h on the x-axis.

In Figures (4.2) and (4.3) we observe the effects of varying the width and the strength of the type IV region. In both of these figures the ratio $A^{(\mathrm{iv})}/A^{(\mathrm{p})}$ takes the values 10, 5 and 2 respectively, with the ratio $A^{(\mathrm{haz})}/A^{(\mathrm{p})}$ and the weld material $A^{(\mathrm{w})}/A^{(\mathrm{p})}$ taking the values 0.1 and 3.0 respectively. In the Figure (4.2) the widths of each region are $x^{(\mathrm{iv})} = x^{(\mathrm{haz})} = x^{(\mathrm{w})} = 0.2$, whereas in Figure (4.3) the width of the type IV region is 0.5, with the widths of the other two regions remaining unaltered.

In Figure (4.2) we observe that for the case of the relatively soft material $\left(A^{(\mathrm{iv})}/A^{(\mathrm{p})} = 10\right)$, within the type IV region the strain-rate dramatically increases, before being severely restricted by the hard heat affected zone. When the width of the type IV

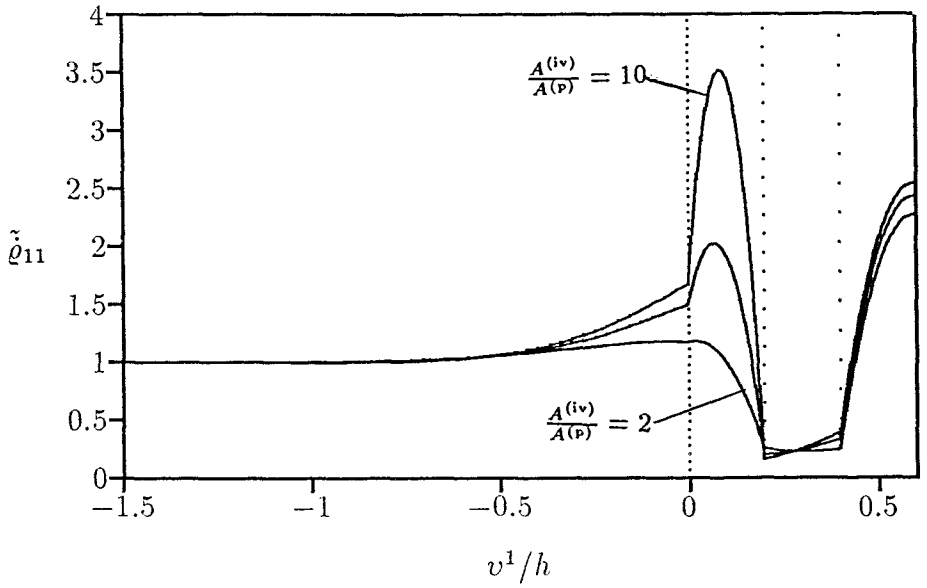

Figure 4.2: strain-rates for a plate with stress free surfaces, $x^{(iv)} = 0.2$

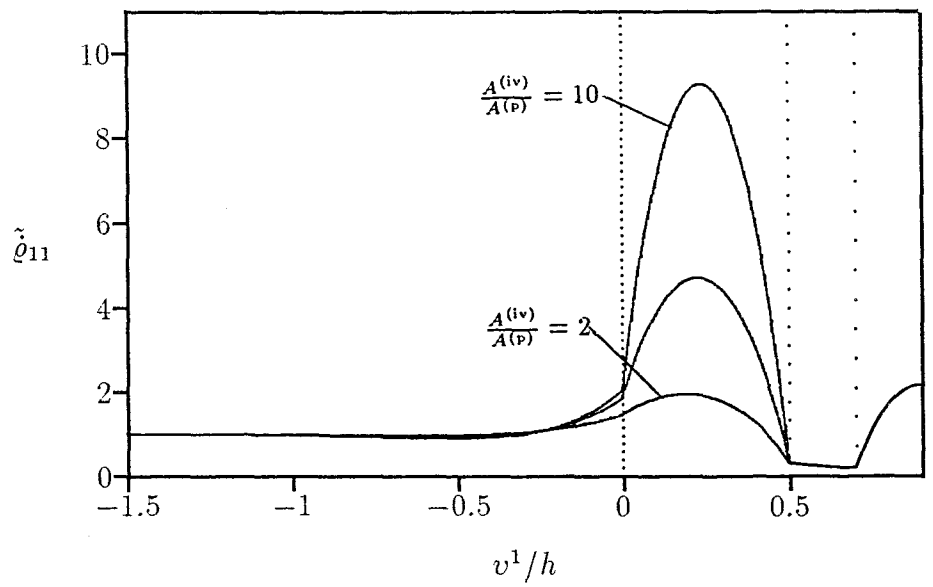

Figure 4.3: strain-rates for a plate with stress free surfaces, $x^{(iv)} = 0.5$

region is increased (Figure (4.3)) we observe a further dramatic rise in the strain-rate

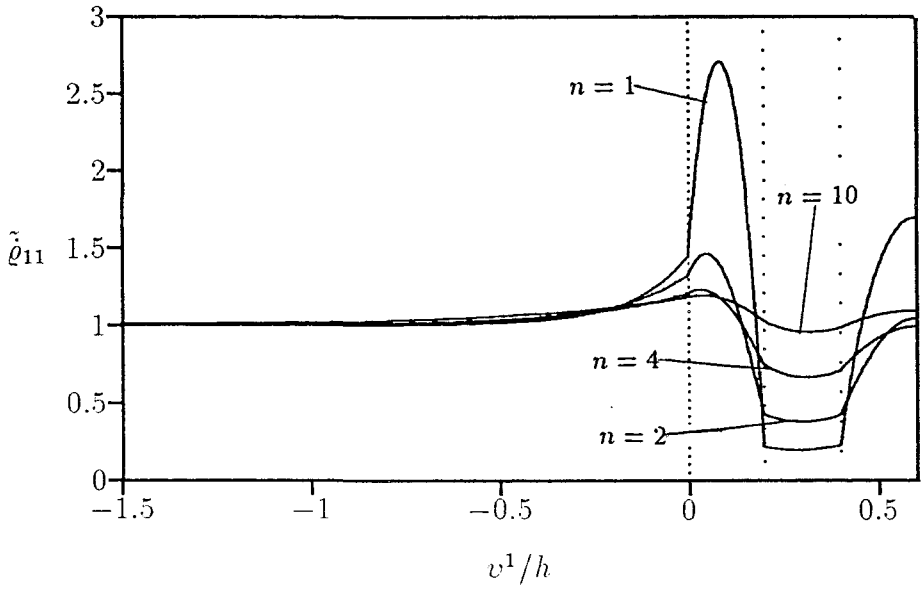

Figure 4.4: strain-rates for different values of n using method of chapter 3

in this region, and with $x^{(\mathrm{iv})} = 0.5$ the maximum strain-rate almost reaches the value expected of a homogeneous plate of type IV material. From Figures (4.2) and (4.3) we conclude that the imposition of a stress free constraint on the top and bottom surfaces of the plate produces less interaction between adjacent regions with the tendency for the strain-rate within each region to tend towards its homogeneous limit.

Although the results presented here are for the elastic case when $n = 1$, it is possible to make some comments about the strain-rates for the weld when $n \neq 1$. Figure (4.4) shows strain-rates for a weldment having exactly the same material properties and parameters as Figure (4.2), for different values of n, using the method described in chapter 3. We see that higher values of the index tend to equalise the strain-rates (as observed by Nicol and Hawkes) such that as $n \to \infty$ the strain-rate tends to a constant throughout the plate. We would expect the same behaviour for the weldment under consideration in this chapter and hence, as n increases, a reduction in the strain rates within the type IV region and weld material. This reduction would be expected to increase the lifetime of the

weld, and so acts against the trend discussed earlier in this section. An accurate numerical solution would be required for these more complicated situations in order to determine the actual failure time, but in view of the assumed parameter values the position of rupture is expected to remain in the type IV region.

Chapter 5

MATHEMATICAL MODEL OF AN INITIALLY FLAT PLATE CONTAINING A WELD WITH THE INTERFACE AT AN ANGLE θ_0 TO THE CENTRAL SURFACE OF THE PLATE

The models discussed so far in this thesis have all been appropriate for the modelling of a low alloy ferritic ($\frac{1}{2}$Chromium, $\frac{1}{2}$ Molybdenum, $\frac{1}{4}$Vanadium) weld, produced by TIG welding. This arises when an arc is struck between the tungsten electrode and the work piece, the electrode being surrounded by an inert gas shield.

If the plate being welded is thin, typically about 2–3 mm, then a single pass of the arc will complete the joining process leaving four regions within the weldment, with the interfaces between the regions approximately normal to the surface of the plate (Figure (3.1)). If the plate is thicker than 3mm , then the weld is produced by a series of passes of the arc, thereby producing a weld in which the interfaces of each region are now at angle θ_0 to the surfaces of the plate (Figure (5.1)). These types of weld are found, for example, in boiler tubes in power stations operating at about 500°C under constant uniaxial loading, and so are operating in the creep regime.

In this chapter we shall apply the Cosserat theory, already successfully developed for a simple butt-weld with the interface normal to the surface of the plate, to the more complicated geometry of the so called 'V-shaped' weld. We shall obtain a model for this type of weld by introducing directors which are no longer normal to the central surface, but more accurately mimic the actual geometry of the weld.

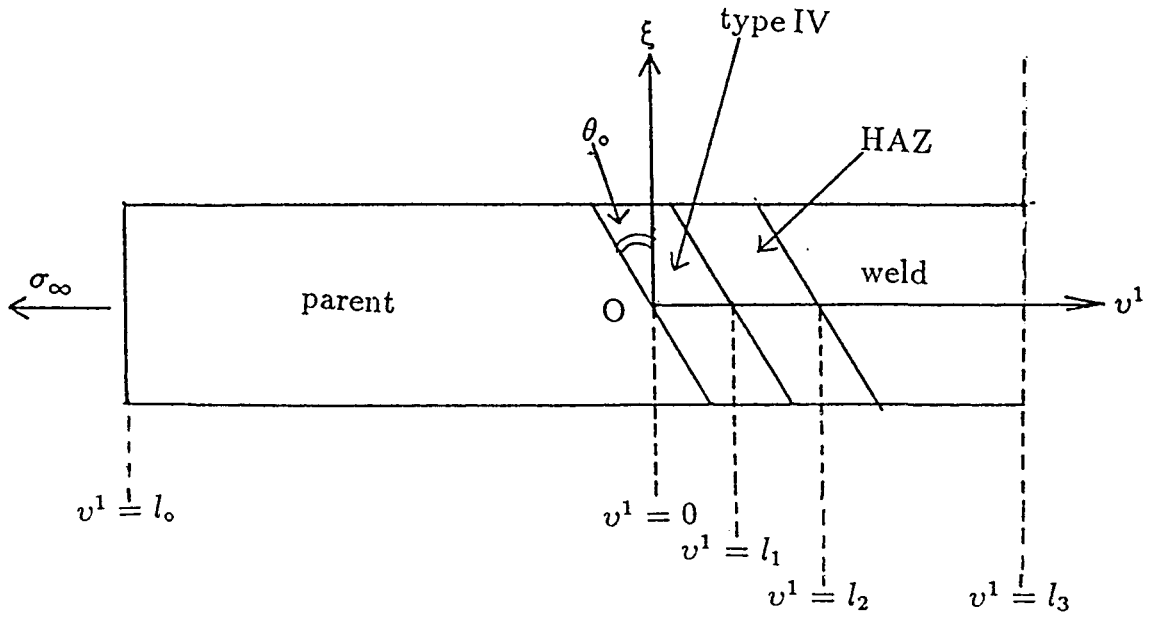

Figure 5.1: Cross-section of a V-shaped weld containing 4 regions

5.1 Geometry of the Plate.

The geometry of the plate and associated co-ordinate system are identical to those defined in section §4.1 and hence the reader will be referred back to equations in the previous chapter where appropriate.

5.2 Kinematic Results.

In this chapter we shall adopt a single director model. Before we derive the relevant kinematic results, we need to define this director in terms of the base vectors $\mathbf{a}_i$. In the initial configuration ($t = 0$) we wish to introduce the director such that it will represent a flat plate with each of the respective interfaces at an angle θ_o to the ξ-axis, see Figure (5.1).

Naghdi (1972) states that the director is intended to represent the "thickening" about

the surface $\xi = 0$ of the three-dimensional shell or plate, and that the component along the unit normal to the Cosserat surface can be regarded as representing the thickness of the three-dimensional shell or plate. Thus if D^i is the initial value of the director component d^i, then we assume that

$$D^3 = 1. \tag{5.1}$$

The geometry of the weldment implies the existence of important directions which are not normal to the central surface. In our model we assume that the director lies along these preferred directions. Hence, we assume that at a position $v^1 = l_\circ$ the director is normal to the surface of the plate. The director varies continuously with distance such that at the interface between the parent material and the type IV region it lies in the plane of the interface. The director is then required to stay parallel to the interfaces within the type IV region and the HAZ, before reaching the weld metal in which it again varies continuously with distance until the centre of the weld, where it returns to being normal to the central surface. We define therefore, the initial value of the director component d^1 as

$$D^1 = -\tan\theta\left(v^1\right), \tag{5.2}$$

where

$$\theta\left(v^1\right) = \begin{cases} \theta_\circ\left(\frac{l_\circ - v^1}{l_\circ}\right) & , \quad l_\circ \leq v^1 \leq 0 \\ \theta_\circ & , \quad 0 < v^1 \leq l_2 \\ \theta_\circ\left(1 - \left(\frac{v^1 - l_2}{l_3 - l_2}\right)\right) & , \quad l_2 < v^1 \leq l_3 \end{cases} \tag{5.3}$$

We assume that there is no variation in the v^2 direction and hence that

$$d^2 = D^2 = 0. \tag{5.4}$$

Assuming that only infinitesimal deformations occur, we can expand the components of the director d about their initial values and therefore we express the director as

$$\mathrm{d} = \left(-\tan\theta + \epsilon\,\delta_1\right)\mathrm{a}_1 + \left(1 + \epsilon\,\delta_3\right)\mathrm{a}_3 + O\left(\epsilon^2\right), \tag{5.5}$$

where we have omitted terms of $O(\epsilon^2)$ in (5.5). Using the relations $(2.67)_{(ii),(iii)}$ and (4.11) we obtain the covariant form of the director components as

$$d_1 = -\tan\theta + \epsilon\left(\delta_1 - 2f_{1,1}\tan\theta\right) + O\left(\epsilon^2\right), \tag{5.6}$$

$$d_2 = 0, \tag{5.7}$$

$$d_3 = 1 + \epsilon\delta_3 + O\left(\epsilon^2\right). \tag{5.8}$$

Then, using the definitions (2.71) to (2.73), the kinematic expressions associated with a single director model for the V-shaped weld can be expressed

$$\dot{\varrho}_{11} = \epsilon\dot{f}_{1,1} + O\left(\epsilon^2\right), \tag{5.9}$$

$$\dot{\varrho}_{12} = \dot{\varrho}_{21} = \dot{\varrho}_{22} = 0, \tag{5.10}$$

$$\dot{\kappa}_{11} = \epsilon\left(\dot{\delta}_{1,1} - \dot{f}_{1,11}\tan\theta - \dot{h}_{1,11}\right) + O\left(\epsilon^2\right), \tag{5.11}$$

$$\dot{\kappa}_{12} = \dot{\kappa}_{21} = \dot{\kappa}_{22} = 0, \tag{5.12}$$

$$\dot{\kappa}_{13} = \epsilon\left(\dot{\delta}_{3,1} - \dot{h}_{1,11}\tan\theta\right) + O\left(\epsilon^2\right), \tag{5.13}$$

$$\dot{\kappa}_{23} = 0, \tag{5.14}$$

$$\dot{\gamma}_1 = \epsilon\left(\dot{\delta}_1 - 2\dot{f}_{1,1}\tan\theta\right) + O\left(\epsilon^2\right), \tag{5.15}$$

$$\dot{\gamma}_2 = 0, \tag{5.16}$$

$$\dot{\gamma}_3 = \epsilon\dot{\delta}_3 + O\left(\epsilon^2\right), \tag{5.17}$$

where the superposed dot denotes the partial derivative with respect to time, holding all other material variables constant. In deriving (5.9) to (5.17) we have also assumed that

$$\frac{\partial\theta}{\partial v^1} \ll \frac{1}{h}. \tag{5.18}$$

This assumption is valid for sufficiently small angles, and since it greatly simplifies the algebra it is used in this chapter. We shall discuss this condition further in section §5.10.

The components of the metric $g_{\alpha\beta}$ can be easily expressed in terms of the variables introduced above, and using equations (2.77) to (2.79) we obtain (ignoring terms of $O(\epsilon^2)$)

$$g_{11} = 1 + \epsilon\left(2f_{1,1} + 2\xi\left(\delta_{1,1} - f_{1,11}\tan\theta - h_{1,11}\right)\right), \tag{5.19}$$

$$g_{12} = g_{21} = 0, \tag{5.20}$$

$$g_{22} = 1, \tag{5.21}$$

$$g_{13} = -\tan\theta + \epsilon\left(\delta_1 - 2f_{1,1}\tan\theta + \xi\left(\delta_{3,1} - \delta_{1,1}\tan\theta + f_{1,1}\tan^2\theta\right)\right), \tag{5.22}$$

$$g_{23} = 0, \tag{5.23}$$

$$g_{33} = 1 + \tan^2\theta + \epsilon\left(2\delta_3 + 2f_{1,11}\tan^2\theta - 2\,\delta_1\tan\theta\right). \tag{5.24}$$

We observe that at this stage in our analysis we have retained the bending terms in the expressions for the kinematic results. From (4.20) we see that the curvature of the plate is a function of $h_1(v^1, t)$, and although the curvature is identically zero at $t = 0$ we would expect that at later times the plate would bend due to the presence of the V-shaped weld. If this is not the case, and the plate remains flat, then both h_1 and the curvature will be identically zero in the solution.

In the following section we derive the continuity equation for a V-shaped weld.

5.3 Continuity Equation.

Recalling equations (4.116) and (4.117), the continuity equation can be written

$$\nabla \cdot \mathbf{v}^* = \frac{1}{\sqrt{g}}\frac{\partial}{\partial v^k}\left(\sqrt{g}v^{*k}\right) = 0, \tag{5.25}$$

where

$$\mathbf{v}^* = \dot{\mathbf{r}} + \xi\dot{\mathbf{d}}. \tag{5.26}$$

Using equations (4.6), (5.6), and (4.8) to (4.10) in (5.26) we obtain, to leading order,

$$\mathbf{v}^* = \epsilon\left(\left[\dot{f}_1 + \xi\left(\dot{\delta}_1 - \tan\theta\dot{f}_{1,1} - \dot{h}_{1,1}\right)\right]\mathrm{i} + \left[\dot{h}_1 + \xi\left(\dot{\delta}_3 - \tan\theta\dot{h}_{1,1}\right)\right]\mathrm{k}\right) \tag{5.27}$$

Also, it follows from (4.17) and (5.19)–(5.24) that, to leading order, we have

$$\begin{aligned} \mathrm{i} &= \mathrm{a}_1 + O(\epsilon), \\ \mathrm{k} &= \mathrm{a}_3 + O(\epsilon), \\ g^{\frac{1}{2}} &= 1 + O(\epsilon). \end{aligned} \tag{5.28}$$

The components of the three-dimensional velocity expressed in terms of the base vectors a_i are

$$\begin{aligned} v^{*1} &= \dot{f}_1 + \xi\left(\dot{\delta}_1 - \tan\theta\dot{f}_{1,1} - \dot{h}_{1,1}\right), \\ v^{*2} &= 0, \\ v^{*3} &= \dot{h}_1 + \xi\left(\dot{\delta}_3 - \tan\theta\dot{h}_{1,1}\right). \end{aligned} \tag{5.29}$$

Substituting expressions (5.28)–(5.29) into equation (5.25) and integrating the resulting expressions through the plate (i.e. with respect to ξ from $\xi = -\frac{h}{2}$ to $\xi = \frac{h}{2}$), we obtain the condition

$$\dot{f}_{1,1} + \dot{\delta}_3 + \tan\theta\ \dot{h}_{1,1} = 0. \tag{5.30}$$

5.4 Stress Variables.

Next we must express the components of the three-dimensional stress tensor σ^{ij} in terms of the two-dimensional generalised stress measures appropriate to the geometry of the weld under investigation. On using the definition (2.91) in the expressions (2.102) and (2.112), the two-dimensional stress measures are related to the components of the three-

dimensional stress tensor σ^{ij} through the expressions

$$\mathrm{N}^{\alpha} a^{\frac{1}{2}} = \int_{-\frac{h}{2}}^{\frac{h}{2}} g^{\frac{1}{2}} \sigma^{\alpha j} \mathrm{g}_j \, d\xi, \tag{5.31}$$

$$\mathrm{M}^{\alpha} a^{\frac{1}{2}} = \int_{-\frac{h}{2}}^{\frac{h}{2}} g^{\frac{1}{2}} \sigma^{\alpha j} \mathrm{g}_j \xi \, d\xi, \tag{5.32}$$

$$\mathrm{m}\, a^{\frac{1}{2}} = \int_{-\frac{h}{2}}^{\frac{h}{2}} g^{\frac{1}{2}} \sigma^{3 j} \mathrm{g}_j \, d\xi, \tag{5.33}$$

Taking the dot product of each of equations (5.31) to (5.33) with the contravariant base vector a^i, we obtain expressions relating the contravariant components of the two-dimensional stress measures to the three dimensional stress tensor, through

$$N^{\alpha i} a^{\frac{1}{2}} = \int_{-\frac{h}{2}}^{\frac{h}{2}} g^{\frac{1}{2}} \sigma^{\alpha j} \left(\mathrm{g}_j \cdot \mathrm{a}^i \right) d\xi, \tag{5.34}$$

$$M^{\alpha i} a^{\frac{1}{2}} = \int_{-\frac{h}{2}}^{\frac{h}{2}} g^{\frac{1}{2}} \sigma^{\alpha j} \left(\mathrm{g}_j \cdot \mathrm{a}^i \right) \xi \, d\xi, \tag{5.35}$$

$$m^i a^{\frac{1}{2}} = \int_{-\frac{h}{2}}^{\frac{h}{2}} g^{\frac{1}{2}} \sigma^{3 j} \left(\mathrm{g}_j \cdot \mathrm{a}^i \right) d\xi. \tag{5.36}$$

As in the previous chapter, the case of the weld with the stress-free top and bottom surfaces, expressions (5.34) to (5.36) can be simplified by assuming that only small deformations occur. In such situations the three-dimensional stress components are small, which in turn implies the existence of small two-dimensional stresses. Hence all stresses involved in the model can be rescaled such that

$$\begin{aligned} N^{\alpha i} = \epsilon \tilde{N}^{\alpha i} \quad , \quad M^{\alpha i} = \epsilon \tilde{M}^{\alpha i}, \\ m^i = \epsilon \tilde{m}^i \quad , \quad \sigma^{ij} = \epsilon \tilde{\sigma}^{ij}. \end{aligned} \tag{5.37}$$

The rescaling of the stress variables in (5.37) means that we require only the leading order terms in ϵ of $a^{\frac{1}{2}}$, $g^{\frac{1}{2}}$ and $(\mathrm{g}_j \cdot \mathrm{a}^i)$. Hence from the expressions (4.23) and (4.24) for a single director and the definition (5.5), we obtain

$$\mathrm{g}_1 = \mathrm{i} + O(\epsilon),$$

$$\begin{aligned} \mathbf{g}_2 &= \mathbf{j}, \\ \mathbf{g}_3 &= -\tan\theta\,\mathbf{i} + \mathbf{k} + O(\epsilon). \end{aligned} \tag{5.38}$$

Recalling expressions (4.13) to (4.16) for the contravariant base vectors we have

$$\begin{aligned} \mathbf{a}^1 &= \mathbf{i} + O(\epsilon), \\ \mathbf{a}^2 &= \mathbf{j}, \\ \mathbf{a}^3 &= \mathbf{k} + O(\epsilon), \end{aligned} \tag{5.39}$$

and we also note that

$$a^{\frac{1}{2}} = 1 + O(\epsilon). \tag{5.40}$$

Using the definitions (5.28), (5.37), (5.39) to (5.40) in (5.34) to (5.36) we obtain

$$\tilde{N}^{\alpha 1} = \int_{-\frac{h}{2}}^{\frac{h}{2}} \left(\tilde{\sigma}^{\alpha 1} - \tan\theta\tilde{\sigma}^{\alpha 3}\right) d\xi \quad , \alpha = 1,2 \tag{5.41}$$

$$\tilde{N}^{\alpha 2} = \int_{-\frac{h}{2}}^{\frac{h}{2}} \tilde{\sigma}^{\alpha 2} d\xi \quad , \alpha = 1,2 \tag{5.42}$$

$$\tilde{N}^{\alpha 3} = \int_{-\frac{h}{2}}^{\frac{h}{2}} \tilde{\sigma}^{\alpha 3} d\xi \quad , \alpha = 1,2 \tag{5.43}$$

$$\tilde{M}^{\alpha 1} = \int_{-\frac{h}{2}}^{\frac{h}{2}} \left(\tilde{\sigma}^{\alpha 1} - \tan\theta\tilde{\sigma}^{\alpha 3}\right) \xi\, d\xi \quad , \alpha = 1,2 \tag{5.44}$$

$$\tilde{M}^{\alpha 2} = \int_{-\frac{h}{2}}^{\frac{h}{2}} \tilde{\sigma}^{\alpha 2} \xi\, d\xi \quad , \alpha = 1,2 \tag{5.45}$$

$$\tilde{M}^{\alpha 3} = \int_{-\frac{h}{2}}^{\frac{h}{2}} \tilde{\sigma}^{\alpha 3} \xi\, d\xi \quad , \alpha = 1,2 \tag{5.46}$$

$$\tilde{m}^1 = \int_{-\frac{h}{2}}^{\frac{h}{2}} \left(\tilde{\sigma}^{31} - \tan\theta\tilde{\sigma}^{33}\right) d\xi, \tag{5.47}$$

$$\tilde{m}^2 = \int_{-\frac{h}{2}}^{\frac{h}{2}} \tilde{\sigma}^{32} d\xi, \tag{5.48}$$

$$\tilde{m}^3 = \int_{-\frac{h}{2}}^{\frac{h}{2}} \tilde{\sigma}^{33} d\xi. \tag{5.49}$$

For simplicity we shall now omit the tildes from the above variables.

We assume that the three-dimensional stress distribution can be represented by truncated power series of the forms

$$\begin{aligned} \sigma^{\alpha\beta} &= a^{\alpha\beta} + b^{\alpha\beta}\,\xi, \\ \sigma^{\alpha 3} &= a^{\alpha 3} + b^{\alpha 3}\,\xi, \\ \sigma^{3\alpha} &= a^{3\alpha} + b^{3\alpha}\,\xi, \\ \sigma^{33} &= a^{33}. \end{aligned} \tag{5.50}$$

Substituting (5.50) into the expressions (5.41) to (5.49) and performing the relevant calculations and back substitutions leads to

$$\sigma^{11} = \frac{1}{h}\left(N^{11} + \tan\theta N^{13}\right) + \frac{12}{h^3}\left(M^{11} + \tan\theta M^{13}\right)\xi, \tag{5.51}$$

$$\sigma^{12} = \frac{N^{12}}{h} + \frac{12}{h^3}M^{12}\xi, \tag{5.52}$$

$$\sigma^{21} = \frac{1}{h}\left(N^{21} + \tan\theta N^{23}\right) + \frac{12}{h^3}\left(M^{21} + \tan\theta M^{23}\right)\xi, \tag{5.53}$$

$$\sigma^{22} = \frac{N^{22}}{h} + \frac{12}{h^3}M^{22}\xi, \tag{5.54}$$

$$\sigma^{13} = \frac{N^{13}}{h} + \frac{12}{h^3}M^{13}\xi, \tag{5.55}$$

$$\sigma^{23} = \frac{N^{23}}{h} + \frac{12}{h^3}M^{23}\xi, \tag{5.56}$$

$$\sigma^{33} = \frac{m^3}{h}. \tag{5.57}$$

We also have expressions for σ^{31} and σ^{32} in the forms

$$\sigma^{31} = \frac{1}{h}\left(m^1 + \tan\theta m^3\right) + b^{31}\xi, \tag{5.58}$$

$$\sigma^{32} = \frac{m^2}{h} + b^{32}\xi, \tag{5.59}$$

In order that the three-dimensional stress tensor σ^{ij} is symmetric we require that, in particular, $\sigma^{13} = \sigma^{31}$ which leads to

$$b^{31} = \frac{12}{h^3}M^{13}, \tag{5.60}$$

$$N^{13} = m^1 + \tan\theta m^3. \tag{5.61}$$

According to the Cosserat theory, if no body forces are acting then the linearized field equations (2.140)–(2.143), for an initially flat plate with a single director, become

$$N^{\alpha\beta}{}_{,\alpha} = 0, \tag{5.62}$$

$$N^{\alpha 3}{}_{,\alpha} = 0, \tag{5.63}$$

$$M^{\alpha\beta}{}_{,\alpha} = m^\beta, \tag{5.64}$$

$$M^{\alpha 3}{}_{,\alpha} = m^3. \tag{5.65}$$

Applying the plane strain condition

$$\frac{\partial}{\partial v^2} = 0, \tag{5.66}$$

the field equations (5.62) to (5.65) reduce further to

$$N^{11}{}_{,1} = 0, \tag{5.67}$$

$$N^{12}{}_{,1} = 0, \tag{5.68}$$

$$N^{13}{}_{,1} = 0, \tag{5.69}$$

$$M^{11}{}_{,1} = m^1, \tag{5.70}$$

$$M^{12}{}_{,1} = m^2, \tag{5.71}$$

$$M^{13}{}_{,1} = m^3. \tag{5.72}$$

As $v^1 \to -\infty$ we assume that the plate acts as if it were a single material plate under simple uniaxial tension and so the only non-zero component of the three-dimensional stress tensor is σ^{11}, where

$$\sigma^{11} = \sigma^\infty. \tag{5.73}$$

On integrating the field equations (5.67) to (5.69), using the expressions (5.51), (5.52) and (5.55) and noting that as $v^1 \to -\infty$ then $\tan\theta(v^1) \to 0$, it follows that

$$N^{11} = N^{\infty} = \sigma^{\infty} h, \tag{5.74}$$

$$N^{12} = N^{13} = 0. \tag{5.75}$$

Now from equation (2.145), for a single director we have

$$N^{\alpha 3} + m^3 D^{\alpha} - m^{\alpha} D^3 = 0 \tag{5.76}$$

Using the definitions (5.1), (5.2) and (5.4) with the identities (5.75) and (5.76) we deduce that

$$N^{13} = m^1 + \tan\theta m^3 = 0, \tag{5.77}$$

$$N^{23} = m^2. \tag{5.78}$$

Substituting for m^1 and m^3 into (5.77), using the field equations (5.70) and (5.72), and integrating with respect to v^1 (recalling that $\theta_{,1} \ll 1$), we obtain

$$M^{11} + \tan\theta M^{13} = constant. \tag{5.79}$$

Using the expression (5.51) and observing that $\tan\theta(v^1) \to 0$ as $v^1 \to -\infty$, then the constant in equation (5.79) becomes identically zero, and hence the expressions for the three-dimensional stresses in terms of the two-dimensional generalised stress measures reduce to

$$\sigma^{11} = \frac{N^{11}}{h}, \tag{5.80}$$

$$\sigma^{12} = \frac{12}{h^3} M^{12} \xi, \tag{5.81}$$

$$\sigma^{13} = \frac{12}{h^3} M^{13} \xi, \tag{5.82}$$

$$\sigma^{23} = \frac{m^2}{h} + \frac{12}{h^3} M^{23}\xi, \tag{5.83}$$

$$\sigma^{22} = \frac{N^{22}}{h} + \frac{12}{h^3} M^{22}\xi, \tag{5.84}$$

$$\sigma^{33} = \frac{m^3}{h}. \tag{5.85}$$

From equations (4.90) and (4.94) we obtain the mixed mode form of the Von Mises equivalent stress as

$$(\sigma^*)^2 = \left(\sigma_1^1\right)^2 + \left(\sigma_2^2\right)^2 + \left(\sigma_3^3\right)^2 - \sigma_1^1\sigma_2^2 - \sigma_2^2\sigma_3^3 - \sigma_3^3\sigma_1^1 + 3\left(\sigma_2^1\sigma_1^2 + \sigma_3^2\sigma_2^3 + \sigma_1^3\sigma_3^1\right). \tag{5.86}$$

Since the field equations in the Cosserat theory are derived in terms of the contravariant components of the two-dimensional generalised stresses, then we require the equivalent stress also to be defined in terms of the contravariant components of the three-dimensional stress tensor σ^{ij}. Thus, we need to raise the indices of the mixed mode form of the components of the stress tensor. Using equation (2.17) in conjunction with the leading order terms of the metric g_{ij}, we then obtain

$$\sigma_1^1 = \sigma^{11} - \tan\theta\sigma^{13}, \tag{5.87}$$

$$\sigma_2^2 = \sigma^{22}, \tag{5.88}$$

$$\sigma_3^3 = -\tan\theta\sigma^{13} + \left(1 + \tan^2\theta\right)\sigma^{23}, \tag{5.89}$$

$$\sigma_2^1 = \sigma^{12}, \tag{5.90}$$

$$\sigma_1^2 = \sigma^{21} - \tan\theta\sigma^{23}, \tag{5.91}$$

$$\sigma_3^2 = -\tan\theta\sigma^{21} + \left(1 + \tan^2\theta\right)\sigma^{23}, \tag{5.92}$$

$$\sigma_2^3 = \sigma^{32}, \tag{5.93}$$

$$\sigma_3^1 = -\tan\theta\sigma^{11} + \left(1 + \tan^2\theta\right)\sigma^{23}, \tag{5.94}$$

$$\sigma_1^3 = \sigma^{13} - \tan\theta\sigma^{23}. \tag{5.95}$$

Upon substituting (5.87) to (5.95), after use of the expressions (5.80) to (5.85), into (5.86) we finally derive

$$\begin{aligned}(\sigma^*)^2 &= \frac{1}{h^2}\Big[\left(N^{11}\right)^2+\left(N^{22}\right)^2+\left(1+\tan^2\theta\right)^2\left(m^3\right)^2-N^{11}N^{22}\\ &- \left(1+\tan^2\theta\right)N^{22}m^3-\left(1-2\tan^2\theta\right)N^{11}m^3+3\left(1+\tan^2\theta\right)\left(m^2\right)^2\Big]\\ &+ \frac{12}{h^4}\xi\Big[2N^{22}M^{22}-N^{11}M^{22}-\left(1+\tan^2\theta\right)m^3M^{22}+6\left(1+\tan^2\theta\right)m^3M^{23}\\ &- 4\tan\theta N^{11}M^{13}-4\tan\theta\left(1+\tan^2\theta\right)m^3M^{13}+2\tan\theta M^{13}N^{22}\\ &- 6\tan\theta M^{12}m^2\Big]+\frac{144}{h^6}\xi^2\Big[\left(M^{22}\right)^2+\left(3+4\tan^2\theta\right)\left(M^{13}\right)^2+3\left(M^{12}\right)^2\\ &+ 3\left(1+\tan^2\theta\right)\left(M^{23}\right)^2+2\tan\theta M^{13}M^{22}-6\tan\theta M^{12}M^{23}\Big], \qquad (5.96)\end{aligned}$$

where we have assumed that the contravariant components of the three-dimensional stress tensor are symmetric i.e.

$$\sigma^{ij}=\sigma^{ji}. \qquad (5.97)$$

5.5 Derivation of the Constitutive Equations.

First let us recall the generalised form of Norton's Law, derived for non-Cartesian tensors in section §4.4. If the kinematic variables and generalised stresses are defined by the two sets,

$$\Psi = \left(N'^{\alpha\beta}, M^{\alpha i}, m^i\right), \qquad (5.98)$$

$$\Theta = \left(\varrho_{\alpha\beta}, \kappa_{\alpha i}, \gamma_i\right), \qquad (5.99)$$

in which we have introduced the invariant stress variable

$$N'^{\alpha\beta}=N'^{\beta\alpha}=N^{\alpha\beta}-m^\alpha d^\beta-M^{\gamma\alpha}\lambda^\beta_{\ \gamma}, \qquad (5.100)$$

then the generalised forms of the Kachanov-Rabotnov equations, appropriate for use with the Cosserat shell theory, are

$$\dot{\Theta} = \frac{A}{2\sigma_c h}\left(\frac{N^*}{\sigma_c h}\right)^{n-1} \frac{1}{\psi^p} \frac{\partial (N^*)^2}{\partial \Psi}, \tag{5.101}$$

and

$$\dot{\psi} = -B\left(\frac{N^*}{\sigma_c h}\right)^m \frac{1}{\psi^q}, \tag{5.102}$$

with N^* being given by (4.109).

Assuming small deformations, the linearized form of equation (5.100) for use with the kinematic variables associated with the geometry of the weld is

$$N'^{\alpha\beta} = N'^{\beta\alpha} = N^{\alpha\beta} - m^\alpha D^\beta. \tag{5.103}$$

Thus, in the derivation of the constitutive equations we require

$$N'^{11} = N^{11} + \tan\theta\, m^1, \tag{5.104}$$

$$N'^{22} = N^{22}. \tag{5.105}$$

As noted in the previous section , we require the three-dimensional stress tensor to be symmetric. We will show later that the components $\sigma^{23}, \sigma^{32}, \sigma^{12}$ and σ^{21} are identically zero and hence we require, in particular , that

$$\sigma^{13} = \sigma^{31}. \tag{5.106}$$

In deriving the three-dimensional stress components, we obtained the relations

$$m^1 + \tan\theta\, m^3 = 0, \tag{5.107}$$

$$M^{11} + \tan\theta M^{13} = 0, \tag{5.108}$$

(see (5.77) and (5.79)) and so it is possible to add the expressions on the left-hand sides of (5.107) and (5.108) to $(N^*)^2$ without altering the value of $(N^*)^2$. After performing

the integration (4.109) on (5.96), replacing N^{11}, N^{22} by the invariants N'^{11}, N'^{22}, and adding on (5.107) and (5.108) with the use of Lagrange multipliers λ, μ respectively, we obtain an expression for $(N^*)^2$ as

$$\begin{aligned}
(N^*)^2 &= \left(N'^{11}\right)^2 - 2\tan\theta N'^{11}m^1 + \tan^2\theta\left(m^1\right)^2 + \left(N'^{22}\right)^2 + \left(1+\tan^2\theta\right)^2\left(m^3\right)^2 \\
&- N'^{11}N'^{22} + \tan\theta m^1 N'^{22} - \left(1+\tan^2\theta\right)N'^{22}m^3 - \left(1-2\tan^2\theta\right)N'^{11}m^3 \\
&+ \tan\theta\left(1-2\tan^2\theta\right)m^1m^3 + 3\left(1+\tan^2\theta\right)\left(m^2\right)^2 \\
&+ \frac{12}{h^2}\left(3+4\tan^2\theta\right)\left(M^{13}\right)^2 + \frac{36}{h^2}\left(M^{12}\right)^2 + \frac{36}{h^2}\left(1+\tan^2\theta\right)\left(M^{23}\right)^2 \\
&+ \frac{24}{h^2}\tan\theta M^{13}M^{22} - \frac{72}{h^2}\tan\theta M^{12}M^{23} + \lambda\left(m^1+\tan\theta m^3\right) \\
&+ \mu\left(M^{11}+\tan\theta M^{13}\right). \qquad (5.109)
\end{aligned}$$

Using the generalised form of Norton's Law (5.98) to (5.101), and using the results (5.9) to (5.17) for the strain-rates, we obtain

$$\begin{aligned}
\dot{f}_{1,1} &= \frac{A}{2\sigma_c h}\left(\frac{N^*}{\sigma_c h}\right)^{n-1}\frac{1}{\psi^p}\left(2N'^{11} - 2\tan\theta m^1 - N'^{22}\right. \\
&- \left.\left(1-2\tan^2\theta\right)m^3\right), \qquad (5.110) \\
0 &= \frac{A}{2\sigma_c h}\left(\frac{N^*}{\sigma_c h}\right)^{n-1}\frac{1}{\psi^p}\left(2N'^{22} - N'^{11} + \tan\theta m^1\right. \\
&- \left.\left(1+\tan^2\theta\right)m^3\right), \qquad (5.111) \\
\dot{\delta}_{1,1} &= \frac{A}{2\sigma_c h}\left(\frac{N^*}{\sigma_c h}\right)^{n-1}\frac{\mu}{\psi^p}, \qquad (5.112) \\
0 &= \frac{A}{2\sigma_c h}\left(\frac{N^*}{\sigma_c h}\right)^{n-1}\frac{1}{\psi^p}\left(\frac{72}{h^2}M^{12} - \frac{72}{h^2}\tan\theta M^{23}\right), \qquad (5.113) \\
0 &= \frac{A}{2\sigma_c h}\left(\frac{N^*}{\sigma_c h}\right)^{n-1}\frac{1}{\psi^p}\left(\frac{24}{h^2}M^{22} + \frac{24}{h^2}\tan\theta M^{13}\right), \qquad (5.114) \\
\dot{\delta}_{3,1} - \tan\theta\dot{h}_{1,11} &= \frac{A}{2\sigma_c h}\left(\frac{N^*}{\sigma_c h}\right)^{n-1}\frac{1}{\psi^p}\left(\frac{24}{h^2}\left(3+4\tan^2\theta\right)M^{13}\right. \\
&+ \left.\frac{24}{h^2}\tan\theta M^{22} + \mu\tan\theta\right), \qquad (5.115)
\end{aligned}$$

$$
\begin{aligned}
0 &= \frac{A}{2\sigma_c h}\left(\frac{N^*}{\sigma_c h}\right)^{n-1}\frac{1}{\psi^p}\left(\frac{72}{h^2}\left(1+\tan^2\theta\right)M^{23}\right. \\
&- \left.\frac{72}{h^2}\tan\theta M^{12}\right), \qquad (5.116)\\
\dot{\delta}_1 - 2\tan\theta\dot{f}_{1,1} &= \frac{A}{2\sigma_c h}\left(\frac{N^*}{\sigma_c h}\right)^{n-1}\frac{1}{\psi^p}\left(-2\tan\theta N'^{11}+2\tan^2\theta m^1+\tan\theta N'^{22}\right. \\
&+ \left.\tan\theta\left(1-2\tan^2\theta\right)m^3+\lambda\right), \qquad (5.117)\\
0 &= \frac{A}{2\sigma_c h}\left(\frac{N^*}{\sigma_c h}\right)^{n-1}\frac{1}{\psi^p}\left(6\left(1+\tan^2\theta\right)m^2\right), \qquad (5.118)\\
\dot{\delta}_3 &= \frac{A}{2\sigma_c h}\left(\frac{N^*}{\sigma_c h}\right)^{n-1}\frac{1}{\psi^p}\left(2\left(1+\tan^2\theta\right)^2 m^3-\left(1+\tan^2\theta\right)N'^{22}\right. \\
&- \left(1-2\tan^2\theta\right)N'^{11}+\tan\theta\left(1-2\tan^2\theta\right)m^1 \\
&+ \left.\lambda\tan\theta\right). \qquad (5.119)
\end{aligned}
$$

The field equations (5.62) to (5.65), have been derived in terms of N^{11} and so it is helpful to substitute back for N^{11} and N^{22}, using (5.104) and (5.105). For non-trivial solutions to the system of equations we require from equations (5.111) and (5.114) that

$$
\begin{aligned}
N^{22} &= \frac{1}{2}\left(N^{11}+\left(1+\tan^2\theta\right)m^3\right), \qquad (5.120)\\
M^{22} &= -\tan\theta M^{13}, \qquad (5.121)
\end{aligned}
$$

and, in order that the equations (5.113), (5.116) and (5.118) are satisfied for a general angle θ , it is necessary that

$$
M^{23} = M^{12} = m^2 = 0. \qquad (5.122)
$$

Eliminating N^{22} and M^{22} from the system of equations then gives

$$
\begin{aligned}
\dot{f}_{1,1} &= \frac{3}{4}\frac{A}{\sigma_c h}\left(\frac{N^*}{\sigma_c h}\right)^{n-1}\frac{1}{\psi^p}\left(N^{11}-\left(1-\tan^2\theta\right)m^3\right), \qquad (5.123)\\
\dot{\delta}_{3,1}-\tan\theta\dot{h}_{1.11} &= \frac{A}{2\sigma_c h}\left(\frac{N^*}{\sigma_c h}\right)^{n-1}\frac{1}{\psi^p}\left(\frac{72}{h^2}\left(1+\tan^2\theta\right)M^{13}+\mu\tan\theta\right), \qquad (5.124)
\end{aligned}
$$

$$\dot{\delta}_1 - \tan\theta \dot{f}_{1,1} = \frac{A}{2\sigma_c h}\left(\frac{N^*}{\sigma_c h}\right)^{n-1}\frac{1}{\psi^p}\lambda, \tag{5.125}$$

$$\dot{\delta}_3 = \frac{3}{4}\frac{A}{\sigma_c h}\left(\frac{N^*}{\sigma_c h}\right)^{n-1}\frac{1}{\psi^p}\left(\left(1+\tan^2\theta\right)^2 m^3 - \left(1-\tan^2\theta\right)N^{11} + \frac{2}{3}\lambda\tan\theta\right). \tag{5.126}$$

Differentiating (5.125) with respect to v^1 and then eliminating $\dot{\delta}_1$ from the system using equation (5.112) leads to

$$\dot{h}_{1,11} = \frac{A}{2\sigma_c h}\left(\frac{N^*}{\sigma_c h}\right)^{n-1}\frac{1}{\psi^p}\left[\left((n-1)\left(\frac{N^*{}_{,1}}{N^*}\right) - p\left(\frac{\psi_{,1}}{\psi}\right)\right)\lambda + \lambda_{,1} - \mu\right]. \tag{5.127}$$

In a somewhat similar way, differentiating (5.126) with respect to v^1 and using equations (5.67) and (5.127) leads to the differential equation

$$\dot{\delta}_{3,1} - \tan\theta\dot{h}_{1,11} = \frac{3}{4}\frac{A}{\sigma_c h}\left(\frac{N^*}{\sigma_c h}\right)^{n-1}\frac{1}{\psi^p}\left[\left((n-1)\left(\frac{N^*{}_{,1}}{N^*}\right) - p\left(\frac{\psi_{,1}}{\psi}\right)\right) \times \left(\left(1+\tan^2\theta\right)^2 m^3 - \left(1-\tan^2\theta\right)N^{11}\right) + \left(1+\tan^2\theta\right)^2 m^3{}_{,1}\right] + \frac{A}{2\sigma_c h}\left(\frac{N^*}{\sigma_c h}\right)^2\frac{1}{\psi^p}\mu\tan\theta. \tag{5.128}$$

Comparing (5.128) with the differential equation (5.124) and recalling the field equation (5.72) we finally derive the following system of partial differential equations

$$m^3{}_{,1} = \frac{48}{h^2}\frac{1}{(1+\tan^2\theta)}M^{13} - \left((n-1)\left(\frac{N^*{}_{,1}}{N^*}\right) - p\left(\frac{\psi_{,1}}{\psi}\right)\right)\left(m^3 - \frac{(1-\tan^2\theta)}{(1+\tan^2\theta)^2}N^{11}\right), \tag{5.129}$$

$$M^{13}{}_{,1} = m^3, \tag{5.130}$$

with

$$\dot{\psi} = -B\left(\frac{N^*}{\sigma_c h}\right)^m\frac{1}{\psi^q}. \tag{5.131}$$

Before introducing the boundary conditions we shall discuss briefly the use of the Lagrange multipliers λ and μ. The latter have been introduced into (5.109) to make full

use of the symmetry of σ^{ij} and this extra flexibility is necessary in order that the continuity condition (5.30) is identically satisfied. Differentiating (5.30) leads to

$$\dot{f}_{1,11} + \dot{\delta}_{3,1} - \tan\theta \dot{h}_{1,11} = 0. \tag{5.132}$$

Hence on differentiating equation (5.110) with respect to v^1, and using equations (5.124), (5.129), (5.130) and (5.67) we deduce that equation (5.132) is satisfied only if the Lagrange multiplier μ satisfies

$$\mu = -\frac{72\tan\theta}{h^2}\left(\frac{3+\tan^2\theta}{1+\tan^2\theta}\right)M^{13} - \frac{6\tan\theta}{(1+\tan^2\theta)^2}\left((n-1)\left(\frac{N^*{}_{,1}}{N^*}\right) - p\left(\frac{\psi_{,1}}{\psi}\right)\right)N^{11}. \tag{5.133}$$

The other Lagrange multiplier λ can be calculated from equation (5.127). In both the expressions for λ and μ we have

$$\begin{aligned}(N^*)^2 &= \frac{3}{4}\left(N^{11}\right)^2 - \frac{3}{2}\left(1-\tan^2\theta\right)N^{11}m^3 + \frac{3}{4}\left(1+\tan^2\theta\right)^2\left(m^3\right)^2 \\ &+ \frac{36}{h^2}\left(1+\tan^2\theta\right)\left(M^{13}\right)^2,\end{aligned} \tag{5.134}$$

and

$$\begin{aligned}N^*{}_{,1} &= \left[\left(-\left(1-\tan^2\theta\right)N^{11} + \left(1+\tan^2\theta\right)^2 m^3\right)\left(\frac{48}{h^2}\frac{M^{13}}{(1+\tan^2\theta)}\right.\right. \\ &+ \left.\left. p\left(\frac{\psi_{,1}}{\psi}\right)\left(m^3 - \frac{(1-\tan^2\theta)}{(1+\tan^2\theta)^2}N^{11}\right)\right) + .\frac{48}{h^2}\left(1+\tan^2\theta\right)M^{13}m^3\right] \\ &\times \left[\frac{4}{3}N^* + \frac{(n-1)}{N^*}\left(-\left(1-\tan^2\theta\right)N^{11} + \left(1+\tan^2\theta\right)^2 m^3\right)\right. \\ &\times \left.\left(m^3 - \frac{(1-\tan^2\theta)}{(1+\tan^2\theta)^2}N^{11}\right)\right]^{-1}.\end{aligned} \tag{5.135}$$

5.6 Boundary Conditions.

The boundary conditions and continuity conditions for the V-shaped weld are identical to those stated in chapter 3 of this thesis for the weld with the interface normal to the

central surface of the plate. Thus we require

$$\text{as } v^1 \to -\infty \quad , \quad M^{13} \to 0, \tag{5.136}$$

$$\text{at } v^1 = l_3 \quad , \quad M^{13} = 0, \tag{5.137}$$

where l_3 is the position of the centre of the weld. The continuity conditions are that at each respective interface

$$M^{13}, \dot{\varrho}_{11} \text{ are continuous.} \tag{5.138}$$

The initial conditions and failure criterion are those defined by (2.43). In view of the form of conditions (5.136) and (5.137) we must solve a two point boundary value problem.

5.7 Non-Dimensionalisation.

The equations (5.129) to (5.131) and the expressions (5.134) and (5.135) can be rescaled and non-dimensionalised by redefining the variables through

$$\tilde{N}^* = \left(\frac{4}{3}\right)^{\frac{1}{2}} \frac{N^*}{N^\infty} \quad , \quad \tilde{\psi} = \psi \quad , \quad \tilde{v}^1 = \frac{v^1}{h}\sqrt{48},$$

$$\tilde{m}^3 = m^3 \quad , \quad \tilde{M}^{13} = \frac{M^{13}}{h}\frac{\sqrt{48}}{N^\infty} \quad , \quad \tilde{t} = \frac{t}{T}, \tag{5.139}$$

$$\tilde{A} = T\left(\frac{3}{4}\right)^{\frac{n+1}{2}} \left(\frac{N^\infty}{\sigma_c h}\right)^n A \quad , \quad \tilde{B} = \left(\frac{N^\infty}{\sigma_c h}\right)^m \left(\frac{3}{4}\right)^{\frac{m}{2}} TB,$$

to give

$$\tilde{m}^3{}_{,1} = \frac{\tilde{M}^{13}}{(1+\tan^2\theta)} - \left((n-1)\left(\frac{\tilde{N}^*{}_{,1}}{\tilde{N}^*}\right) - p\left(\frac{\tilde{\psi}_{,1}}{\tilde{\psi}}\right)\right)\left(\tilde{m}^3 - \frac{(1-\tan^2\theta)}{(1+\tan^2\theta)^2}\right), \tag{5.140}$$

$$\tilde{M}^{13}{}_{,1} = \tilde{m}^3, \tag{5.141}$$

$$\dot{\tilde{\psi}} = -\tilde{B}\frac{\left(\tilde{N}^*\right)^m}{\tilde{\psi}^q}, \tag{5.142}$$

with

$$\left(\tilde{N}^*\right)^2 = 1 - 2\left(1 - \tan^2\theta\right)\tilde{m}^3 + \left(1 + \tan^2\theta\right)^2\left(\tilde{m}^3\right)^2 + \left(1 + \tan^2\theta\right)\left(\tilde{M}^{13}\right)^2 \quad (5.143)$$

and

$$\begin{aligned}\left(\tilde{N}^*\right)_{,1} &= \left[\left(-\left(1 - \tan^2\theta\right) + \left(1 + \tan^2\theta\right)^2\tilde{m}^3\right)\left(\frac{\tilde{M}^{13}}{\left(1 + \tan^2\theta\right)}\right.\right. \\ &+ \left.\left. p\left(\frac{\dot{\psi}_{,1}}{\dot{\psi}}\right)\left(\tilde{m}^3 - \frac{\left(1 - \tan^2\theta\right)}{\left(1 + \tan^2\theta\right)^2}\right)\right) + \left(1 + \tan^2\theta\right)\tilde{M}^{13}\tilde{m}^3\right] \\ &\times \left[\tilde{N}^* + \frac{(n_1)}{\tilde{N}^*}\left(-\left(1 - \tan^2\theta\right) + \left(1 + \tan^2\theta\right)^2\tilde{m}^3\right)\right. \\ &\times \left.\left(\tilde{m}^3 - \frac{\left(1 - \tan^2\theta\right)}{\left(1 + \tan^2\theta\right)^2}\right)\right]^{-1}. \end{aligned} \quad (5.144)$$

The system of partial differential equations is now solved numerically.

5.8 Numerical Solution.

To solve the system of partial differential equations (5.140) to (5.142) we must specify values for the indices m, n, p and q and also values for $A^{(\mathrm{p})}$, $A^{(\mathrm{iv})}$, $A^{(\mathrm{haz})}$ and $A^{(\mathrm{w})}$ and the corresponding values for B. It seems sensible to use the same values for these parameters as those used in chapter 3, (namely (3.114) to (3.118)), so that direct comparisons can be made with the results in chapter 3 . The system of differential equations is solved as follows;

Step 1: At $t = 0$, we know that $\psi = 1$ everywhere. Hence (5.140) and (5.141) can be solved using a fourth order Runge-Kutta technique, which is accurate to $O\left(\Delta x^5\right)$ where Δx defines the step size. Let M_i and m_i represent the values of M^{13} and m^3 respectively at the i'th node along the v^1 axis, dropping the tildes of the non-dimensional quantity for convenience. Then if we define

$$M^{13}{}_{,1} = f\left(m^3\right), \quad (5.145)$$

$$m^3{}_{,1} = g\left(v^1, M^{13}, m^3\right), \tag{5.146}$$

we deduce

$$M_{i+1} = M_i + \frac{1}{6}\left(j_1 + 2j_2 + 2j_3 + j_4\right), \tag{5.147}$$

$$m_{i+1} = m_i + \frac{1}{6}\left(k_1 + 2k_2 + 2k_3 + k_4\right), \tag{5.148}$$

where

$$j_1 = \Delta x\, f\left(m_i\right), \tag{5.149}$$

$$k_1 = \Delta x\, g\left(v^1, M_i, m_i\right), \tag{5.150}$$

$$j_2 = \Delta x\, f\left(m_i + \frac{k_1}{2}\right), \tag{5.151}$$

$$k_2 = \Delta x\, g\left(v^1 + \frac{\Delta x}{2}, M_i + \frac{j_1}{2}, m_i + \frac{k_1}{2}\right), \tag{5.152}$$

$$j_3 = \Delta x\, f\left(m_i + \frac{k_2}{2}\right), \tag{5.153}$$

$$k_3 = \Delta x\, g\left(v^1 + \frac{\Delta x}{2}, M_i + \frac{j_2}{2}, m_i + \frac{k_2}{2}\right), \tag{5.154}$$

$$j_4 = \Delta x\, f\left(m_i + k_3\right), \tag{5.155}$$

$$k_4 = \Delta x\, g\left(v^1 + \Delta x, M_i + j_3, m_i + k_3\right). \tag{5.156}$$

The ordinary differential equations (5.140) and (5.141) are solved using a shooting and matching technique, which changes the two point boundary value problem to an initial value problem with m^3 unknown as $v^1 \to -\infty$. In the numerical solution minus infinity is replaced by l_∞, which is a position chosen to be far enough away from the weld region that M^{13} and m^3 have attained their limiting values. The Runge-Kutta method is then initiated at l_∞ with $M^{13} = 0$ and a "guess" for m^3. Let this guess be denoted by $m_\circ$. The solution for this initial value will give a value for M^{13} at l_3 which we hope will satisfy the boundary condition (5.137). If it is sufficiently close, i.e. within some

tolerance of zero, then we proceed with step 3 (below), otherwise $m_\circ$ needs to be revised. The improvement to $m_\circ$ is carried out using the Newton-Raphson method for finding the root of a function.

Step 2: We wish to find the root of

$$M^{13}|_{v^1=l_3} = M(m_\circ) = 0, \tag{5.157}$$

and so can update the guess for $m_\circ$ using

$$m_1 = m_\circ - \frac{M(m_\circ)}{M'(m_\circ)}, \tag{5.158}$$

where

$$M'(m_\circ) = \frac{dM}{dm_\circ} \tag{5.159}$$

We cannot write down an explicit function for $M(m_\circ)$, however, and so we must approximate (5.159) by slightly altering the initial guess, and then using the Runge-Kutta procedure to obtain a different boundary value for M^{13}. The derivative can then be approximated through the formula

$$\frac{dM}{dm_\circ} \approx \frac{M(m_\circ + \Delta m_\circ) - M(m_\circ)}{\Delta m_\circ}, \tag{5.160}$$

where $\Delta m_\circ$ is the change in the initial guess. This process is repeated continually until (5.157) is satisfied to some tolerance level.

Step 3:After solving the ordinary differential equations (5.140) and (5.141) at a particular time step the quantity ψ can be updated to the next time step using a forward difference scheme giving

$$\frac{\left(\psi_i^{j+1}\right)^{q+1} - \left(\psi_i^{j}\right)^{q+1}}{\Delta t} = -B(q+1)(N^*)^n, \tag{5.161}$$

where ψ_i^j represents the value of ψ at the i^{th} node along the v^1 axis at the j^{th} time step.

Steps 1 to 3 are repeated until the failure criterion

$$\left(\psi_i^{j+1}\right)^{q+1} \leq 0, \tag{5.162}$$

holds at a single node. If the condition (5.162) is true at more than one node then the time step Δt is reduced by a factor of 10 and the process is repeated for that time step until (5.162) is satisfied uniquely.

In using the above numerical method we assume that there are 51 nodes in each region and that at each interface the continuity conditions (5.138) hold. Thus at the interface between the parent material and the type IV region , for example, we have

$$M_{51}^{(\mathrm{p})} = M_{1}^{(\mathrm{iv})}, \tag{5.163}$$

and

$$\dot{\varrho}_{51}^{(\mathrm{p})} = \dot{\varrho}_{1}^{(\mathrm{iv})}, \tag{5.164}$$

where $\dot{\varrho}_i^{(p)}, \dot{\varrho}_i^{(iv)}$ represents the strain-rate $\dot{\varrho}_{11}$ in each respective region. On using (5.9), (5.123) and (5.139) condition (5.164) becomes

$$\begin{aligned} &\frac{A^{(\mathrm{p})}}{\left(\psi^{(\mathrm{p})}\right)^{n}}\left(N^{*(\mathrm{p})}\right)^{n-1}\left(1-\left(1-\tan^{2}\theta\right)m^{(\mathrm{p})}\right) \\ &\quad=\frac{A^{(\mathrm{iv})}}{\left(\psi^{(\mathrm{iv})}\right)^{n}}\left(N^{*(\mathrm{iv})}\right)^{n-1}\left(1-\left(1-\tan^{2}\theta\right)m^{(\mathrm{iv})}\right) \end{aligned} \tag{5.165}$$

where a parameter or variable with an index of (p) or (iv) represents the limiting value of the parameter/variable at the interface in the parent or type IV region respectively. Since the only unknown in (5.165) is $m^{(\mathrm{iv})}$, we can solve (5.165) iteratively, from an initial guess of $m_{\circ}^{(\mathrm{iv})}$, by using

$$m_{1}^{(\mathrm{iv})} = m_{\circ}^{(\mathrm{iv})} - \frac{f\left(m_{\circ}^{(\mathrm{iv})}\right)}{f'\left(m_{\circ}^{(\mathrm{iv})}\right)}, \tag{5.166}$$

where

$$\begin{aligned} f\left(m^{(\mathrm{iv})}\right) \;=\; &\frac{A^{(\mathrm{iv})}}{\left(\psi^{(\mathrm{iv})}\right)^{n}}\left(N^{*(\mathrm{iv})}\right)^{n-1}\left(1-\left(1-\tan^{2}\theta\right)m^{(\mathrm{iv})}\right) \\ &-\frac{A^{(\mathrm{p})}}{\left(\psi^{(\mathrm{p})}\right)^{n}}\left(N^{*(\mathrm{p})}\right)^{n-1}\left(1-\left(1-\tan^{2}\theta\right)m^{(\mathrm{p})}\right) \end{aligned} \tag{5.167}$$

and

$$\begin{aligned} f'\left(m^{(\mathrm{iv})}\right) &= \frac{df}{dm^{(\mathrm{iv})}} \\ &= \frac{A^{(\mathrm{iv})}}{\psi^{(\mathrm{iv})^n}}\left[(n-1)\left(N^{*(\mathrm{iv})}\right)^{n-3}\left(1-\left(1-\tan^2\theta\right)m^{(\mathrm{iv})}\right)\left(-1+\tan^2\theta\right.\right. \\ &\quad \left.\left.+\left(1+\tan^2\theta\right)^2 m^{(\mathrm{iv})}\right)-\left(N^{*(\mathrm{iv})}\right)^{n-1}\left(1-\tan^2\theta\right)\right]. \end{aligned} \tag{5.168}$$

In the above procedure a separate Newton-Raphson iteration must be performed at each interface, and hence the computer time required to solve this system is much greater than for the solution obtained in chapter 3. The initial guesses for m^3 at $v^1 = l_\infty$ and for the guesses of m^3 at each of the interfaces can be improved by using the values obtained for the solution of the ordinary differential equations at the previous time step.

Using the above method rupture times and position of rupture can be obtained for various prescribed values of the parameters.

5.9 Results.

This section divides naturally into two subsections. The first contains results for the strain-rates at $t = 0$, together with the rupture times and rupture positions for the situation where the interface of each region is normal to the central surface of the plate ($\theta_\circ = 0$). These results can then be directly compared with the results obtained using the method of chapter 3.

The second subsection considers the effects on the strain-rates at $t = 0$, rupture times and rupture positions in the weldment, caused by varying the angle of the interface ($\theta_\circ$). We recall the definitions (3.140) to (3.142) for $x^{(\mathrm{iv})}, x^{(\mathrm{haz})}$ and $x^{(\mathrm{w})}$. We shall also use the same values for B stated in (3.143).

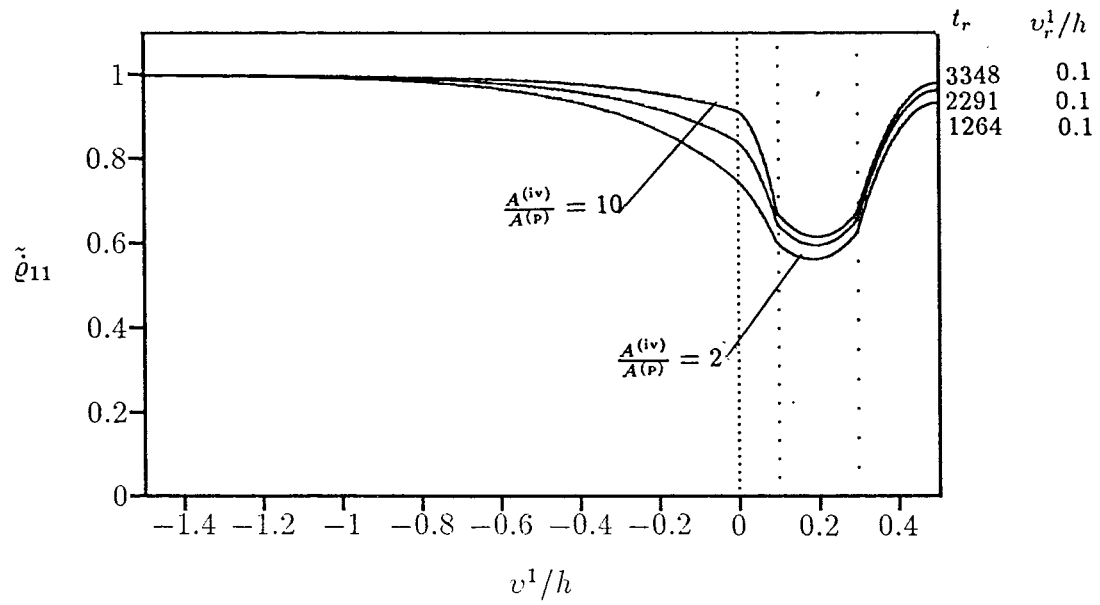

Figure 5.2: strain-rates for various $A^{(iv)}/A^{(p)}$ with $x^{(iv)}$=0.1

5.9.1 $\theta_o = 0$.

In Figures (5.2)–(5.4), (5.6)–(5.8) and (5.14)–(5.16) the non-dimensional position v^1/h is plotted on the horizontal axis against the non-dimensional strain-rate $\tilde{\dot{\varrho}}_{11}$ on the vertical axis. On the right hand side of each figure are shown the corresponding rupture times t_r and rupture positions v_r^1 respectively.

Figures (5.2) to (5.5) show the changes in the strain-rate at $t = 0$ and the time to rupture caused by varying the parameters associated with the type IV region, namely $x^{(iv)}$ and the ratio $A^{(iv)}/A^{(p)}$. In all three figures $A^{(iv)}$ takes the values 10, 5 and 2 respectively, but in all cases $A^{(haz)}/A^{(p)} = 0.1$ and $A^{(w)}/A^{(p)} = 3.0$ and the widths of the heat affected zone and weld metal are given by $x^{(haz)} = x^{(w)} = 0.2$. The difference between the figures is due to the variation in $x^{(iv)}$:

- Figure (5.2), $x^{(iv)} = 0.1$,

- Figure (5.3), $x^{(\mathrm{iv})} = 0.2$,
- Figure (5.4), $x^{(\mathrm{iv})} = 0.5$.

The analogous results to Figures (5.2)–(5.4), using the method described in chapter 3, are shown in Figures (3.2) to (3.4). Comparing directly Figure (3.2) with Figure (5.2) we observe that although the plots of the initial strain-rates are similar, the rupture times and positions of rupture are dramatically different. In Figure (5.2) the positions of rupture, for the three chosen values of $A^{(\mathrm{iv})}/A^{(\mathrm{p})}$, are at the interface between the type IV region and the heat affected zone. The reason for these rupture positions being located at this point becomes clear upon examination of the generalised effective stress N^*, which attains its maximum value within the type IV region at this position, and as the rate of damage $\dot{\psi}$ is dependent upon N^* (with a high B in the type IV region) we would expect the maximum rate of damage to occur at this point.

The time to rupture for each specific value of $A^{(\mathrm{iv})}/A^{(\mathrm{p})}$ has been reduced significantly for each of the Figures (5.2)–(5.4) compared to the analogous results shown in Figures (3.2)–(3.4). The results display the same characteristic trends in rupture times, however, since the rupture time decreases as the relative strength of the type IV region is increased. It should be noted that we have again not altered the value of the parameter B in the type IV region when changing the value of $A^{(\mathrm{iv})}/A^{(\mathrm{p})}$.

If the value of B is changed in the type IV region such that B satisfies equation (3.149) with $p = 0.9$, then the times to rupture, as $A^{(\mathrm{iv})}/A^{(\mathrm{p})}$ decreases become 3348, 4184 and 4514 hours respectively. This agrees with the argument expressed in §3.8 that the relationship between the parameters A and B is very important, and in realistic situations increasing the strength of the type IV region increases the rupture time.

Widening the type IV region to $x^{(\mathrm{iv})} = 0.2$ (Figure (5.3)) produces an increase in the initial strain-rates for each value of $A^{(\mathrm{iv})}/A^{(\mathrm{p})}$, and a decrease in the corresponding rupture times. The rupture positions are again at the interface between the type IV region and the

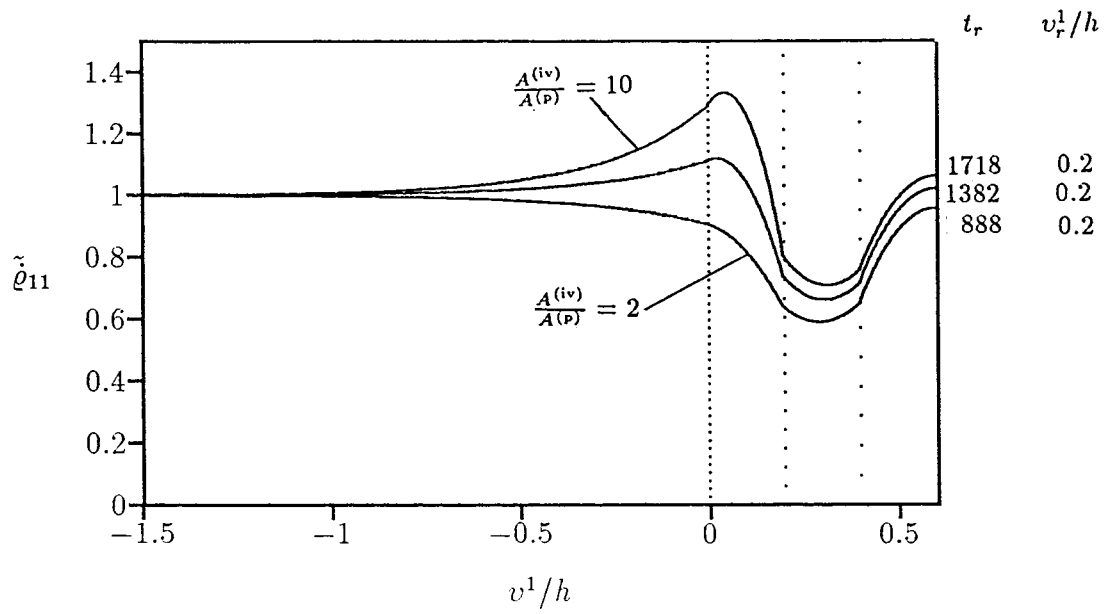

Figure 5.3: strain-rates for various $A^{(iv)}/A^{(p)}$ with $x^{(iv)}$=0.2

HAZ. We observe that the percentage decrease in the rupture time from the previous case $\left(x^{(iv)} = 0.1,\ \text{Figure (5.2)}\ \right)$ is greatest for the softer type IV region $\left(A^{(iv)}/A^{(p)} = 10\right)$.

This trend continues when the width of the type IV region is increased to $x^{(iv)} = 0.5$, when the rupture time has decreased so much for the soft type IV region that the weld ruptures quicker than for the stronger type IV region $\left(A^{(iv)}/A^{(p)} = 5\right)$. Examination of the initial $(t = 0)$ generalised effective stress N^* within the type IV region (Figure (5.5)), for the same parameters used to obtain Figure (5.4), gives the mathematical reason for this anomaly. From Figure (5.5), for the very soft type IV region there is, according to our model, an increase in the value of N^* as v^1/h approaches the interface between the type IV region and the HAZ. This raises the value of N^* above the corresponding plot for $A^{(iv)}/A^{(p)} = 5$ and hence the damage rate is greater for the softer type IV region, which in turn implies that the weld ruptures quicker for this softer type IV region.

When the value of B is altered, using the equation (3.149) with $p = 0.9$, and using the appropriate parameter values associated with Figure (5.3), the rupture times corresponding

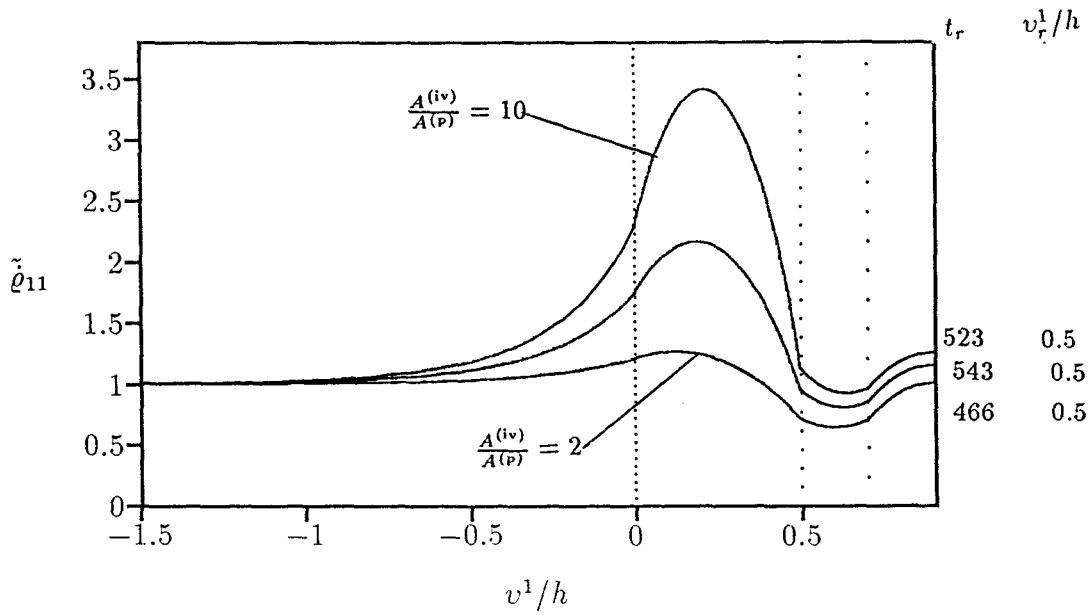

Figure 5.4: strain-rates for various $A^{(iv)}/A^{(p)}$ with $x^{(iv)}$=0.5

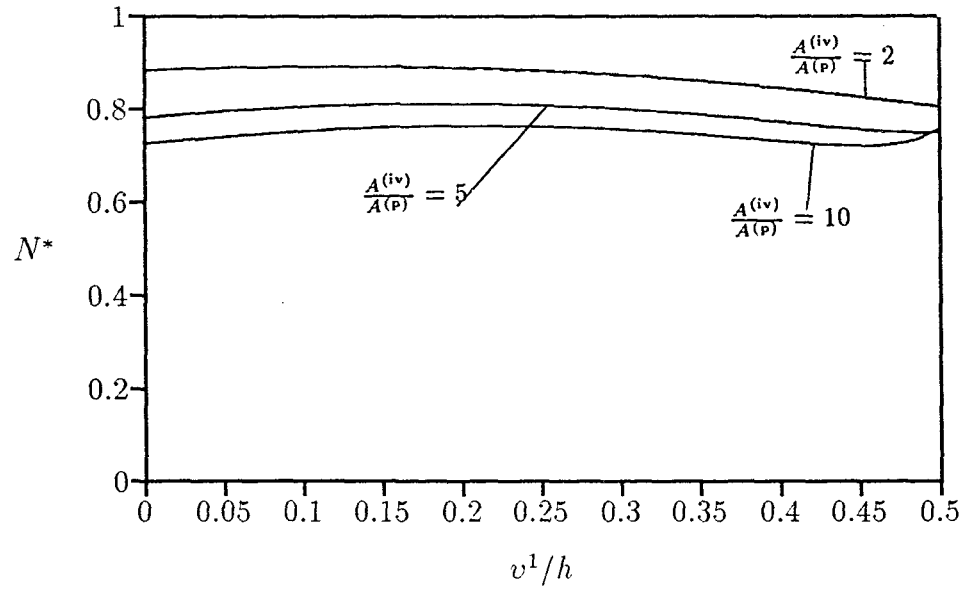

Figure 5.5: Variation of $\hat{N}^*$ in the type IV region, corresponding to Figure (5.4)

to the chosen values of $A^{(iv)}/A^{(p)}$=10, 5 and 2 are 1718, 2514 and 3174 hours respectively.

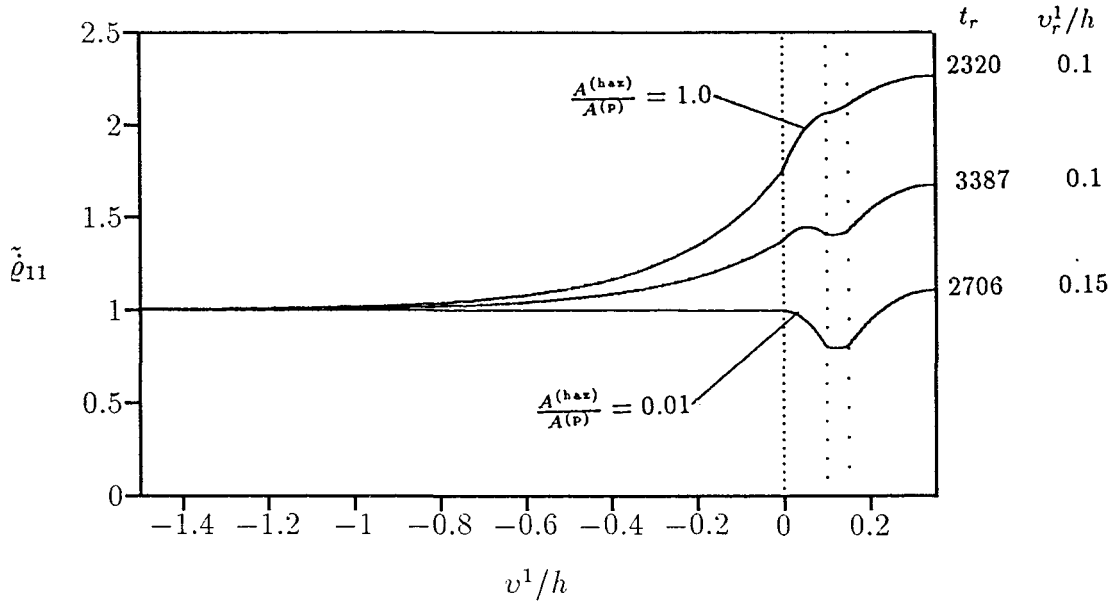

Figure 5.6: strain-rates for various $A^{(\mathrm{haz})}/A^{(\mathrm{p})}$ with $x^{(\mathrm{haz})}$=0.05

When $x^{(\mathrm{iv})} = 0.5$ (Figure (5.4)) the corresponding rupture times are 523, 987, and 1661 hours. Thus counter intuitive solutions obtained without a variation in B have been removed.

From Figure (5.5) it appears that the maximum value of N^* occurs at some position within the type IV region (the maximum value of N^* within the type IV region actually occurs at v^1/h =0.21, 0.19 and 0.12 for $A^{(\mathrm{iv})}/A^{(\mathrm{p})}$ =10, 5 and 2 respectively) and so we would expect rupture to occur at these positions. However,in a similar manner to the behaviour of the strain-rates in Figure (3.11), where the position of the maximum value of the strain rate moved with time, using the method of this chapter the position of the maximum value of N^*, and hence the position of the maximum damage rate, is also time-dependent.

In Figures (5.6) to (5.8) the parameters associated with the HAZ are varied. Each of the figures show plots of the strain-rate at $t = 0$ for $A^{(\mathrm{haz})}/A^{(\mathrm{p})}$ taking the values 1.0, 0.1 and 0.01 respectively. The widths of the type IV region and the weld metal are kept

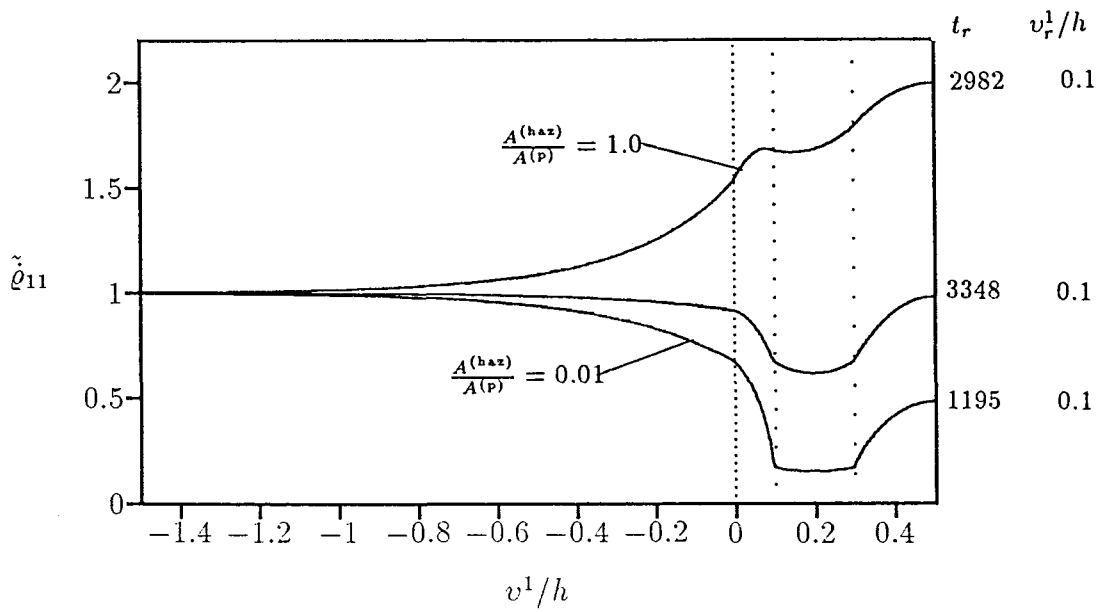

Figure 5.7: strain-rates for various $A^{(\mathrm{haz})}/A^{(\mathrm{p})}$ with $x^{(\mathrm{haz})}$=0.2

constant at $x^{(\mathrm{iv})}$=0.1 and $x^{(\mathrm{w})}$= 0.2, with the relative strength of these two regions being fixed at $A^{(\mathrm{iv})}/A^{(\mathrm{p})} = 10.0$ and $A^{(\mathrm{w})}/A^{(\mathrm{p})} = 3.0$. The only parameter varying from figure to figure is $x^{(\mathrm{haz})}$, which takes the values

- Figure (5.6), $x^{(\mathrm{haz})} = 0.05$,
- Figure (5.7), $x^{(\mathrm{haz})} = 0.2$,
- Figure (5.8), $x^{(\mathrm{haz})} = 0.5$.

Comparing Figure (5.6) with Figure (3.5) we observe a similar pattern in the initial strain-rates and rupture times. We deduce again that for a very hard HAZ $\left(A^{(\mathrm{haz})}/A^{(\mathrm{p})} = 0.01\right)$ the position of rupture is at the interface between the HAZ and the weld metal and, for this case, the actual time to rupture is comparable to that obtained using the direct method of chapter 3.

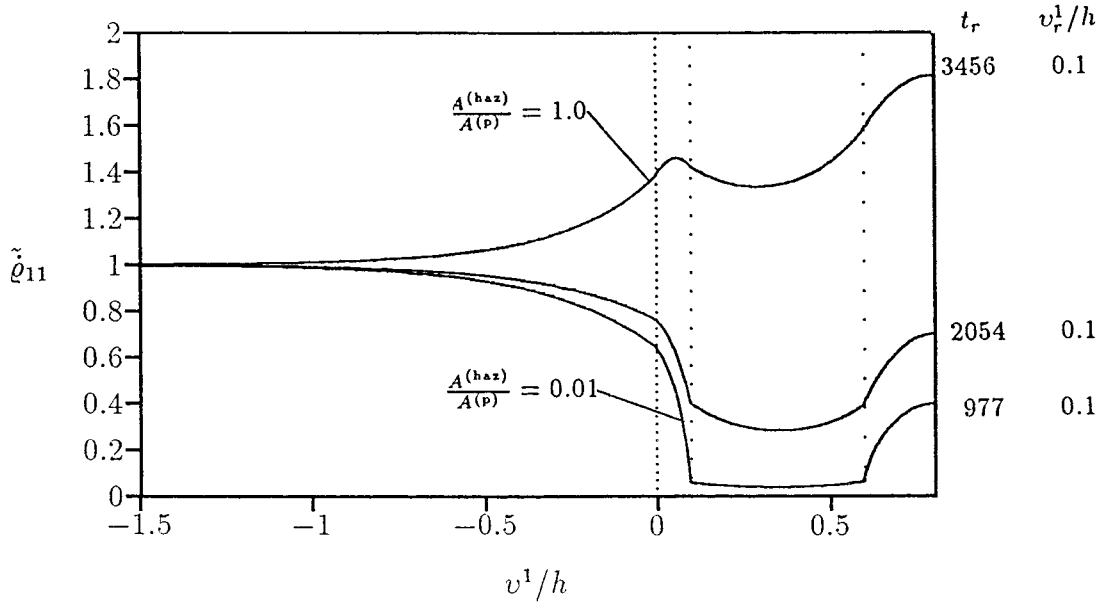

Figure 5.8: strain-rates for various $A^{(\mathrm{haz})}/A^{(\mathrm{p})}$ with $x^{(\mathrm{haz})}$=0.5

When B is altered, the time to rupture for $A^{(\mathrm{haz})}/A^{(\mathrm{p})} = 1.0$ is 2881 hours. This value is of a similar order to that obtained without this variation in B, indicating that the influence of HAZ on the damage accumulated in the type IV region is minimal when $A^{(\mathrm{haz})}/A^{(\mathrm{p})} = 1.0$. When $A^{(\mathrm{haz})}/A^{(\mathrm{haz})} = 0.1$ the rupture times are identical as this is the standard value used for $A_\circ$ in equation (3.149). With $A^{(\mathrm{haz})}/A^{(\mathrm{p})} = 0.01$ and B altered accordingly, the position of rupture is now at the interface between the type IV region and the HAZ. The rupture time has also increased to 3743 hours.

When the width of the HAZ is increased to $x^{(\mathrm{haz})} = 0.2$, we observe that the rupture times do not follow the pattern obtained using the method of chapter 3 (Figure 3.6), where strengthening the HAZ produced a decrease in the strain-rates and thus an increase in the time to rupture. Figure (5.7) reveals that strengthening the HAZ from $A^{(\mathrm{haz})}/A^{(\mathrm{p})} = 1.0$ to $A^{(\mathrm{haz})}/A^{(\mathrm{p})} = 0.1$ and subsequently to $A^{(\mathrm{haz})}/A^{(\mathrm{p})}$ =0.01 leads to apparently contradictory results for the respective rupture times when compared with Figure (3.6). With the generalised Nicol model used in this chapter there is no simple

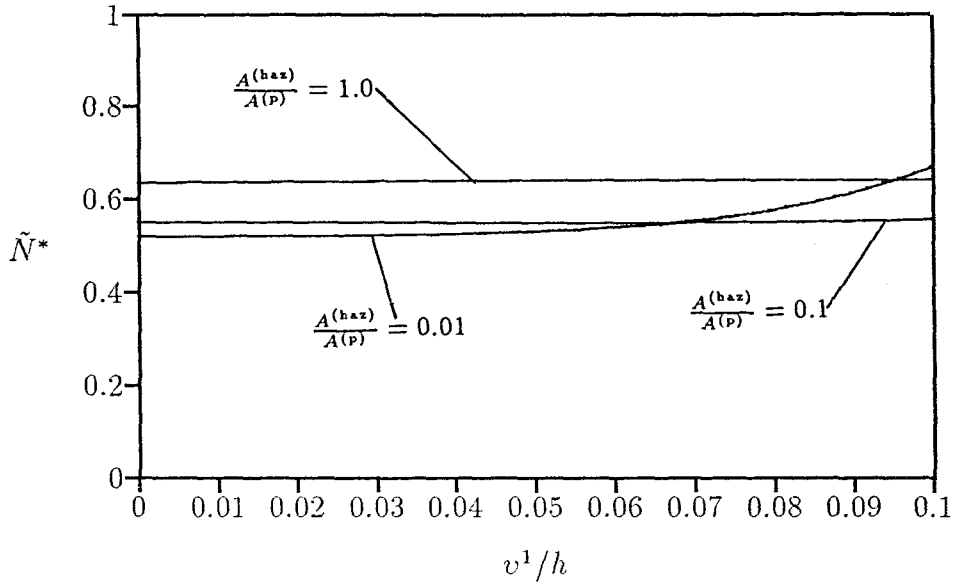

Figure 5.9: Variation of $\tilde{N}^*$ in the type IV region, corresponding to Figure (5.7)

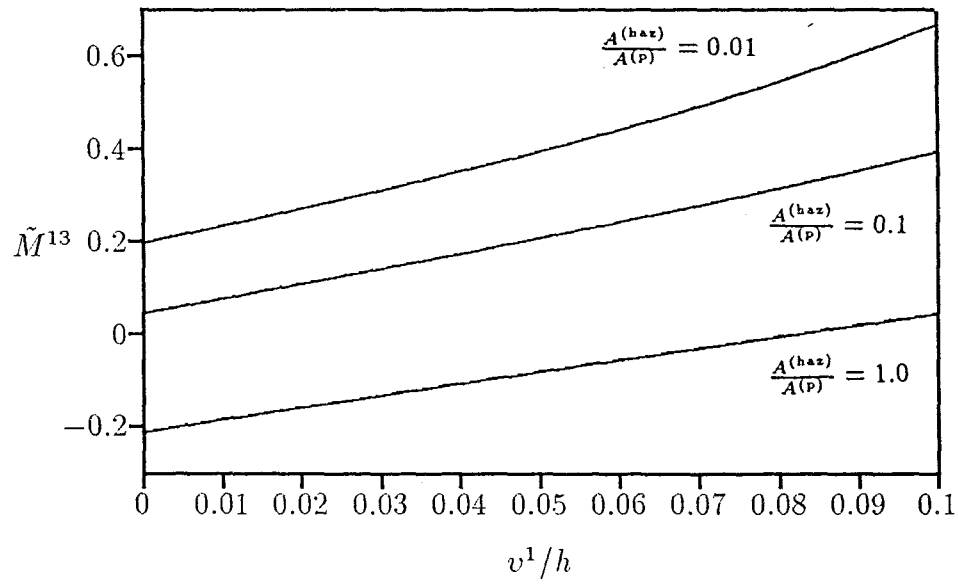

Figure 5.10: Variation of $\tilde{M}^{13}$ in the type IV region, corresponding to Figure (5.7)

analogy to equation (3.144) and so we must investigate the behaviour of N^* to ascertain

the reason for the confusing variation in rupture time. Figure (5.9) shows the initial value of N^* within the type IV region , using the same parameters and method adopted in determining Figure (5.7). It becomes apparent from Figure (5.9) that the extremely hard HAZ $\left(A^{(\mathrm{haz})}/A^{(\mathrm{p})} = 0.01\right)$ causes an increase in the value of N^* when approaching the interface with the HAZ and it is this increase that causes the observed variation in rupture time.

The latter argument becomes clearer when observing the initial values of M^{13} in the type IV region (Figure (5.10)), since increasing the strength of the HAZ increases the value of M^{13}. From equation (5.143) the contribution to N^* is through the term $(M^{13})^2$, and so it seems that for the anomalous case with $A^{(\mathrm{haz})}/A^{(\mathrm{p})}$=0.01, the value of M^{13} has become sufficiently large to increase significantly the value of N^* and hence affect the rupture time.

When the value of B is altered then the respective rupture times for $p = 0.9$ are 2883, 3348 and 1195 hours for $A^{(\mathrm{haz})}/A^{(\mathrm{p})}$=1.0, 0.1 and 0.01. Thus the rate of accumulated damage in the HAZ has little effect on the time to rupture within the type IV region.

In Figure (5.8) the width of the HAZ is now $x^{(\mathrm{haz})} = 0.5$. Comparing Figure (5.8) with Figure (3.7) we observe that the strain rates at $t = 0$ are comparable throughout the weld for each of the three values of the ratio $A^{(\mathrm{haz})}/A^{(\mathrm{p})}$. Again plotting the value of M^{13} (on the y-axis) against v^1/h (on the x-axis), for the type IV region only (Figure (5.11)), we note that as the ratio $A^{(\mathrm{haz})}/A^{(\mathrm{p})}$ decreases then the value of M^{13} within the type IV region increases. In this case the values of M^{13} when $A^{(\mathrm{haz})}/A^{(\mathrm{p})}$=0.01 and $A^{(\mathrm{haz})}/A^{(\mathrm{p})}$=0.1 are sufficiently large to influence N^* and the rupture time.

In both of the previous cases it seems clear that the rupture time has local maxima for some value of $A^{(\mathrm{haz})}/A^{(\mathrm{p})}$. Figures (5.10) and (5.11) suggest that the optimal values lie within the ranges $0.01 \leq A^{(\mathrm{haz})}/A^{(\mathrm{p})} \leq 1.0$ for $x^{(\mathrm{haz})} = 0.2$ and $0.1 \leq A^{(\mathrm{haz})}/A^{(\mathrm{p})} \leq 1.0$ for $x^{(\mathrm{haz})} = 0.5$ respectively (see Figures (5.12) and (5.13)).

For the case of the wide HAZ, with $x^{(\mathrm{haz})} = 0.5$, changing the value of B as

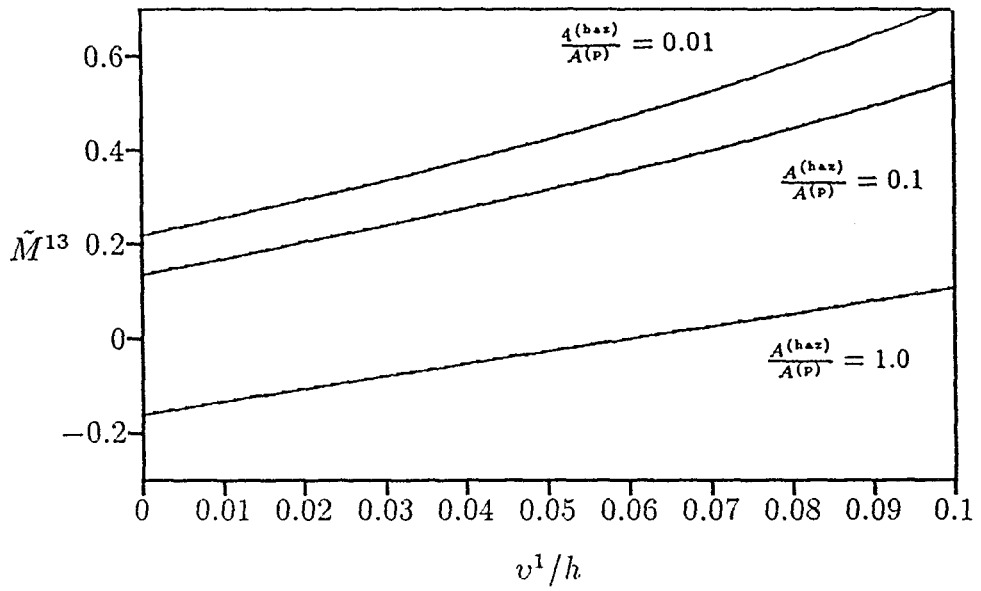

Figure 5.11: Variation of $\tilde{M}^{13}$ in the type IV region, corresponding to Figure (5.8)

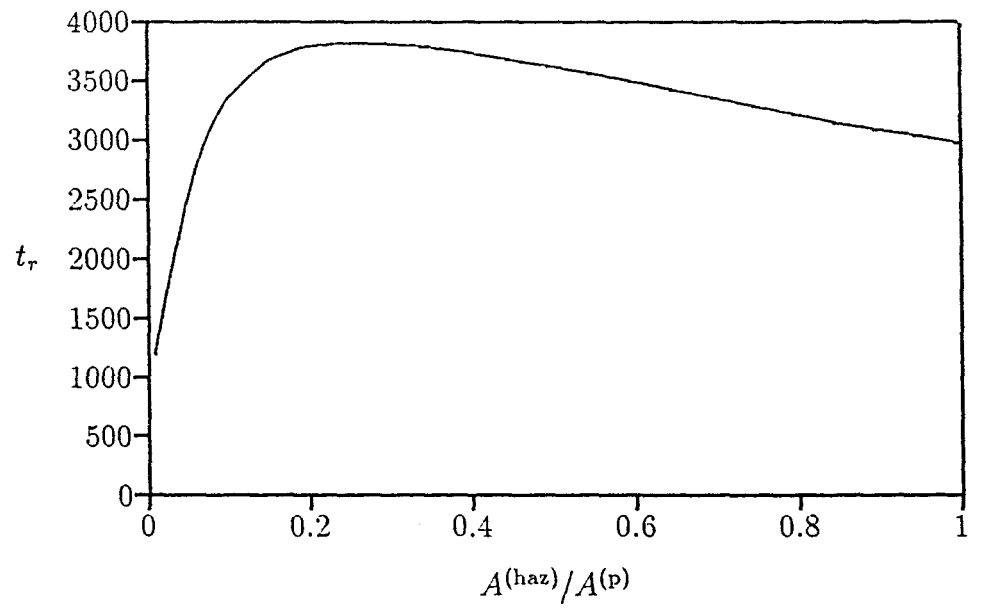

Figure 5.12: Variation in rupture time with $A^{(haz)}/A^{(p)}$, for $x^{(haz)}$=0.2

$A^{(haz)}/A^{(p)}$ changed produced the following rupture times:t_r=3867, 2054 and 977 hours

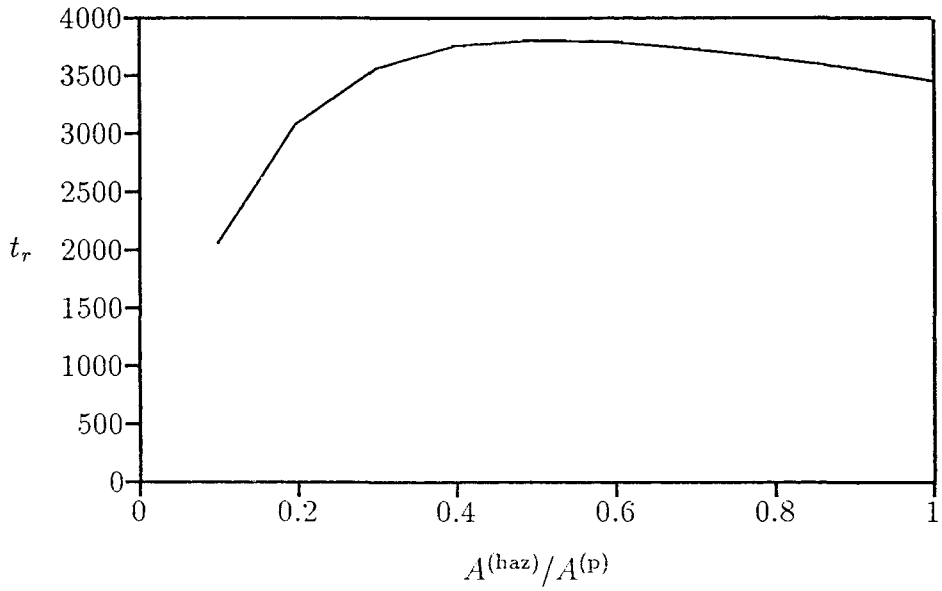

Figure 5.13: Variation in rupture time with $A^{(haz)}/A^{(p)}$, for $x^{(haz)}$=0.5

for $A^{(haz)}/A^{(p)}$=1.0, 0.1 and 0.01.

Figures (5.14) to (5.16) show the effects on the strain-rate at $t = 0$, the position of rupture and time to rupture, through variations in the width and relative strength of the weld metal. In each figure the ratio $A^{(w)}/A^{(p)}$ takes the values 30.0, 3.0 and 0.3 respectively. The values of the other parameters are $A^{(iv)}/A^{(p)} = 10.0, A^{(haz)}/A^{(p)} = 0.1$, with the widths of these two regions being $x^{(iv)}$=0.1 and $x^{(haz)} = 0.2$ respectively. The remaining parameter $x^{(w)}$ changes as follows:

- Figure (5.14), $x^{(w)} = 0.05$,
- Figure (5.15), $x^{(w)} = 0.2$,
- Figure (5.16), $x^{(w)} = 0.5$.

The most interesting feature of these series of figures is that as the width of the weld metal increases the time to rupture continues to increase for the 'standard' value of the

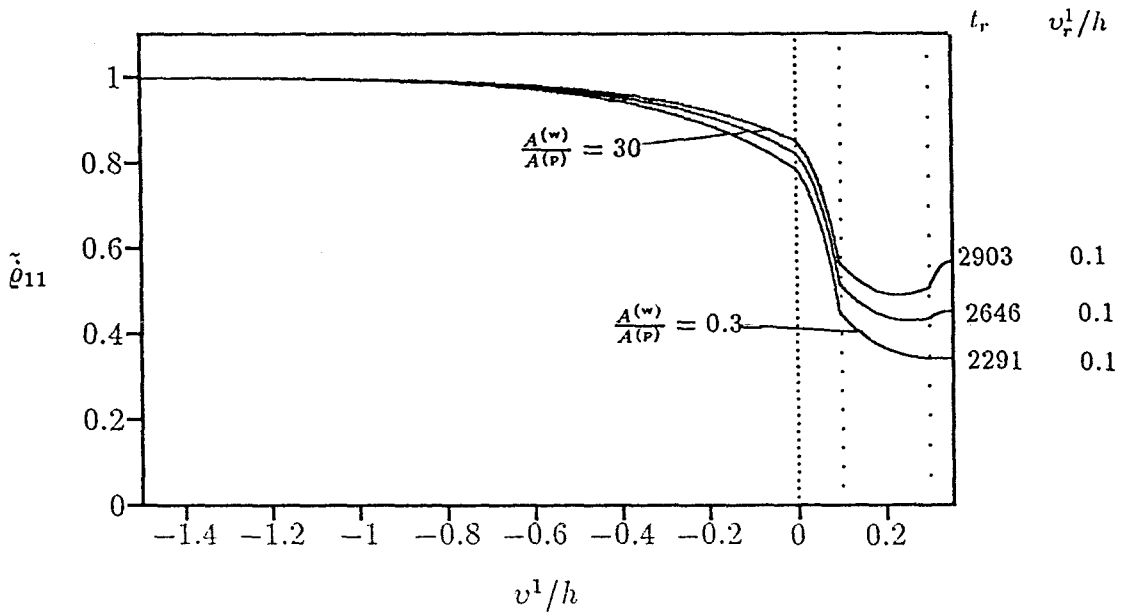

Figure 5.14: strain-rates for various $A^{(w)}/A^{(p)}$ with $x^{(w)}$=0.05

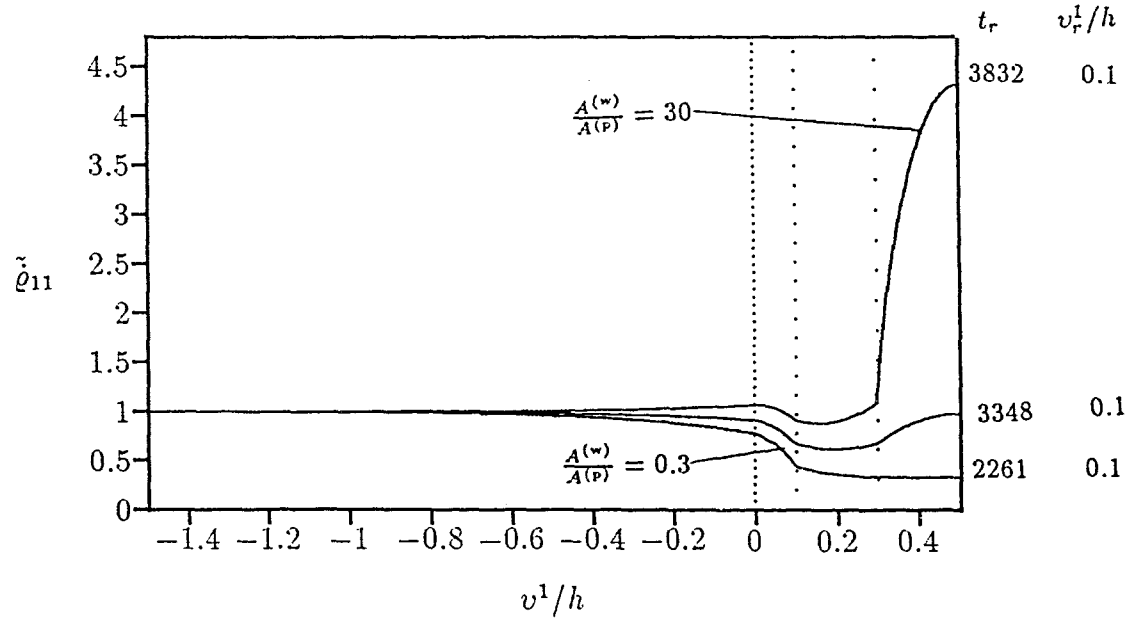

Figure 5.15: strain-rates for various $A^{(w)}/A^{(p)}$ with $x^{(w)}$=0.2

ratio $A^{(w)}/A^{(p)}$=3.0, whereas, for the softer weld metal $\left(A^{(w)}/A^{(p)} = 30.0\right)$, the time to

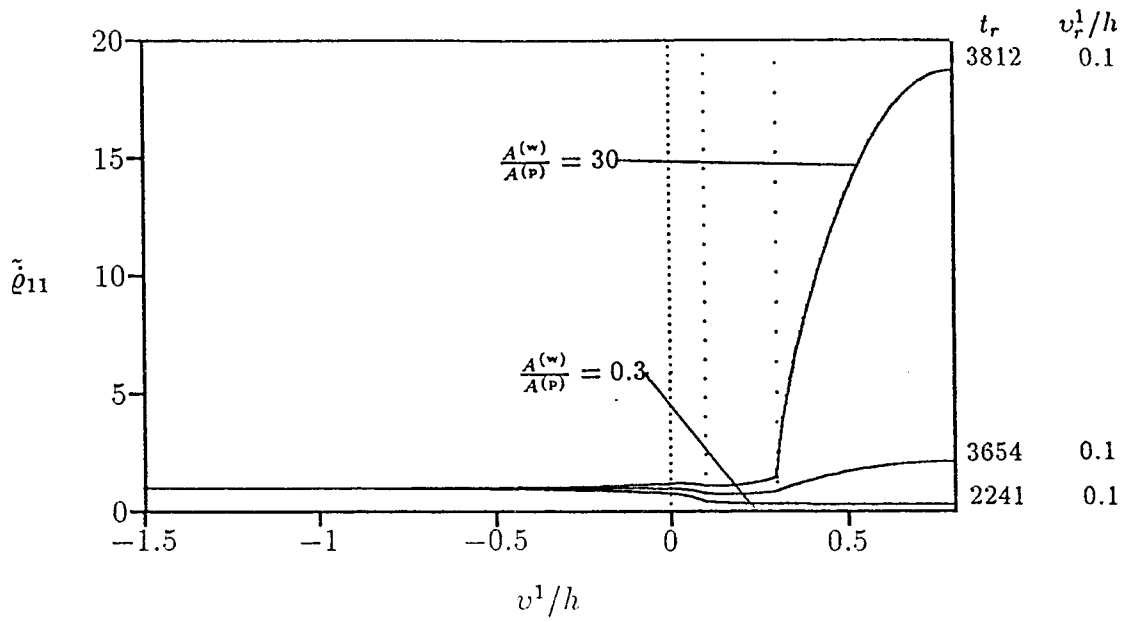

Figure 5.16: strain-rates for various $A^{(w)}/A^{(p)}$ with $x^{(w)}$=0.5

rupture increases to a value of 3832 hours when $x^{(w)} = 0.2$ and then decreases slightly to 3812 hours when the width of the weld metal is increased to $x^{(w)}$=0.5. . This would imply that there exists an optimal value for $x^{(w)}$ in the range $0.05 \leq x^{(w)} \leq 0.5$.

The reason for this slightly confusing result may be that as the width of the weld metal is increased, the strain-rate within this zone tends to its homogeneous limit. Once the strain-rate has reached this limit it is unlikely to increase further for a wide weld and this has a constraining affect on the strain-rates within the other zones of the weld.

Upon changing the value of the B in Figures (5.14)–(5.16) using $p = 0.9$ we obtain the following rupture times, omitting the case when $A^{(w)}/A^{(p)}$=3.0 since this is assumed to be the 'standard' value. For Figure (5.14), t_r=2903 and 2281 for $A^{(w)}/A^{(p)}$=30.0 and 0.3. For Figure (5.15), t_r=3832 and 2232 hours for the respective values of $A^{(w)}/A^{(p)}$ and, finally for Figure (5.16), t_r=3124 and 2212 hours for the chosen values of the strength ratio.

We note that altering the value of B in the weld region has very little effect on the

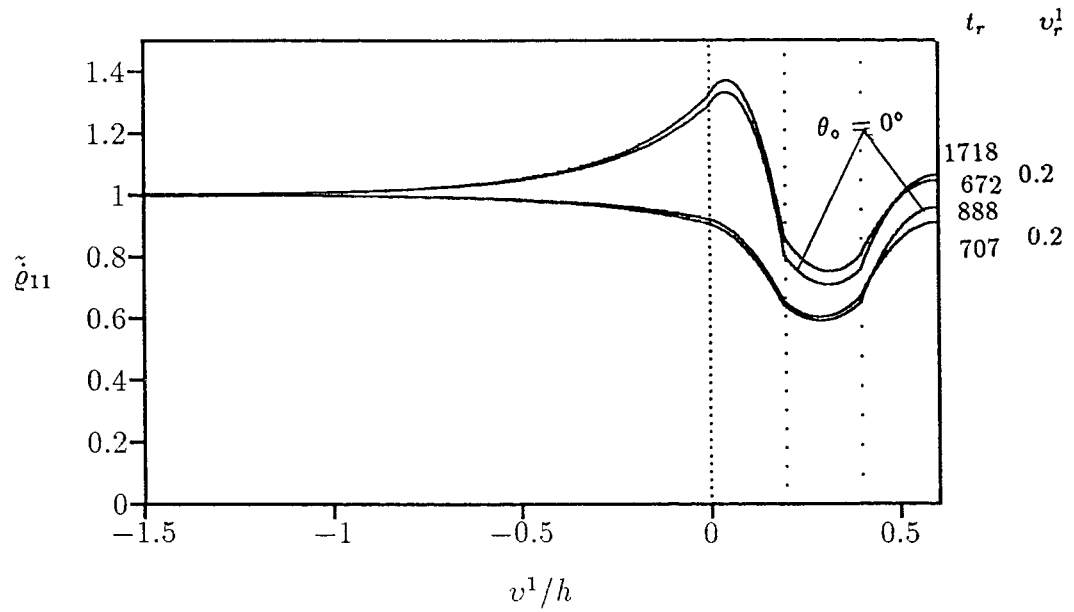

Figure 5.17: strain-rates for various $A^{(\mathrm{iv})}/A^{(\mathrm{p})}$ with angled interfaces

rupture times apart from the case when $A^{(\mathrm{w})}/A^{(\mathrm{p})}$=30.0 and $x^{(\mathrm{w})} = 0.5$. The large change in rupture time in the latter case occurs because the rupture position has now moved to within the weld metal at $v^1/h = 0.71$, whereas for all the other cases the rupture position was at the interface between the type IV region and the HAZ.

The results in this section emphasize that complex interactions occur within a weldment and these can cause unexpected variations in rupture times.

5.9.2 $\theta_\circ \neq 0.$

Figure (5.17) shows the changes in the strain-rate caused when the interfaces are at an angle $\theta_\circ(\neq 0)$ to the central surface of the plate. The plots shown are for the ratio $A^{(\mathrm{iv})}/A^{(\mathrm{p})}$ taking the values 10 and 2, with the angle $\theta_\circ$ taking the values 0° and 10°. All other parameters involved in the problem have the same values as used to produce Figure (5.3). We observe that for both situations an angled interface produces a small variation in the non-dimensional strain-rate at $t = 0$, and a decrease in the rupture time of the

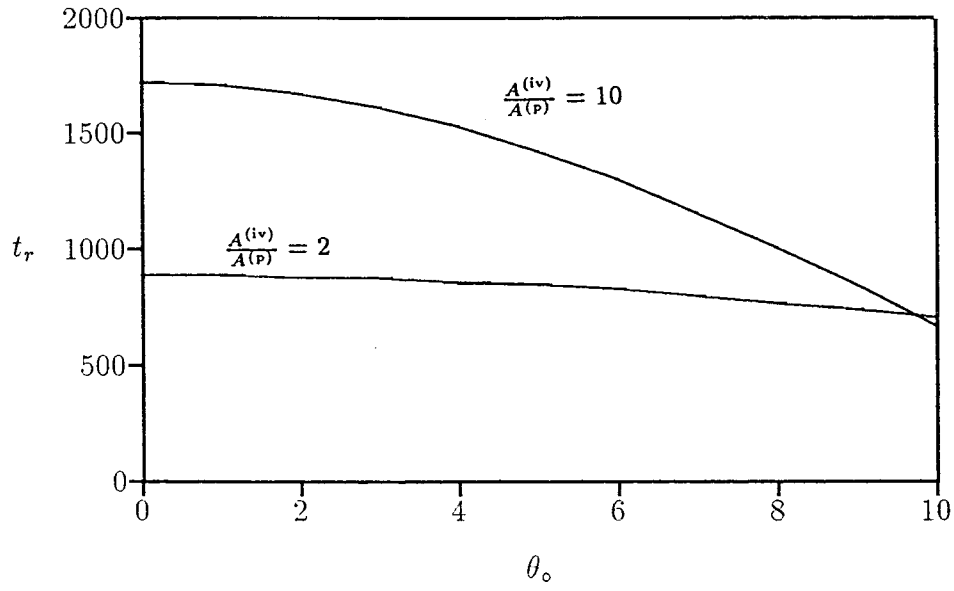

Figure 5.18: Variation in lifetime t_r with angle of the interfaces θ_o

weld.

Figure (5.18) shows the variation in the rupture time as a function of the angle of the interface θ_o, for the two welds described in the previous paragraph. We observe that the percentage decrease in rupture time varies dramatically depending on the value of the strength ratio $A^{(iv)}/A^{(p)}$. For $A^{(iv)}/A^{(p)} = 10.0$ there has been a 60% reduction in the lifetime of the weld, whereas for the case of $A^{(iv)}/A^{(p)} = 2.0$ the lifetime of the weld has been reduced by 20%.

Figure (5.19) shows the effect of an angled interface on the strain-rate at $t = 0$ for different strengths of the weld metal where $A^{(w)}/A^{(p)}$ takes the values 30.0 and 0.3 respectively. The other parameters of the weld are $x^{(iv)} = 0.1, x^{(haz)} = x^{(w)} = 0.2, A^{(iv)}/A^{(p)} = 10.0$ and $A^{(haz)}/A^{(p)} = 0.1$. Again we observe a large difference in the rupture times arising from the angled interface.

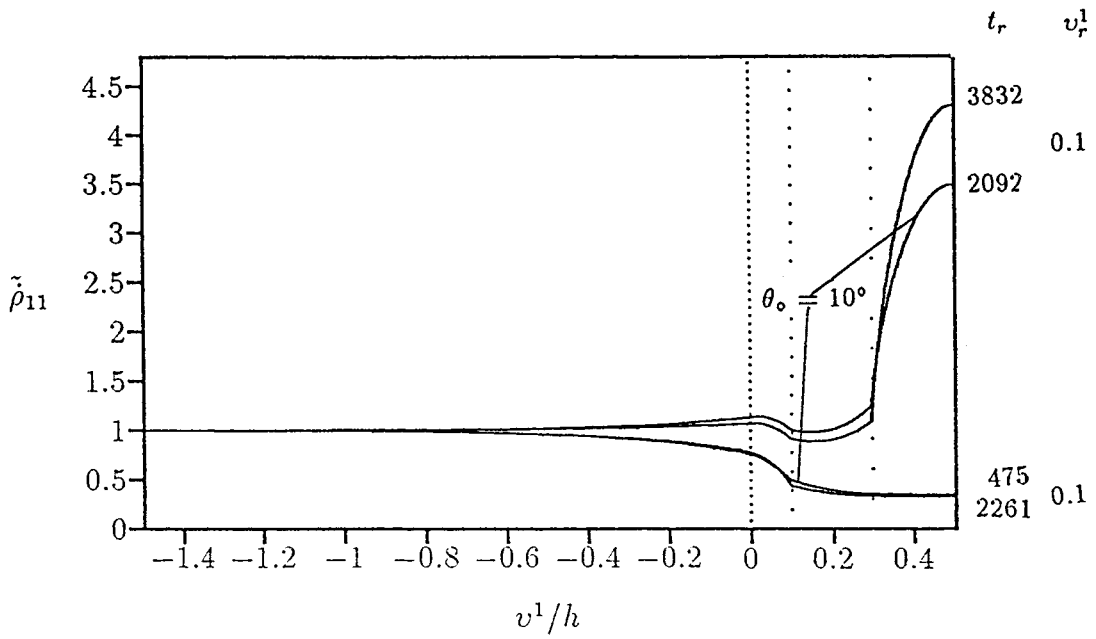

Figure 5.19: strain-rates for various $A^{(w)}/A^{(p)}$ with angled interfaces

5.10 Discussion.

It has been shown in the previous section §5.9 that, using the generalised Nicol method, we can obtain results for the strain-rates at $t = 0$,and the corresponding rupture times and rupture positions for welds containing four zones with different material properties, when the interfaces between each region are at an angle θ_o to the central surface of the plate. The results produced, using this method, show that for all the different welds considered the presence of the angled interfaces has caused a reduction in the lifetime of the weld. The size of this reduction has been somewhat larger than expected.

The condition (5.18), when non-dimensionalised using (5.139), requires that

$$\frac{\partial \theta}{\partial \tilde{v}^1} \ll \frac{1}{\sqrt{48}}. \tag{5.169}$$

For a typical weldment with the width approximately equal to the thickness of the plate the inequality is strictly satisfied for very small angles. The derivative in (5.169), however,

becomes significant even for angles as small as 10°. Consequently, the results presented in the previous section should be used only to indicate the trend in the behaviour of the lifetime of the weld due to the presence of angled interfaces. At larger angles we would not expect a reversal of this trend, but the magnitude of reduction might be significantly changed. The trend indicated by our results is in agreement with results obtained by Shakhmatov et al.(1987) who examined welds with different geometries using a model which included slip lines.

Clearly it would be useful to industry if a model applicable to large angles could be developed. In principle our method is easily extended but since the algebraic complexity is increased the problem is not considered further in this thesis.

Chapter 6

CLOSING REMARKS

This thesis has used the basic ideas of Continuum Damage Mechanics to introduce an explicit time dependence into the constitutive equations derived by Nicol (1985) and Hawkes (1989). We have used coupled damage equations to model the creep and creep rupture of a plate containing a weldment comprising parent material, type IV region, heat affected zone and the weld metal.

It has been found that both models introduced by Nicol and Hawkes produce results that are in close agreement for the initial strain-rates, but that the positions of rupture and the rupture times differ significantly from one model to the other. These differences in rupture times appear to be caused by how the different models cope with the large mismatch of material properties at the interfaces separating each region. Large differences in creep strength between the materials lead to rapid changes in stresses close to the interface. Hayhurst (1983) argues that a more realistic evolution equation should include a specific dependence on the maximum principal stress as well as the equivalent stress. We have obtained results using such an evolution equation and observe that for the weldment considered in this thesis there was a resulting large reduction in the rupture time. It is clear from the work in this thesis that the Nicol approach does incorporate some of the variations in stresses into the model but, as yet there is no firm evidence to suggest which model is best.

The obvious advantage of the Cosserat models discussed here is that they produce results for the rupture time and position of rupture in a fraction of the time taken to operate a full finite element scheme. Each set of results displayed earlier in this thesis was

produced in about 1 minute, typically, compared with the many hours necessary to obtain a solution using a finite element code. This comment alone justifies further investigation as to the accuracy and reliability of the results obtained using the Cosserat models.

During the progression of this thesis it has become clear that it is unrealistic to change the value of the material parameter A without alterating the corresponding value of B. It has been shown that the rupture results depend sensitively on the relationship between these two material quantities. Without detailed information about all the material parameters it is impossible to make lifetime predictions with any confidence and hence the results obtained in this thesis should only be used as an observation on the trends in rupture behaviour. However, it should be stated that the qualitative results obtained up to now with the Cosserat models do not contradict the experimental evidence derived over many years of testing.

In chapter 5, we investigated the effect on the rupture time of a plate containing a V-shaped weld. It has been found that the presence of a weld in the plate with the interfaces between each region at an angle to the central surface causes a reduction in the time to rupture. This is in agreement with results obtained by Shakhmatov et al.(1987), in their investigation of butt welded joints using the method of slip lines. The results of chapter 5 have shown that small differences in the values of the initial strain-rate can cause large changes in the calculated lifetime of a plate. Consequently the approach used by Storesund, Tu and Wu (1992) to predict the lifetime seems to be a little simplistic.

Clearly there are many problems that have been left incomplete or untouched by this present work. It would be desirable, for instance, to model a weld with a larger bevel angle than that considered in this thesis. Although the increase in algebra would be considerable, one expects the form of the resulting constitutive equations would be similar to the form of the equations in chapter 5 and hence could be solved using a similar numerical scheme. It would also be useful to obtain failure times for a pipe instead of a plate, since pipes are used much more extensively in practical situations. Such a solution would then allow

a direct comparison with the finite element method of Hall and Hayhurst (1991).

The Cosserat approach might also be used to model plates and pipes containing welds with other geometrical shapes, such as an 'X-shaped' weld, a weld with the interfaces at an oblique angle to the surface of the plate, or a 'chevron' weld. It may be possible to model an X-shaped weld by imposing a symmetry condition on a laminate containing two V-shaped welds. The oblique angled weld could be modelled in a similar manner to the V-shaped weld without the initial value of the director in the weld needing to vary with distance.

The chevron weld could then be modelled as a composite of two of the oblique welds. One feature of the last two problems is the loss of symmetry at the centre of the welds. Another situation that has recently been studied by Robinson, Binienda and Miti-Kavuma (1992), using a method somewhat similar to Cosserat theory, is that of a thin-walled pressure vessel, with reinforced fibres at an arbitrary helical angle, operating in the creep regime. This problem has a geometrical structure which would require the initial values of all the director components to be non-zero.

The overall conclusion which emanates from this thesis is that the Cosserat model coupled with the Kachanov-Rabotnov damage equation, of a weldment, provide much useful information to the design engineer on the time and position of rupture. The derivation of the governing equations for the mathematical model may sometimes be somewhat lengthy, but the resulting partial differential equations can be solved very quickly using a computer and the results are potentially useful, therefore, in an efficient design process.

REFERENCES

Abram, J., *Tensor Calculus through Differential Geometry*, Butterworth and Co., (1965).

Ashby, M.F. and Embury, J.D., *The Influence of Dislocation Density on the Ductile-Transition in BCC Metals*, Scripta Met. **19**, 557–562, (1985).

Chaboche, J.L., *Continuum Damage Mechanics, Parts I–II*, Trans. ASME J. Appl. Mech. **55**, 59–72, (1988).

Cocks, A.C.F. and Ashby, M.F., *The Growth of a Dominant Crack in a Creeping Material*, Scripta Met. **16** 109–114, (1981).

Coleman, M.C., *The Structure of Weldments and it's Relevance to High Temperature Failure*, Proceedings of the Fifth Bolton Land Conference (edited by R. J. Christoffel, E. F. Nippes and H. D. Solomon), (1978).

Dyson, B.F., *Continuous Cavity Nucleation and Creep Fracture*, Scripta Met. **17**, 31–37, (1983).

Eringen, A.C., *Mechanics of Continua*, Wiley, (1967).

Evans, R.W., Parker, J.D. and Wilshire, B., *An Extrapolation Procedure for Long-Term Creep Strain and Creep Life Prediction with Special Reference to 1/2Cr1/2Mo1/4V Ferritic Steels*, in Recent Advances in Creep and Fracture of Engineering Materials and Structures (edited by B. Wilshire and D. R. J. Owen), Pineridge Press, (1982).

Giessen van der, E. and Tvergaard, V., *A Creep Rupture Model Accounting for Cavitation at Sliding Grain Boundaries*, Int. J. Frac. **48**, 153–178, (1991).

Green, A.E., Laws, N. and Naghdi, P.M., *Rods, Plates and Shells*, Proc. Camb. Soc. **64**, 895–913, (1968).

Green, A.E. and Naghdi, P.M, *Some Remarks on the Linear Theory of Shells*, Quart. J. Mech. and Applied Math. **XVIII**, 257–276, (1965).

Green, A.E., Naghdi, P.M. and Osborn, R.B., *Theory of an Elastic-Plastic Cosserat Surface*, Int. J. Solids Structures, **4**, 907–927, (1968).

Green, A.E., Naghdi, P.M. and Wainwright, W.L., *A General Theory of a Cosserat Surface*, Arch. Rat. Mech. Anal. **20**, 287–308, (1965).

Green, A.E., Naghdi, P.M. and Wenner, M.L., *Linear Theory of Cosserat Surface and Elastic Plates of Variable Thickness*, Proc. Camb. Phil. Soc. **69**, 227–254, (1971).

Green, A.E. and Zerna, W. *Theoretical Elasticity*, Clarendon Press, (1968).

Hall, F.R. and Hayhurst, D.R., *Modelling of Grain Size in Creep Crack Growth using a Non-Local Continuum Damage Approach*, Proc. R. Soc. Lond. A **433**, 405–421, (1991a).

Hall, F.R. and Hayhurst, D.R., *Continuum Damage Mechanics Modelling of High Temperature Deformation and Failure in a Pipe Weldment*, Proc. R. Soc. Lond. A **433**, 383–403, (1991b).

Hawkes, T.D., *Mathematical Modelling of Creep of Weldments using the Cosserat Theory of Plates and Shells*, Ph.D. Thesis, University of Southampton, (1989).

Hayhurst, D.R., *Creep Rupture Under Multi-Axial States of Stress*, J. Mech. Phys. Solids. **20**, 381–390, (1972).

Hayhurst, D.R., *On the Rôle of Creep Continuum Damage in Structural Mechanics*, in Engineering Approaches to High Temperature Design (edited by B. Wilshire and D. R. J. Owen), Pineridge Press, (1983).

Johnson, A.E., *Creep under Complex Stress Systems at Elevated Temperatures*, Proc. Inst. Mech. Engrs **164**, 432–447, (1951).

Jonas, J.J. and Baudelet, B., *Effect of Crack and Cavity Generation on Tensile Stability*, Acta Met. **25**, 43–50, (1977).

Kachanov, L.M., *Introduction to Continuum Damage Mechanics*, Martinus-Nijhoff, Dordrecht, the Netherlands, (1986).

Kachanov, L.M., *Time of the Fracture Process under Creep Conditions*, Izv. Akad. Nauk. S.S.S.R., Otd. Teck. Nauk. 8, 26–31, (1958).

Leckie, F.A., *The Micro- and Macro-Mechanics of Creep Rupture*, Eng. Frac. Mech. **25** Nos. 5/6, 505–521, (1986).

Leckie, F.A. and Hayhurst, F.R., *Constitutive Equations for Creep Rupture*, Acta Metall. **25**, 1059–1070, (1977).

Maruyama, K., Tanaka, C. and Oikawa, H., *Long-Term Creep Curve Prediction Based on the Modified θ Projection Concept*, Trans. ASME Int. Press. Vess. Tech. **112**, 92–97, (1990).

Monkman, F.C. and Grant, N.J., *An Empirical Relationship between Rupture Life amd Minimum Creep Rate*, Proc. ASTM **56**, 593, (1956).

Naghdi, P.M, *The Theory of Shells and Plates*, Handbuch der Physik, Vol. VIa/2, (1972). Re-issued as Mechanics of Solids Vol. II (edited by C. Truesdell), Springer-Verlag (1984).

Nicol, D.A.C. and Williams, J.A., *The Creep Behaviour of Cross-Weld Specimens Under Uniaxial Loading*, Res Mechanica, **14**, 197–223, (1985).

Nicol, D.A.C., *Creep Behaviour of Butt Welded Joints*, Int. J. Engng. Sci., **23**, 541–553, (1985).

Norton, F.H., *Creep of Steel at High Temperatures*, McGraw-Hill, New York, (1929).

Odqvist, F.K.G., *Mathematical Theory of Creep and Creep Rupture*, Clarendon Press, (1974).

Othman, A.M. and Hayhurst, D.R., *Multi-Axial Creep Rupture of a Model Structure using a Two Parameter Material Model*, Int. J. Mech. Sci. **32** No. 1, 35–88. (1990)

Rabotnov, Y.N., *Creep in Structural Members*, North Holland, Amsterdam, (1969).

Robinson, D.N., Binienda, W.K. and Miti-Kavuma, M., *Creep and Creep Rupture of Metallic Composites*, J. Engng. Mech. ASCE **118** No. 8, 1646–1660, (1992).

Shakhmatov, M.V. et al., *Optimisation of Design and Geometrical Parameters of Butt Welded Joints in Heat Resisting Dissimilar Steels*, Welding International No. 8, (1988).

Storesund, J., Tu, S.T. and Wu, R., *A Study of the Stress Distribution in Uniaxial Cross Weld Creep Test Specimens*, Int. Symposiuym, Baltica II, Tallin, R Estonia, (1992).

Truesdell, C., *The Physical Components of Vectors and Tensors*, Z. Angew. Math. Mech. **33**, 345–356, (1953).

Wilshire, B., *Microscopic Models and Macroscopic Constitutive Laws for High Temperature Creep and Creep Fracture of Metallic and Ceramic Materials*, in Mechanics of Creep Brittle Materials-2 (edited by A. C. F. Cocks and A. R. S. Ponter), Elsevier Applied Science, London and New York, 112–123, (1991).